Handbook of
Yield Point Engineering

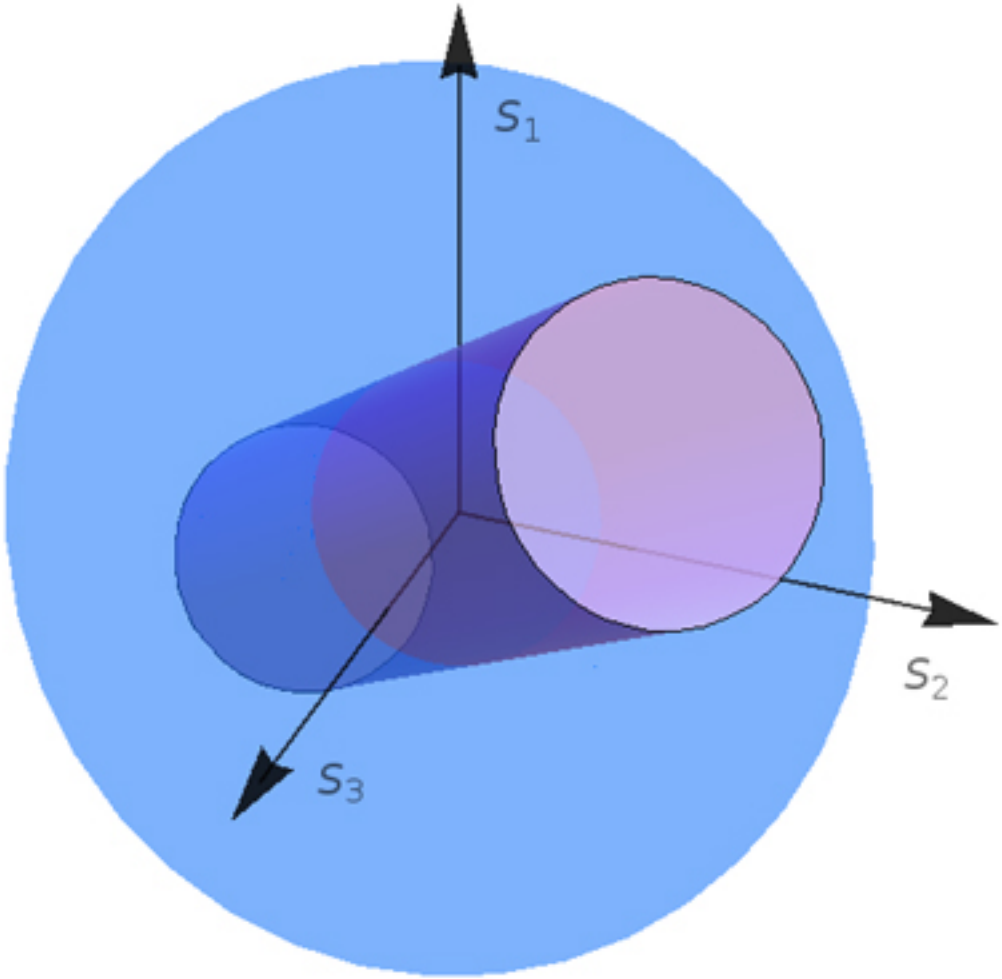

Clifford Boudreau
Cierra Cowell

First Edition, 2012

ISBN 978-81-323-0934-5

Published by:
Academic Studio
4735/22 Prakashdeep Bldg,
Ansari Road, Darya Ganj,
Delhi - 110002
Email: info@wtbooks.com

Table of Contents

Chapter 1

Yield (Engineering)

The **yield strength** or **yield point** of a material is defined in engineering and materials science as the stress at which a material begins to deform plastically. Prior to the yield point the material will deform elastically and will return to its original shape when the applied stress is removed. Once the yield point is passed some fraction of the deformation will be permanent and non-reversible.
In the three-dimensional space of the principal stresses (σ_1,σ_2,σ_3), an infinite number of yield points form together a yield surface.

Knowledge of the yield point is vital when designing a component since it generally represents an upper limit to the load that can be applied. It is also important for the control of many materials production techniques such as forging, rolling, or pressing. In structural engineering, this is a soft failure mode which does not normally cause catastrophic failure or ultimate failure unless it accelerates buckling.

Definition

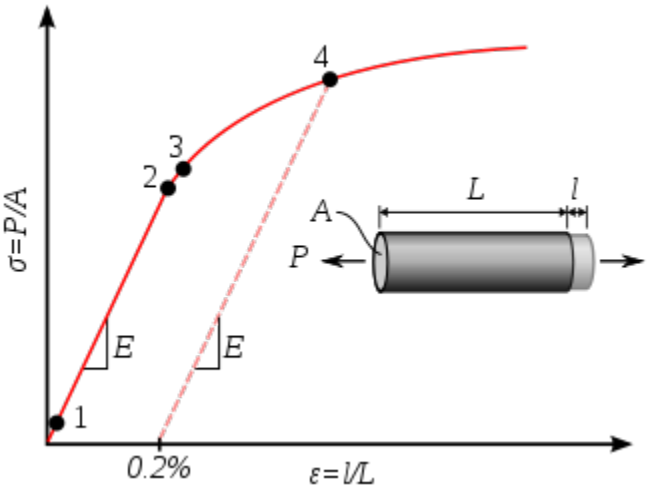

Typical yield behavior for non-ferrous alloys.
1: True elastic limit

2: Proportionality limit
3: Elastic limit
4: Offset yield strength

It is often difficult to precisely define yielding due to the wide variety of stress–strain curves exhibited by real materials. In addition, there are several possible ways to define yielding:

True elastic limit
: The lowest stress at which dislocations move. This definition is rarely used, since dislocations move at very low stresses, and detecting such movement is very difficult.

Proportionality limit
: Up to this amount of stress, stress is proportional to strain (Hooke's law), so the stress-strain graph is a straight line, and the gradient will be equal to the elastic modulus of the material.

Elastic limit (yield strength)
: Beyond the elastic limit, permanent deformation will occur. The lowest stress at which permanent deformation can be measured. This requires a manual load-unload procedure, and the accuracy is critically dependent on equipment and operator skill. For elastomers, such as rubber, the elastic limit is much larger than the proportionality limit. Also, precise strain measurements have shown that plastic strain begins at low stresses.

Yield point
: The point in the stress-strain curve at which the curve levels off and plastic deformation begins to occur.

Offset yield point (proof stress)
: When a yield point is not easily defined based on the shape of the stress-strain curve an *offset yield point* is arbitrarily defined. The value for this is commonly set at 0.1 or 0.2% of the strain. The offset value is given as a subscript, e.g., $R_{p0.2}$=310 MPa. High strength steel and aluminum alloys do not exhibit a yield point, so this offset yield point is used on these materials.

Upper yield point and lower yield point
: Some metals, such as mild steel, reach an upper yield point before dropping rapidly to a lower yield point. The material response is linear up until the upper yield point, but the lower yield point is used in structural engineering as a conservative value. If a metal is only stressed to the upper yield point, and beyond, luders bands can develop.

Yield criterion

A yield criterion, often expressed as yield surface, or yield locus, is a hypothesis concerning the limit of elasticity under any combination of stresses. There are two interpretations of yield criterion: one is purely mathematical in taking a statistical approach while other models attempt to provide a justification based on established physical principles. Since stress and strain are tensor qualities they can be described on

the basis of three principal directions, in the case of stress these are denoted by σ_1, σ_2, and σ_3.

The following represent the most common yield criterion as applied to an isotropic material (uniform properties in all directions). Other equations have been proposed or are used in specialist situations.

Isotropic yield criteria

Maximum Principal Stress Theory - Yield occurs when the largest principal stress exceeds the uniaxial tensile yield strength. Although this criterion allows for a quick and easy comparison with experimental data it is rarely suitable for design purposes.

$$\sigma_1 \leq \sigma_y$$

Maximum Principal Strain Theory - Yield occurs when the maximum principal strain reaches the strain corresponding to the yield point during a simple tensile test. In terms of the principal stresses this is determined by the equation:

$$\sigma_1 - \nu(\sigma_2 + \sigma_3) \leq \sigma_y.$$

Maximum Shear Stress Theory - Also known as the Tresca yield criterion, after the French scientist Henri Tresca. This assumes that yield occurs when the shear stress τ exceeds the shear yield strength τ_y:

$$\tau = \frac{\sigma_1 - \sigma_3}{2} \leq \tau_{ys}.$$

Total Strain Energy Theory - This theory assumes that the stored energy associated with elastic deformation at the point of yield is independent of the specific stress tensor. Thus yield occurs when the strain energy per unit volume is greater than the strain energy at the elastic limit in simple tension. For a 3-dimensional stress state this is given by:

$$\sigma_1^2 + \sigma_2^2 + \sigma_3^2 - 2\nu(\sigma_1\sigma_2 + \sigma_2\sigma_3 + \sigma_1\sigma_3) \leq \sigma_y^2.$$

Distortion Energy Theory - This theory proposes that the total strain energy can be separated into two components: the *volumetric* (hydrostatic) strain energy and the *shape* (distortion or shear) strain energy. It is proposed that yield occurs when the distortion component exceeds that at the yield point for a simple tensile test. This is generally referred to as the Von Mises yield criterion and is expressed as:

$$\frac{1}{2}\left[(\sigma_1 - \sigma_2)^2 + (\sigma_2 - \sigma_3)^2 + (\sigma_3 - \sigma_1)^2\right] \leq \sigma_y^2.$$

Based on a different theoretical underpinning this expression is also referred to as **octahedral shear stress theory**.

Other commonly used isotropic yield criteria are the

- Mohr-Coulomb yield criterion
- Drucker-Prager yield criterion
- Bresler-Pister yield criterion
- Willam-Warnke yield criterion

The yield surfaces corresponding to these criteria have a range of forms. However, most isotropic yield criteria correspond to convex yield surfaces.

Anisotropic yield criteria

When a metal is subjected to large plastic deformations the grain sizes and orientations change in the direction of deformation. As a result the plastic yield behavior of the material shows directional dependency. Under such circumstances, the isotropic yield criteria such as the von Mises yield criterion are unable to predict the yield behavior accurately. Several anisotropic yield criteria have been developed to deal with such situations. Some of the more popular anisotropic yield criteria are:

- Hill's quadratic yield criterion.
- Generalized Hill yield criterion.
- Hosford yield criterion.

Factors influencing yield stress

The stress at which yield occurs is dependent on both the rate of deformation (strain rate) and, more significantly, the temperature at which the deformation occurs. Early work by Alder and Philips in 1954 found that the relationship between yield stress and strain rate (at constant temperature) was best described by a power law relationship of the form

$$\sigma_y = C(\dot{\epsilon})^m$$

where C is a constant and m is the strain rate sensitivity. The latter generally increases with temperature, and materials where m reaches a value greater than ~0.5 tend to exhibit super plastic behaviour.

Later, more complex equations were proposed that simultaneously dealt with both temperature and strain rate:

$$\sigma_y = \frac{1}{\alpha}\sinh^{-1}\left[\frac{Z}{A}\right]^{(1/n)}$$

where α and A are constants and Z is the temperature-compensated strain-rate - often described by the Zener-Hollomon parameter:

$$Z = (\dot{\epsilon}) \exp\left(\frac{Q_{HW}}{RT}\right)$$

where Q_{HW} is the activation energy for hot deformation and T is the absolute temperature.

Strengthening mechanisms

There are several ways in which crystalline and amorphous materials can be engineered to increase their yield strength. By altering dislocation density, impurity levels, grain size (in crystalline materials), the yield strength of the material can be fine tuned. This occurs typically by introducing defects such as impurities dislocations in the material. To move this defect (plastically deforming or yielding the material), a larger stress must be applied. This thus causes a higher yield stress in the material. While many material properties depend only on the composition of the bulk material, yield strength is extremely sensitive to the materials processing as well for this reason.

These mechanisms for crystalline materials include

- Work Hardening
- Solid Solution Strengthening
- Particle/Precipitate Strengthening
- Grain boundary strengthening

Work Hardening

Where deforming the material will introduce dislocations, which increases their density in the material. This increases the yield strength of the material, since now more stress must be applied to move these dislocations through a crystal lattice. Dislocations can also interact with each other, becoming entangled.

The governing formula for this mechanism is:

$$\Delta\sigma_y = Gb\sqrt{\rho}$$

where σ_y is the yield stress, G is the shear elastic modulus, b is the magnitude of the Burgers vector, and ρ is the dislocation density.

Solid Solution Strengthening

By alloying the material, impurity atoms in low concentrations will occupy a lattice position directly below a dislocation, such as directly below an extra half plane defect.

This relieves a tensile strain directly below the dislocation by filling that empty lattice space with the impurity atom.

The relationship of this mechanism goes as:

$$\Delta\tau = Gb\sqrt{C_s}\epsilon^{3/2}$$

where τ is the shear stress, related to the yield stress, G and b are the same as in the above example, C_s is the concentration of solute and ε is the strain induced in the lattice due to adding the impurity.

Particle/Precipitate Strengthening

Where the presence of a secondary phase will increase yield strength by blocking the motion of dislocations within the crystal. A line defect that, while moving through the matrix, will be forced against a small particle or precipitate of the material. Dislocations can move through this particle either by shearing the particle, or by a process known as bowing or ringing, in which a new ring of dislocations is created around the particle.

The shearing formula goes as:

$$\Delta\tau = \frac{r_{\text{particle}}}{l_{\text{interparticle}}}\gamma_{\text{particle-matrix}}$$

and the bowing/ringing formula:

$$\Delta\tau = \frac{Gb}{l_{\text{interparticle}} - 2r_{\text{particle}}}$$

In these formulas, r_{particle} is the particle radius, $\gamma_{\text{particle-matrix}}$ is the surface tension between the matrix and the particle, $l_{\text{interparticle}}$ is the distance between the particles.

Grain boundary strengthening

Where a buildup of dislocations at a grain boundary causes a repulsive force between dislocations. As grain size decreases, the surface area to volume ratio of the grain increases, allowing more buildup of dislocations at the grain edge. Since it requires a lot of energy to move dislocations to another grain, these dislocations build up along the boundary, and increase the yield stress of the material. Also known as Hall-Petch strengthening, this type of strengthening is governed by the formula:

$$\sigma_y = \sigma_0 + kd^{-1/2}$$

where

σ_0 is the stress required to move dislocations,
k is a material constant, and
d is the grain size.

Testing

Yield strength testing involves taking a small sample with a fixed cross-section area, and then pulling it with a controlled, gradually increasing force until the sample changes shape or breaks. Longitudinal and/or transverse strain is recorded using mechanical or optical extensometers.

Indentation hardness correlates linearly with tensile strength for most steels. Hardness testing can therefore be an economical substitute for tensile testing, as well as providing local variations in yield strength due to e.g. welding or forming operations.

Implications for structural engineering

Yielded structures have a lower stiffness, leading to increased deflections and decreased buckling strength. The structure will be permanently deformed when the load is removed, and may have residual stresses. Engineering metals display strain hardening, which implies that the yield stress is increased after unloading from a yield state. Highly optimized structures, such as airplane beams and components, rely on yielding as a fail-safe failure mode. No safety factor is therefore needed when comparing limit loads (the highest loads expected during normal operation) to yield criteria.

Typical yield and ultimate strengths

Note: many of the values depend on manufacturing process and purity/composition.

Material	Yield strength (MPa)	Ultimate strength (MPa)	Density (g/cm^3)	free breaking length (km)
ASTM A36 steel	250	400	7.8	3.2
Steel, API 5L X65	448	531	7.8	5.8
Steel, high strength alloy ASTM A514	690	760	7.8	9.0
Steel, prestressing strands	1650	1860	7.8	21.6
Piano wire		2200–2482	7.8	28.7
Carbon Fiber (CF, CFK)		5650	1.75	
High density polyethylene (HDPE)	26-33	37	0.95	2.8
Polypropylene	12-43	19.7-80	0.91	1.3
Stainless steel AISI 302 -	520	860		

Cold-rolled				
Cast iron 4.5% C, ASTM A-48	*	172	7.20	2.4
Titanium alloy (6% Al, 4% V)	830	900	4.51	18.8
Aluminium alloy 2014-T6	400	455	2.7	15.1
Copper 99.9% Cu	70	220	8.92	0.8
Cupronickel 10% Ni, 1.6% Fe, 1% Mn, balance Cu	130	350	8.94	1.4
Brass	approx. 200+	550	5.3	3.8
Spider silk	1150 (??)	1200		50
Silkworm silk	500			25
Aramid (Kevlar or Twaron)	3620		1.44	256.3
UHMWPE	21	46	0.97	240
Bone (limb)	104-121	130		3
Nylon, type 6/6	45	75		2
*Grey cast iron does not have a well defined yield strength because the stress-strain relationship is atypical. The yield strength can vary from 65 to 80% of the tensile strength.				

Elements in the annealed state

	Young's modulus (GPa)	**Proof or yield stress (MPa)**	**Ultimate strength (MPa)**
Aluminium	70	15-20	40-50
Copper	130	33	210
Iron	211	80-100	350
Nickel	170	14-35	140-195
Silicon	107	5000-9000	
Tantalum	186	180	200
Tin	47	9-14	15-200
Titanium	120	100-225	240-370
Tungsten	411	550	550-620

Chapter 2

Von Mises Yield Criterion

The **Von Mises yield criterion** suggests that the yielding of materials begins when the second deviatoric stress invariant J_2 reaches a critical value k. For this reason, it is sometimes called the J_2-*plasticity* or J_2 flow theory. It is part of a plasticity theory that applies best to ductile materials, such as metals. Prior to yield, material response is assumed to be elastic.

In materials science and engineering the von Mises yield criterion can be also formulated in terms of the **von Mises stress** or **equivalent tensile stress**, σ_v, a scalar stress value that can be computed from the stress tensor. In this case, a material is said to start yielding when its von Mises stress reaches a critical value known as the yield strength, σ_y. The von Mises stress is used to predict yielding of materials under any loading condition from results of simple uniaxial tensile tests. The von Mises stress satisfies the property that two stress states with equal distortion energy have equal von Mises stress.

Because the von Mises yield criterion is independent of the first stress invariant, I_1, it is applicable for the analysis of plastic deformation for ductile materials such as metals, as the onset of yield for these materials does not depend on the hydrostatic component of the stress tensor.

Although formulated by Maxwell in 1865, it is generally attributed to Richard Edler von Mises (1913). Tytus Maksymilian Huber (1904), in a paper in Polish, anticipated to some extent this criterion. This criterion is also referred to as the Maxwell–Huber–Hencky–von Mises theory.

Mathematical formulation

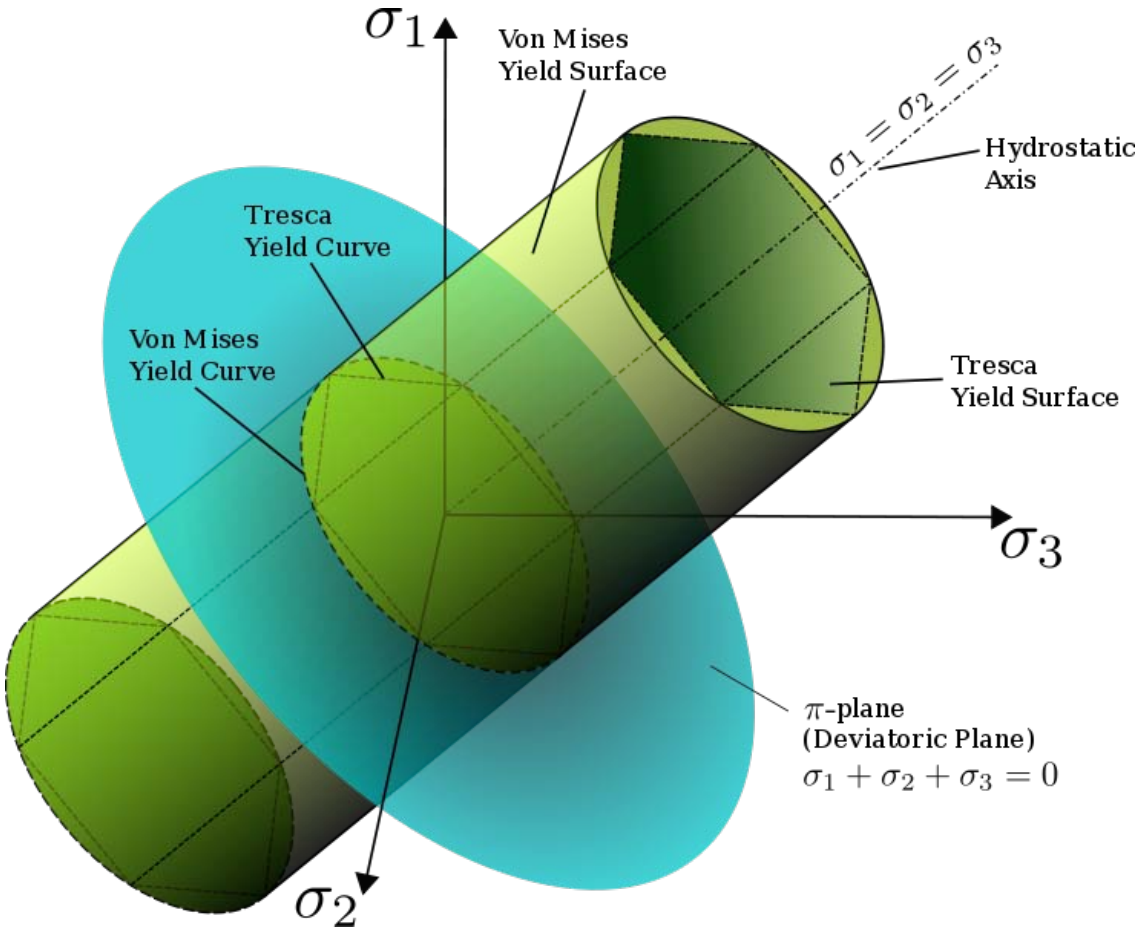

The von Mises yield surfaces in principal stress coordinates circumscribes a cylinder with radius $\sqrt{\frac{2}{3}}\sigma_y$around the hydrostatic axis. Also shown is Tresca's hexagonal yield surface.

Mathematically the yield function for the von Mises condition is expressed as:

$$f(J_2) = \sqrt{J_2} - k = 0$$

An alternative form is:

$$f(J_2) = J_2 - k^2 = 0$$

where *k* can be shown to be the yield stress of the material in pure shear. As it will become evident later, at the onset of yielding, the magnitude of the shear yield stress in pure shear is √3 times lower than the tensile yield stress in the case of simple tension. Thus, we have

$$k = \frac{\sigma_y}{\sqrt{3}}$$

Furthermore, if we define the von Mises stress as $\sigma_v = \sqrt{3J_2}$, the von Mises yield criterion can be expressed as:

$$\begin{aligned} f(J_2) &= \sqrt{3J_2} - \sigma_y \\ &= \sigma_v - \sigma_y = 0 \end{aligned}$$

Substituting J_2 in terms of the principal stresses into the von Mises criterion equation we have

$$(\sigma_1 - \sigma_2)^2 + (\sigma_2 - \sigma_3)^2 + (\sigma_1 - \sigma_3)^2 = 6k^2 = 2\sigma_y^2$$

or

$$(\sigma_1^2 + \sigma_2^2 + \sigma_3^2) - \sigma_1\sigma_2 - \sigma_2\sigma_3 - \sigma_1\sigma_3 = 3k^2 = \sigma_y^2$$

or as a function of the stress tensor components

$$(\sigma_{11} - \sigma_{22})^2 + (\sigma_{22} - \sigma_{33})^2 + (\sigma_{11} - \sigma_{33})^2 + 6(\sigma_{23}^2 + \sigma_{31}^2 + \sigma_{12}^2) = 6k^2 = 2\sigma_y^2$$

This equation defines the yield surface as a circular cylinder whose yield curve, or intersection with the deviatoric plane, is a circle with radius $\sqrt{2}k$, or $\sqrt{\frac{2}{3}}\sigma_y$. This implies that the yield condition is independent of hydrostatic stresses.

Von Mises criterion for different stress conditions

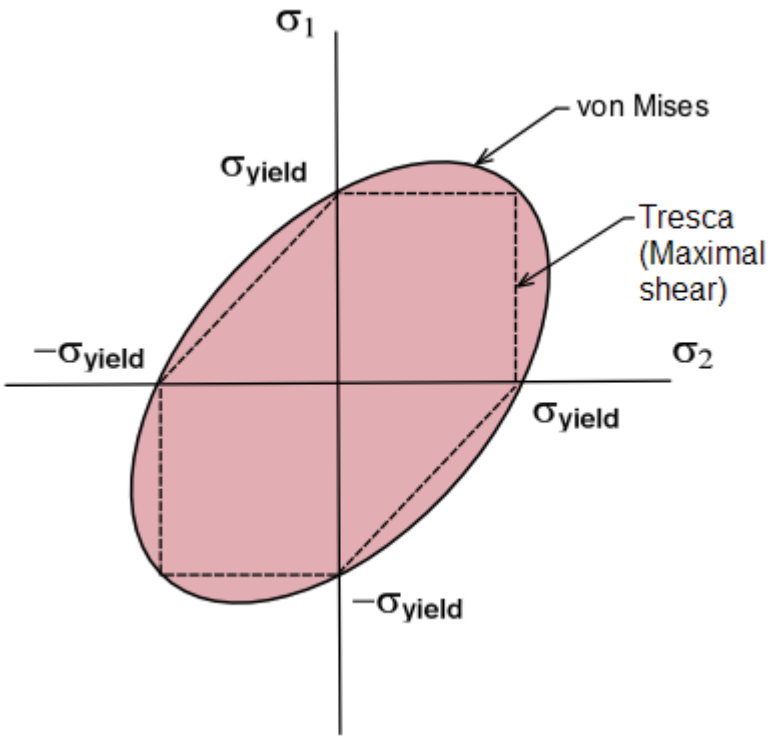

Projection of the von Mises yield criterion into the σ_1,σ_2 plane

In the case of **uniaxial stress** or **simple tension**, $\sigma_1 \neq 0$, $\sigma_3 = \sigma_2 = 0$, the von Mises criterion reduces to

$$\sigma_1 = \sigma_y.$$

Therefore, the material starts to yield, when σ_1 reaches the *yield strength* of the material σ_y, which is a characteristic material property. In practice, this parameter is indeed determined in a tensile test satisfying the uniaxial stress condition.

It is also convenient to define an **Equivalent tensile stress** or **von Mises stress**, σ_v, which is used to predict yielding of materials under **multiaxial loading conditions** using results from simple uniaxial tensile tests. Thus, we define

$$\begin{aligned}
\sigma_v &= \sqrt{3J_2} \\
&= \sqrt{\frac{(\sigma_{11}-\sigma_{22})^2 + (\sigma_{22}-\sigma_{33})^2 + (\sigma_{11}-\sigma_{33})^2 + 6(\sigma_{12}^2+\sigma_{23}^2+\sigma_{31}^2)}{2}} \\
&= \sqrt{\frac{(\sigma_1-\sigma_2)^2 + (\sigma_2-\sigma_3)^2 + (\sigma_1-\sigma_3)^2}{2}} \\
&= \sqrt{\tfrac{3}{2}\, s_{ij}s_{ji}}
\end{aligned}$$

where s_{ij} are the components of the stress deviator tensor $\boldsymbol{\sigma}^{dev}$:

$$\boldsymbol{\sigma}^{dev} = \boldsymbol{\sigma} - \frac{1}{3}(\boldsymbol{\sigma} \cdot \mathbf{I})\,\mathbf{I}$$

In this case, yielding occurs when the equivalent stress, σ_v, reaches the yield strength of the material in simple tension, σ_y. As an example, the stress state of a steel beam in compression differs from the stress state of a steel axle under torsion, even if both specimen are of the same material. In view of the stress tensor, which fully describes the stress state, this difference manifests in six degrees of freedom, because the stress tensor has six independent components. Therefore, it is difficult to tell which of the two specimens is closer to the yield point or has even reached it. However, by means of the von Mises yield criterion, which depends solely on the value of the scalar von Mises stress, i.e., one degree of freedom, this comparison is straightforward: A larger von Mises value implies that the material is closer to the yield point.

In the case of **pure shear stress**, $\sigma_{12} = \sigma_{21} \neq 0$, while all other $\sigma_{ij} = 0$, von Mises criterion becomes:

$$\sigma_{12} = k = \frac{\sigma_y}{\sqrt{3}}$$

This means that, at the onset of yielding, the magnitude of the shear stress in pure shear is $\sqrt{3}$times lower than the tensile stress in the case of simple tension. The von Mises yield criterion for pure shear stress, expressed in principal stresses, is

$$(\sigma_1 - \sigma_2)^2 + (\sigma_2 - \sigma_3)^2 + (\sigma_1 - \sigma_3)^2 = 6\sigma_{12}^2$$

In the case of **plane stress**, $\sigma_3 = 0$, the von Mises criterion becomes:

$$\sigma_1^2 - \sigma_1\sigma_2 + \sigma_2^2 = 3k^2 = \sigma_y^2$$

This equation represents an ellipse in the plane $\sigma_1 - \sigma_2$, as shown in the Figure above.

Physical interpretation of the von Mises yield criterion

Hencky (1924) offered a physical interpretation of von Mises criterion suggesting that yielding begins when the elastic energy of distortion reaches a critical value. For this, the von Mises criterion is also known as the **maximum distortion strain energy criterion**. This comes from the relation between J_2 and the elastic strain energy of distortion W_D:

$$W_D = \frac{J_2}{2G}$$ with the elastic shear modulus $$G = \frac{E}{2(1+\nu)}.$$

In 1937 Arpad L. Nadai suggested that yielding begins when the octahedral shear stress reaches a critical value, i.e. the octahedral shear stress of the material at yield in simple tension. In this case, the von Mises yield criterion is also known as the **maximum octahedral shear stress criterion** in view of the direct proportionality that exist between J_2 and the octahedral shear stress, τ_{oct}, which by definition is

$$\tau_{oct} = \sqrt{\frac{2}{3} J_2}$$

thus we have

$$\tau_{oct} = \frac{\sqrt{2}}{3} \sigma_y$$

Comparison with Tresca yield criterion

Also shown in the figure is Tresca's maximum shear stress criterion (dashed line). Observe that Tresca's yield surface is circumscribed by von Mises'. Therefore, it predicts plastic yielding already for stress states that are still elastic according to the von Mises criterion. As a model for plastic material behavior, Tresca's criterion is therefore more conservative.

Chapter 3

Stress (Mechanics)

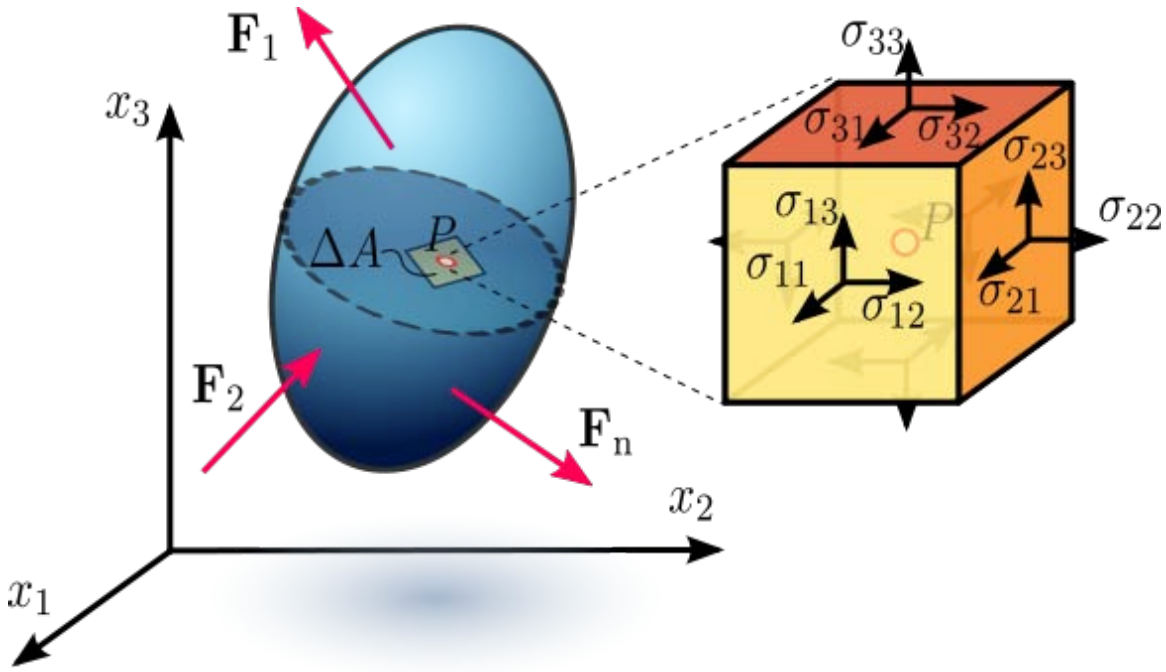

Figure 1.1 Stress in a loaded deformable material body assumed as a continuum.

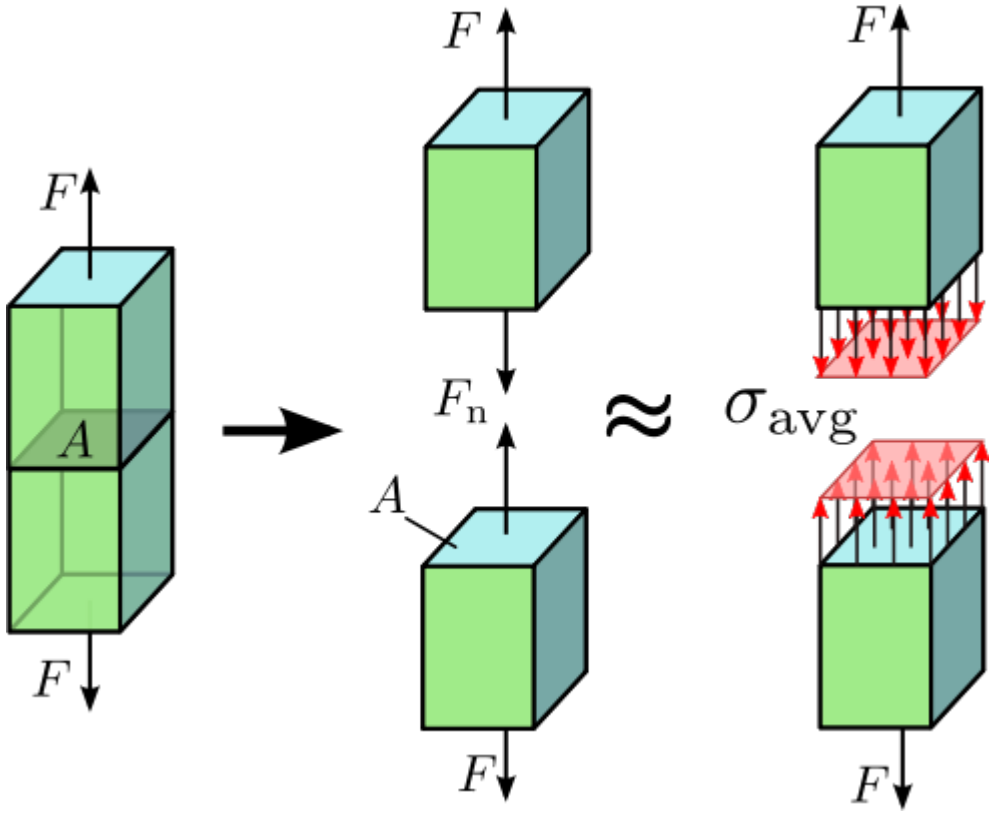

Figure 1.2 Axial stress in a prismatic bar axially loaded

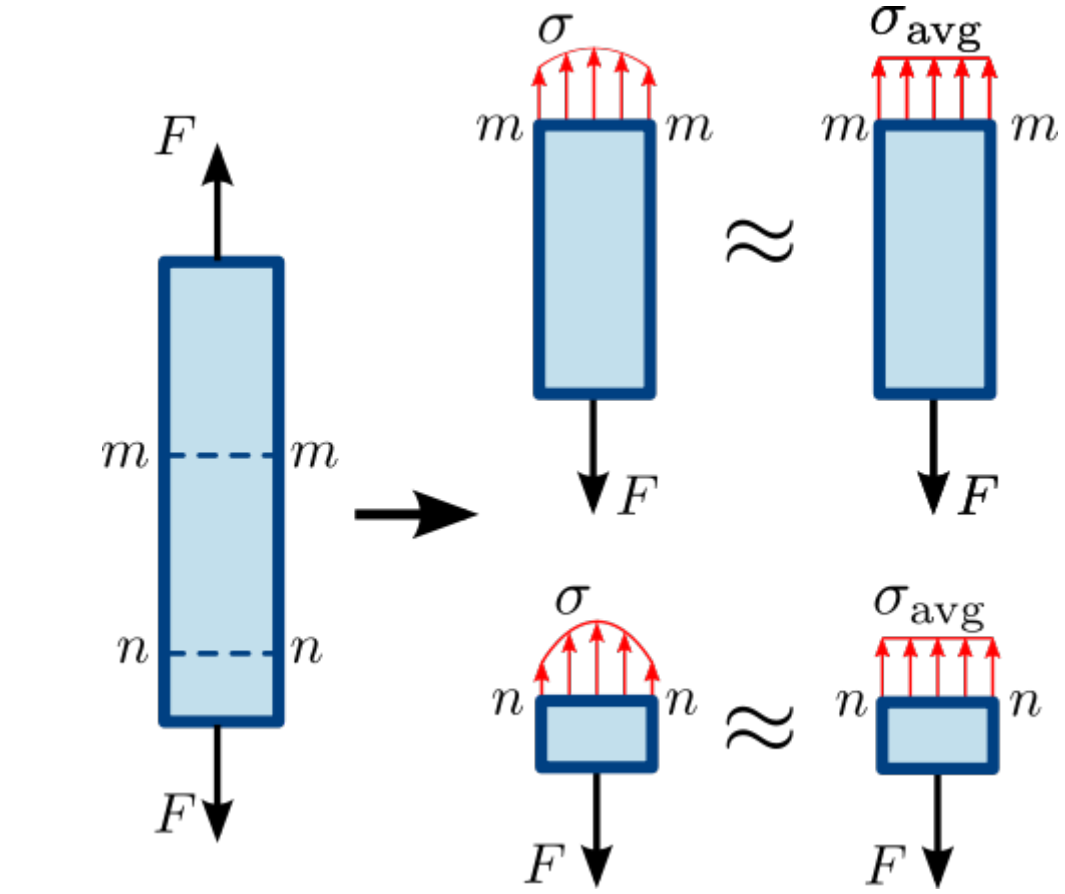

Figure 1.3 Normal stress in a prismatic (straight member of uniform cross-sectional area) bar. The stress or force distribution in the cross section of the bar is not necessarily uniform. However, an average normal stress σ_{avg} can be used

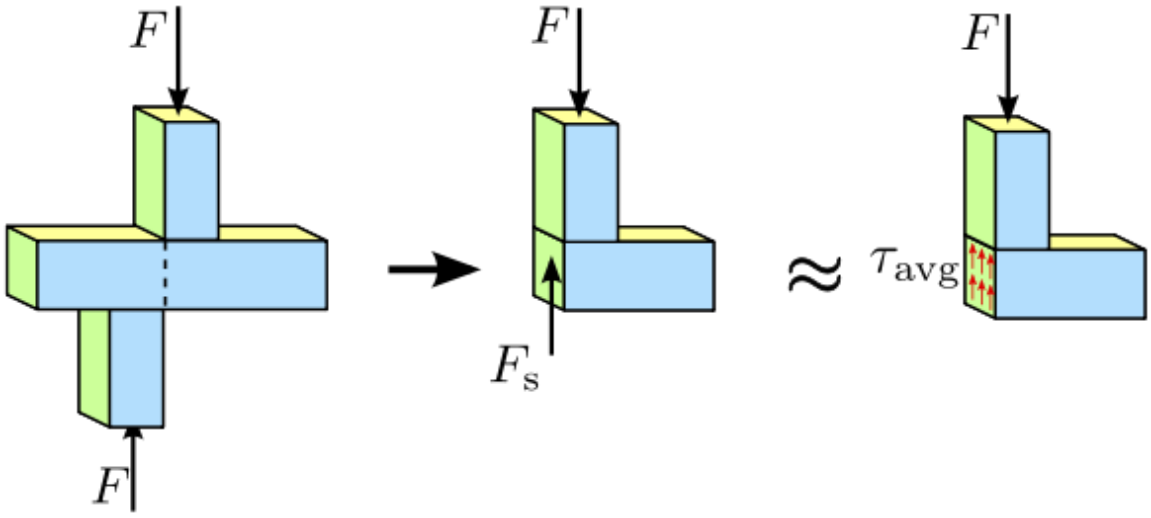

Figure 1.4 Shear stress in a prismatic bar. The stress or force distribution in the cross section of the bar is not necessarily uniform. Nevertheless, an average shear stress τ_{avg} is a reasonable approximation.

In continuum mechanics, **stress** is a measure of the internal forces acting within a deformable body. Quantitatively, it is a measure of the average force per unit area of a surface within the body on which internal forces act. These internal forces are produced between the particles in the body as a reaction to external forces applied on the body. Because the loaded deformable body is assumed to behave as a continuum, these internal forces are distributed continuously within the volume of the material body, and result in deformation of the body's shape. Beyond certain limits of material strength, this can lead to a permanent change of shape or physical failure.

However, treating physical force as a "one dimensional entity", as it is often done in mechanics, creates a few problems. Any model of continuum mechanics which explicitly expresses force as a variable generally fails to merge and describe deformation of matter and solid bodies, because the attributes of matter and solids are three dimensional. Classical models of continuum mechanics assume an average force and fail to properly incorporate "geometrical factors", which are important to describe stress distribution and accumulation of energy during the continuum.

The dimension of stress is that of pressure, and therefore the SI unit for stress is the pascal (symbol Pa), which is equivalent to one newton (force) per square meter (unit area), that is N/m^2. In Imperial units, stress is measured in pound-force per square inch, which is abbreviated as psi.

Introduction

Stress is a measure of the average force per unit area of a surface within a deformable body on which internal forces act. It is a measure of the intensity of the internal forces acting between particles of a deformable body across imaginary internal surfaces. These internal forces are produced between the particles in the body as a reaction to external forces applied on the body. External forces are either surface forces or body forces. Because the loaded deformable body is assumed to behave as a continuum, these internal forces are distributed continuously within the volume of the material body, *i.e.* the stress distribution in the body is expressed as a piecewise continuous function of space coordinates and time.

Normal , shear stresses and virial stresses

For the simple case of a body axially loaded, e.g., a prismatic bar subjected to tension or compression by a force passing through its centroid (Figures 1.2 and 1.3) the stress σ, or intensity of internal forces, can be obtained by dividing the total *normal force* F_{n}, determined from the equilibrium of forces, by the cross-sectional area A of the prism it is acting upon. The normal force can be a *tensile force* if acting outward from the plane, or *compressive force* if acting inward to the plane. In the case of a prismatic bar axially loaded, the stress σ is represented by a scalar called *engineering stress* or *nominal stress* that represents an average stress (σ_{avg}) over the area, meaning that the stress in the cross section is uniformly distributed. Thus, we have

$$\sigma_{\mathrm{avg}} = \frac{F_{\mathrm{n}}}{A} \approx \sigma$$

A different type of stress is obtained when transverse forces F are applied to the prismatic bar as shown in Figure 1.4. Considering the same cross-section as before, from static equilibrium the internal force has a magnitude equal to F_{s} and in opposite direction parallel to the cross-section. F_{s} is called the *shear force*. Dividing the shear force F_{s} by the area A of the cross section we obtain the *shear stress*. In this case the shear stress τ is a scalar quantity representing an average shear stress (τ_{avg}) in the section, *i.e.* the stress in the cross-section is uniformly distributed. In materials science and in engineering aspects the average of the ""scalar"" shear force (τ_{avg}) are true for crystallized materials during brittle fracture and operates through the fractured cross-section or stress plane.

$$\tau_{\mathrm{avg}} = \frac{F_{\mathrm{s}}}{A} \approx \tau$$

In Figure 1.3, the normal stress is observed in two planes $m - m$ and $n - n$ of the axially loaded prismatic bar. The stress on plane $n - n$, which is closer to the point of application of the load F, varies more across the cross-section than that of plane $m - m$. However, if the cross-sectional area of the bar is very small, *i.e.* the bar is slender, the variation of stress across the area is small and the normal stress can be approximated by σ_{avg}. On the other hand, the variation of shear stress across the section of a prismatic bar cannot be assumed to be uniform.

Virial stress is a measure of stress on an atomic scale. It is given by

$$\tau_{ij} = \frac{1}{\Omega} \sum_{k \in \Omega} \left(-m^{(k)} (u_i^{(k)} - \bar{u}_i)(u_j^{(k)} - \bar{u}_j) + \frac{1}{2} \sum_{\ell \in \Omega} (x_i^{(\ell)} - x_i^{(k)}) f_j^{(k\ell)} \right)$$

where

- k and ℓ are atoms in the domain,
- Ω is the volume of the domain,
- $m^{(k)}$ is the mass of atom k,
- $u_i^{(k)}$ is the i^{th} component of the velocity of atom k,
- $\bar{u}_j$ is the j^{th} component of the average velocity of atoms in the volume,
- $x_i^{(k)}$ is the i^{th} component of the position of atom k, and
- $f_i^{(k\ell)}$ is the i^{th} component of the force between atom k and ℓ.

At zero kelvin, all velocities are zero so we have

$$\tau_{ij} = \frac{1}{2\Omega} \sum_{k,\ell \in \Omega} (x_i^{(\ell)} - x_i^{(k)}) f_j^{(k\ell)}$$

.

This can be thought of as follows. The τ_{11} component of stress is the force in the 1 direction divided by the area of a plane perpendicular to that direction. Consider two adjacent volumes separated by such a plane. The 11-component of stress on that interface is the sum of all pairwise forces between atoms on the two sides....

Stress modeling (Cauchy)

In general, stress is not uniformly distributed over the cross-section of a material body, and consequently the stress at a point in a given region is different from the average stress over the entire area. Therefore, it is necessary to define the stress not over a given area but at a specific point in the body (Figure 1.1). According to Cauchy, the *stress at any point* in an object, assumed to behave as a continuum, is completely defined by the nine components σ_{ij} of a second-order tensor of type (0,2) known as the Cauchy stress tensor, $\boldsymbol{\sigma}$:

$$\boldsymbol{\sigma} = \begin{bmatrix} \sigma_{11} & \sigma_{12} & \sigma_{13} \\ \sigma_{21} & \sigma_{22} & \sigma_{23} \\ \sigma_{31} & \sigma_{32} & \sigma_{33} \end{bmatrix} \equiv \begin{bmatrix} \sigma_{xx} & \sigma_{xy} & \sigma_{xz} \\ \sigma_{yx} & \sigma_{yy} & \sigma_{yz} \\ \sigma_{zx} & \sigma_{zy} & \sigma_{zz} \end{bmatrix} \equiv \begin{bmatrix} \sigma_x & \tau_{xy} & \tau_{xz} \\ \tau_{yx} & \sigma_y & \tau_{yz} \\ \tau_{zx} & \tau_{zy} & \sigma_z \end{bmatrix}$$

The Cauchy stress tensor obeys the tensor transformation law under a change in the system of coordinates. A graphical representation of this transformation law is the Mohr's circle of stress distribution.

The Cauchy stress tensor is used for stress analysis of material bodies experiencing small deformations where the differences in stress distribution in most cases can be neglected. For large deformations, also called finite deformations, other measures of stress, such as the first and second Piola-Kirchhoff stress tensors, the Biot stress tensor, and the Kirchhoff stress tensor, are required.

According to the principle of conservation of linear momentum, if a continuous body is in static equilibrium it can be demonstrated that the components of the Cauchy stress tensor in every material point in the body satisfy the equilibrium equations (Cauchy's equations of motion for zero acceleration). At the same time, according to the principle of conservation of angular momentum, equilibrium requires that the summation of moments with respect to an arbitrary point is zero, which leads to the conclusion that the stress tensor is symmetric, thus having only six independent stress components instead of the original nine.

There are certain invariants associated with the stress tensor, whose values do not depend upon the coordinate system chosen or the area element upon which the stress tensor operates. These are the three eigenvalues of the stress tensor, which are called the principal stresses. Solids, liquids, and gases have stress fields. Static fluids support normal stress but will flow under shear stress. Moving viscous fluids can support shear stress (dynamic pressure). Solids can support both shear and normal stress, with ductile materials failing under shear and brittle materials failing under normal stress. All materials have temperature dependent variations in stress-related properties, and non-Newtonian materials have rate-dependent variations.

Stress analysis

Stress analysis means the determination of the internal distribution of stresses in a structure. It is needed in engineering for the study and design of structures such as tunnels, dams, mechanical parts, and structural frames, under prescribed or expected loads. To determine the distribution of stress in a structure, the engineer needs to solve a boundary-value problem by specifying the boundary conditions. These are displacements and forces on the boundary of the structure.

Constitutive equations, such as Hooke's Law for linear elastic materials, describe the stress-strain relationship in these calculations.

When a structure is expected to deform elastically (and resume its original shape), a boundary-value problem based on the theory of elasticity is applied, with infinitesimal strains, under design loads.

When the applied loads permanently deform the structure, the theory of plasticity is used.

The stress analysis can be simplified when the physical dimensions and the distribution of loads allow the structure to be treated as one-dimensional or two-dimensional. For a two-dimensional analysis a plane stress or a plane strain condition can be assumed. Alternatively, experimental determination of stresses can be carried out.

Approximate computer-based solutions for boundary-value problems can be obtained through numerical methods such as the Finite Element Method, the Finite Difference Method, and the Boundary Element Method. Analytical or closed-form solutions can be obtained for simple geometries, constitutive relations, and boundary conditions.

Theoretical background

Continuum mechanics deals with deformable bodies, as opposed to rigid bodies. The stresses considered in continuum mechanics are only those produced by deformation of the body, *sc.* only relative changes in stress are considered, not the absolute values. A body is considered stress-free if the only forces present are those inter-atomic forces (ionic, metallic, and van der Waals forces) required to hold the body together and to keep its shape in the absence of all external influences, including gravitational attraction.

Stresses generated during manufacture of the body to a specific configuration are also excluded.

Following the classical dynamics of Newton and Euler, the motion of a material body is produced by the action of externally applied forces which are assumed to be of two kinds: surface forces and body forces.

Surface forces, or contact forces, can act either on the bounding surface of the body, as a result of mechanical contact with other bodies, or on imaginary internal surfaces that bound portions of the body, as a result of the mechanical interaction between the parts of the body to either side of the surface (Euler-Cauchy's stress principle). When a body is acted upon by external contact forces, internal contact forces are then transmitted from point to point inside the body to balance their action, according to Newton's second law of motion of conservation of linear momentum and angular momentum (for continuous bodies these laws are called the Euler's equations of motion). The internal contact forces are related to the body's deformation through constitutive equations.

The concept of stress can then be thought as a measure of the intensity of the internal contact forces acting between particles of the body across imaginary internal surfaces. In other words, stress is a measure of the average quantity of force exerted per unit area of the surface on which these internal forces act. The intensity of contact forces is related, specifically in an inverse proportion, to the area of contact. For example, if a force applied to a small area is compared to a distributed load of the same resultant magnitude applied to a larger area, one finds that the effects or intensities of these two forces are locally different because the stresses are not the same.

Body forces are forces originating from sources outside of the body that act on the volume (or mass) of the body. Saying that body forces are due to outside sources implies that the *internal forces* are manifested through the contact forces alone. These forces arise from the presence of the body in force fields, (*e.g.*, a gravitational field). As the mass of a continuous body is assumed to be continuously distributed, any force originating from the mass is also continuously distributed. Thus, body forces are assumed to be continuous over the entire volume of the body.

The density of internal forces at every point in a deformable body are not necessarily equal, *i.e.* there is a distribution of stresses throughout the body. This variation of internal forces throughout the body is governed by Newton's second law of motion of conservation of linear momentum and angular momentum, which normally are applied to a mass particle but are extended in continuum mechanics to a body of continuously distributed mass. For continuous bodies these laws are called Euler’s equations of motion. If a body is represented as an assemblage of discrete particles, each governed by Newton’s laws of motion, then Euler’s equations can be derived from Newton’s laws. Euler’s equations can, however, be taken as axioms describing the laws of motion for extended bodies, independently of any particle structure.

Euler–Cauchy stress principle

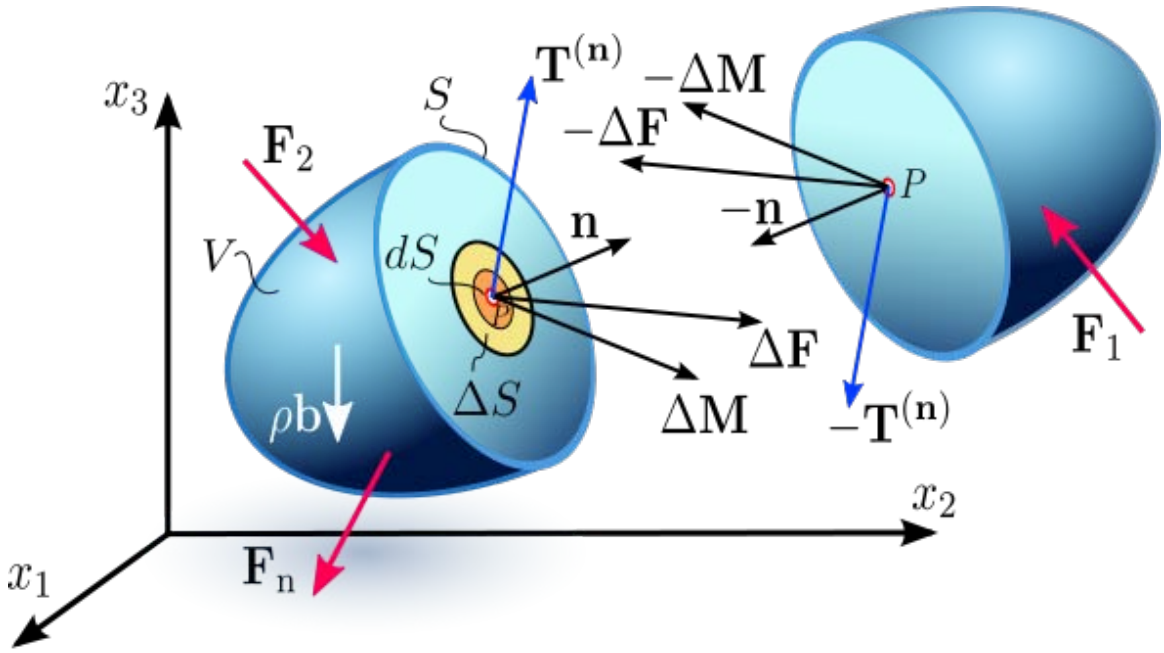

Figure 2.1a Internal distribution of contact forces and couple stresses on a differential dS of the internal surface S in a continuum, as a result of the interaction between the two portions of the continuum separated by the surface

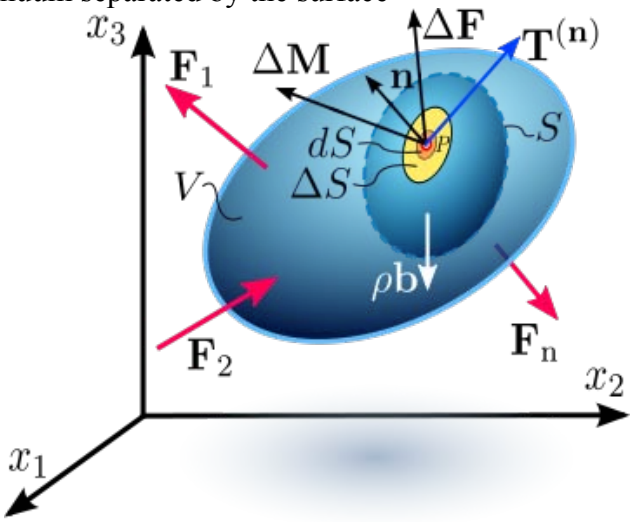

Figure 2.1b Internal distribution of contact forces and couple stresses on a differential dS of the internal surface S in a continuum, as a result of the interaction between the two portions of the continuum separated by the surface

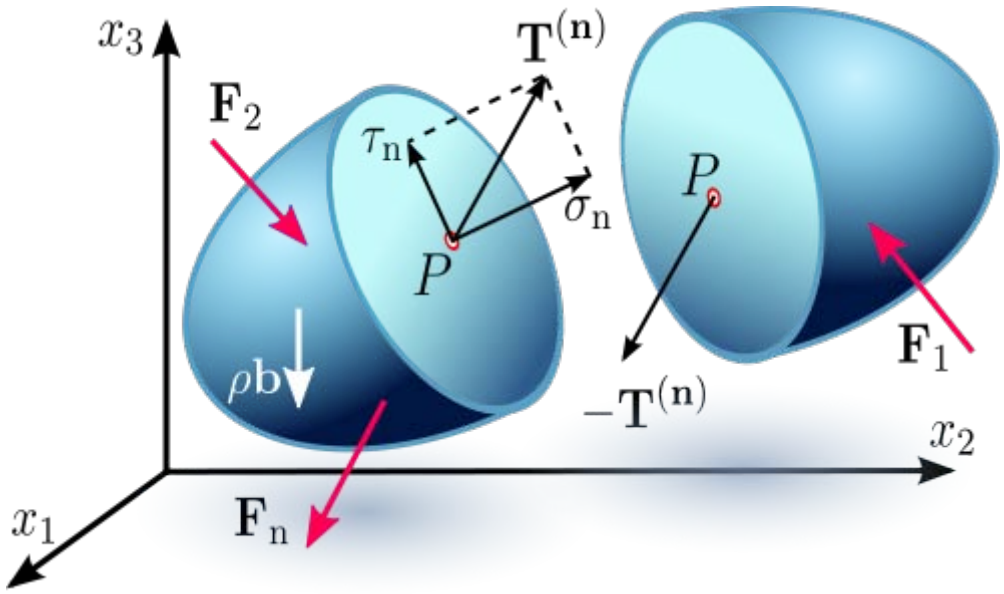

Figure 2.1c Stress vector on an internal surface S with normal vector n. Depending on the orientation of the plane under consideration, the stress vector may not necessarily be perpendicular to that plane, *i.e.* parallel to $\mathbf{n}$, and can be resolved into two components: one component normal to the plane, called *normal stress* σ_{n}, and another component parallel to this plane, called the *shearing stress* τ.

The Euler–Cauchy stress principle states that *upon any surface (real or imaginary) that divides the body, the action of one part of the body on the other is equivalent (equipollent) to the system of distributed forces and couples on the surface dividing the body*, and it is represented by a vector field $\mathbf{T}^{(\mathbf{n})}$, called the stress vector, defined on the surface S and assumed to depend continuously on the surface's unit vector $\mathbf{n}$.

To explain this principle, we consider an imaginary surface S passing through an internal material point P dividing the continuous body into two segments, as seen in Figure 2.1a or 2.1b (some authors use the cutting plane diagram and others use the diagram with the arbitrary volume inside the continuum enclosed by the surface S). The body is subjected to external surface forces $\mathbf{F}$ and body forces $\mathbf{b}$. The internal contact forces being transmitted from one segment to the other through the dividing plane, due to the action of one portion of the continuum onto the other, generate a force distribution on a small area ΔS, with a normal unit vector $\mathbf{n}$, on the dividing plane S. The force distribution is equipollent to a contact force $\Delta\mathbf{F}$ and a couple stress $\Delta\mathbf{M}$, as shown in Figure 2.1a and 2.1b. Cauchy's stress principle asserts that as ΔS becomes very small and tends to zero the ratio $\Delta\mathbf{F}/\Delta S$ becomes $\mathrm{d}\mathbf{F}/\mathrm{d}S$ and the couple stress vector $\Delta\mathbf{M}$ vanishes. In specific fields of continuum mechanics the couple stress is assumed not to vanish; however, as stated previously, in classical branches of continuum mechanics we deal with non-polar materials which do not consider couple stresses and body moments. The resultant vector $\mathrm{d}\mathbf{F}/\mathrm{d}S$ is defined as the *stress vector* or *traction vector* given by $\mathbf{T}^{(\mathbf{n})} = T_{\mathrm{i}}^{(\mathbf{n})}\,\mathbf{e}_{\mathrm{i}}$ at the point P associated with a plane with a normal vector $\mathbf{n}$:

$$T_i^{(\mathbf{n})} = \lim_{\Delta S \to 0} \frac{\Delta F_i}{\Delta S} = \frac{dF_i}{dS}.$$

This equation means that the stress vector depends on its location in the body and the orientation of the plane on which it is acting.

Depending on the orientation of the plane under consideration, the stress vector may not necessarily be perpendicular to that plane, *i.e.* parallel to **n**, and can be resolved into two components:

- one normal to the plane, called *normal stress*

  $$\sigma_{\mathrm{n}} = \lim_{\Delta S \to 0} \frac{\Delta F_{\mathrm{n}}}{\Delta S} = \frac{dF_{\mathrm{n}}}{dS},$$
  where $\mathrm{d}F_{\mathrm{n}}$ is the normal component of the force d**F** to the differential area d*S*

- and the other parallel to this plane, called the *shear stress*

  $$\tau = \lim_{\Delta S \to 0} \frac{\Delta F_{\mathrm{s}}}{\Delta S} = \frac{dF_{\mathrm{s}}}{dS},$$
  where $\mathrm{d}F_{\mathrm{s}}$ is the tangential component of the force d**F** to the differential surface area d*S*. The shear stress can be further decomposed into two mutually perpendicular vectors.

Cauchy's postulate

According to the *Cauchy Postulate*, the stress vector $\mathbf{T}^{(\mathbf{n})}$ remains unchanged for all surfaces passing through the point *P* and having the same normal vector **n** at *P*, *i.e.* having a common tangent at *P*. This means that the stress vector is a function of the normal vector **n** only, and it is not influenced by the curvature of the internal surfaces.

Cauchy's fundamental lemma

A consequence of Cauchy's postulate is *Cauchy's Fundamental Lemma*, also called the *Cauchy reciprocal theorem*, which states that the stress vectors acting on opposite sides of the same surface are equal in magnitude and opposite in direction. Cauchy's fundamental lemma is equivalent to Newton's third law of motion of action and reaction, and it is expressed as

$$-\mathbf{T}^{(\mathbf{n})} = \mathbf{T}^{(-\mathbf{n})}.$$

Cauchy's stress theorem – stress tensor

The state of stress at a point in the body is then defined by all the stress vectors $\mathbf{T}^{(\mathbf{n})}$ associated with all planes (infinite in number) that pass through that point. However,

according to *Cauchy's fundamental theorem*, also called *Cauchy's stress theorem*, merely by knowing the stress vectors on three mutually perpendicular planes, the stress vector on any other plane passing through that point can be found through coordinate transformation equations.

Cauchy's stress theorem states that there exists a second-order tensor field **σ**(**x**, t), called the *Cauchy stress tensor*, independent of **n**, such that **T** is a linear function of **n**:

$$\mathbf{T}^{(\mathbf{n})} = \boldsymbol{\sigma} \cdot \mathbf{n} \quad \text{or} \quad T_j^{(n)} = \sigma_{ij} n_i.$$

This equation implies that the stress vector $\mathbf{T}^{(\mathbf{n})}$ at any point *P* in a continuum associated with a plane with normal vector **n** can be expressed as a function of the stress vectors on the planes perpendicular to the coordinate axes, *i.e.* in terms of the components σ_{ij} of the stress tensor **σ**.

To prove this expression, consider a tetrahedron with three faces oriented in the coordinate planes, and with an infinitesimal area d*A* oriented in an arbitrary direction specified by a normal vector **n** (Figure 2.2). The tetrahedron is formed by slicing the infinitesimal element along an arbitrary plane **n**. The stress vector on this plane is denoted by $\mathbf{T}^{(\mathbf{n})}$. The stress vectors acting on the faces of the tetrahedron are denoted as $\mathbf{T}^{(\mathbf{e}_1)}$, $\mathbf{T}^{(\mathbf{e}_2)}$, and $\mathbf{T}^{(\mathbf{e}_3)}$, and are by definition the components σ_{ij} of the stress tensor **σ**. This tetrahedron is sometimes called the *Cauchy tetrahedron*. From equilibrium of forces, *i.e.* Euler's first law of motion (Newton's second law of motion), we have

$$\mathbf{T}^{(\mathbf{n})}\, dA - \mathbf{T}^{(\mathbf{e}_1)}\, dA_1 - \mathbf{T}^{(\mathbf{e}_2)}\, dA_2 - \mathbf{T}^{(\mathbf{e}_3)}\, dA_3 = \rho \left(\frac{h}{3} dA \right) \mathbf{a},$$

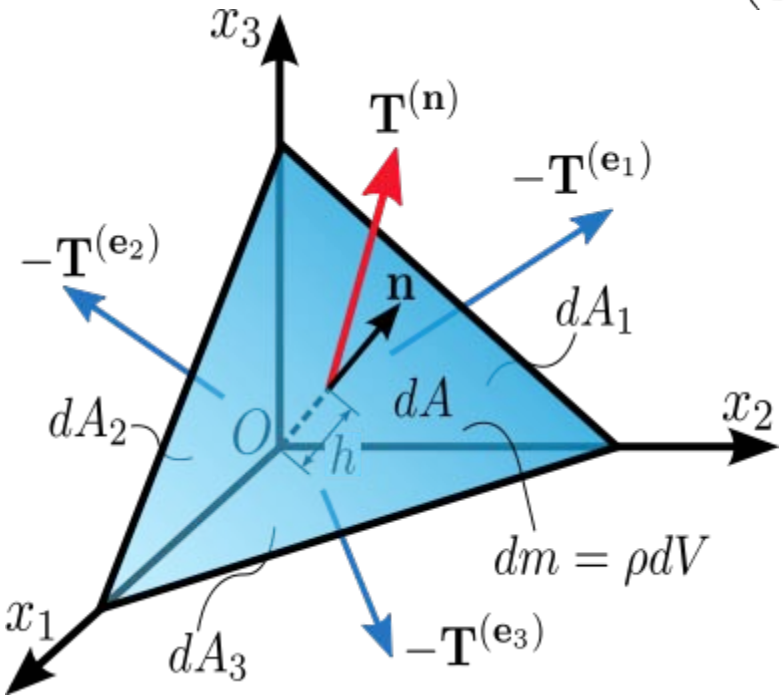

Figure 2.2. Stress vector acting on a plane with normal vector **n**.
A note on the sign convention: The tetrahedron is formed by slicing a parallelepiped along an arbitrary plane **n**. So, the force acting on the plane **n** is the reaction exerted by the other half of the parallelepiped and has an opposite sign.

where the right-hand-side of the equation represents the product of the mass enclosed by the tetrahedron and its acceleration: ρ is the density, **a** is the acceleration, and h is the height of the tetrahedron, considering the plane **n** as the base. The area of the faces of the tetrahedron perpendicular to the axes can be found by projecting dA into each face (using the dot product):

$$\begin{aligned} dA_1 &= (\mathbf{n} \cdot \mathbf{e}_1)\, dA = n_1\, dA, \\ dA_2 &= (\mathbf{n} \cdot \mathbf{e}_2)\, dA = n_2\, dA, \\ dA_3 &= (\mathbf{n} \cdot \mathbf{e}_3)\, dA = n_3\, dA, \end{aligned}$$

and then substituting into the equation to cancel out dA:

$$\mathbf{T}^{(\mathbf{n})} - \mathbf{T}^{(\mathbf{e}_1)} n_1 - \mathbf{T}^{(\mathbf{e}_2)} n_2 - \mathbf{T}^{(\mathbf{e}_3)} n_3 = \rho \left(\frac{h}{3}\right) \mathbf{a}.$$

To consider the limiting case as the tetrahedron shrinks to a point, h must go to 0 (intuitively, the plane **n** is translated along **n** toward O). As a result, the right-hand-side of the equation approaches 0, so

$$\mathbf{T}^{(\mathbf{n})} = \mathbf{T}^{(\mathbf{e}_1)} n_1 + \mathbf{T}^{(\mathbf{e}_2)} n_2 + \mathbf{T}^{(\mathbf{e}_3)} n_3.$$

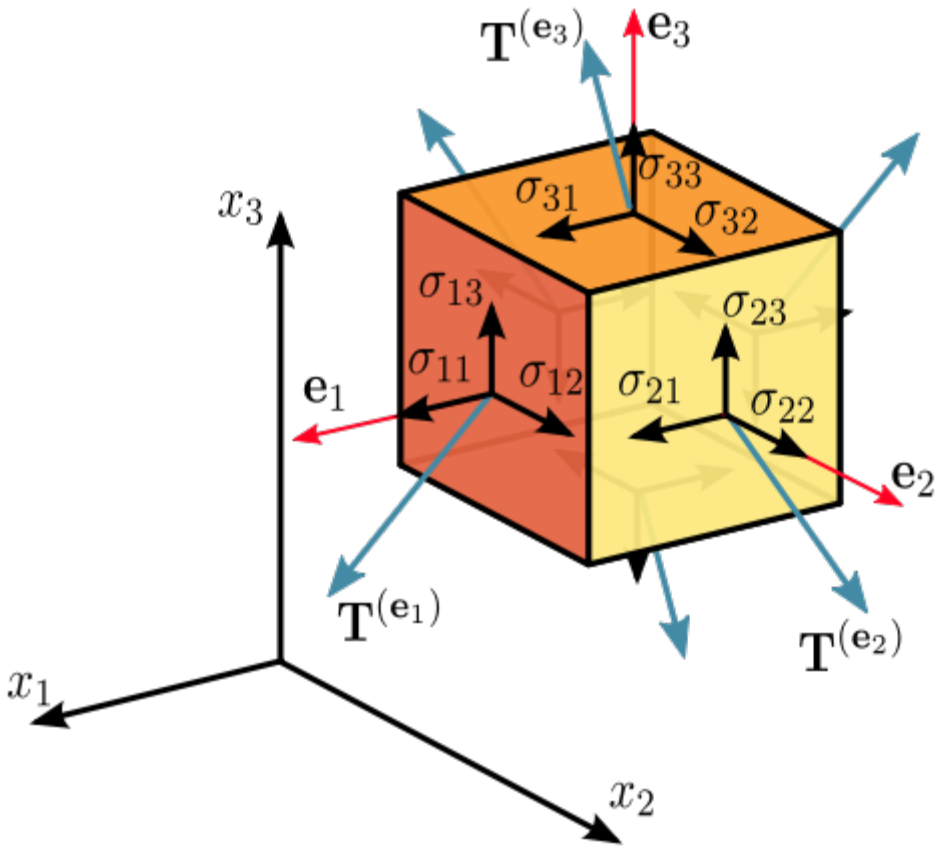

Figure 2.3 Components of stress in three dimensions

Assuming a material element (Figure 2.3) with planes perpendicular to the coordinate axes of a Cartesian coordinate system, the stress vectors associated with each of the element planes, *i.e.* $\mathbf{T}^{(\mathbf{e}_1)}$, $\mathbf{T}^{(\mathbf{e}_2)}$, and $\mathbf{T}^{(\mathbf{e}_3)}$ can be decomposed into a normal component and two shear components, *i.e.* components in the direction of the three coordinate axes. For the particular case of a surface with normal unit vector oriented in the direction of the x_1-axis, the normal stress is denoted by σ_{11}, and the two shear stresses are denoted as σ_{12} and σ_{13}:

$$\begin{aligned}
\mathbf{T}^{(\mathbf{e}_1)} &= T_1^{(\mathbf{e}_1)}\mathbf{e}_1 + T_2^{(\mathbf{e}_1)}\mathbf{e}_2 + T_3^{(\mathbf{e}_1)}\mathbf{e}_3 = \sigma_{11}\mathbf{e}_1 + \sigma_{12}\mathbf{e}_2 + \sigma_{13}\mathbf{e}_3, \\
\mathbf{T}^{(\mathbf{e}_2)} &= T_1^{(\mathbf{e}_2)}\mathbf{e}_1 + T_2^{(\mathbf{e}_2)}\mathbf{e}_2 + T_3^{(\mathbf{e}_2)}\mathbf{e}_3 = \sigma_{21}\mathbf{e}_1 + \sigma_{22}\mathbf{e}_2 + \sigma_{23}\mathbf{e}_3, \\
\mathbf{T}^{(\mathbf{e}_3)} &= T_1^{(\mathbf{e}_3)}\mathbf{e}_1 + T_2^{(\mathbf{e}_3)}\mathbf{e}_2 + T_3^{(\mathbf{e}_3)}\mathbf{e}_3 = \sigma_{31}\mathbf{e}_1 + \sigma_{32}\mathbf{e}_2 + \sigma_{33}\mathbf{e}_3,
\end{aligned}$$

In index notation this is

$$\mathbf{T}^{(\mathbf{e}_i)} = T_j^{(\mathbf{e}_i)}\mathbf{e}_j = \sigma_{ij}\mathbf{e}_j.$$

The nine components σ_{ij} of the stress vectors are the components of a second-order Cartesian tensor called the *Cauchy stress tensor*, which completely defines the state of stress at a point and is given by

$$\boldsymbol{\sigma} = \sigma_{ij} = \begin{bmatrix} \mathbf{T}^{(\mathbf{e}_1)} \\ \mathbf{T}^{(\mathbf{e}_2)} \\ \mathbf{T}^{(\mathbf{e}_3)} \end{bmatrix} = \begin{bmatrix} \sigma_{11} & \sigma_{12} & \sigma_{13} \\ \sigma_{21} & \sigma_{22} & \sigma_{23} \\ \sigma_{31} & \sigma_{32} & \sigma_{33} \end{bmatrix} \equiv \begin{bmatrix} \sigma_{xx} & \sigma_{xy} & \sigma_{xz} \\ \sigma_{yx} & \sigma_{yy} & \sigma_{yz} \\ \sigma_{zx} & \sigma_{zy} & \sigma_{zz} \end{bmatrix} \equiv \begin{bmatrix} \sigma_x & \tau_{xy} & \tau_{xz} \\ \tau_{yx} & \sigma_y & \tau_{yz} \\ \tau_{zx} & \tau_{zy} & \sigma_z \end{bmatrix},$$

where σ_{11}, σ_{22}, and σ_{33} are normal stresses, and σ_{12}, σ_{13}, σ_{21}, σ_{23}, σ_{31}, and σ_{32} are shear stresses. The first index i indicates that the stress acts on a plane normal to the x_i-axis, and the second index j denotes the direction in which the stress acts. A stress component is positive if it acts in the positive direction of the coordinate axes, and if the plane where it acts has an outward normal vector pointing in the positive coordinate direction.

Thus, using the components of the stress tensor

$$\begin{aligned} \mathbf{T}^{(\mathbf{n})} &= \mathbf{T}^{(\mathbf{e}_1)} n_1 + \mathbf{T}^{(\mathbf{e}_2)} n_2 + \mathbf{T}^{(\mathbf{e}_3)} n_3 \\ &= \sum_{i=1}^{3} \mathbf{T}^{(\mathbf{e}_i)} n_i \\ &= \left(\sigma_{ij} \mathbf{e}_j\right) n_i \\ &= \sigma_{ij} n_i \mathbf{e}_j \end{aligned}$$

or, equivalently,

$$T_j^{(\mathbf{n})} = \sigma_{ij} n_i.$$

Alternatively, in matrix form we have

$$\begin{bmatrix} T_1^{(\mathbf{n})} & T_2^{(\mathbf{n})} & T_3^{(\mathbf{n})} \end{bmatrix} = \begin{bmatrix} n_1 & n_2 & n_3 \end{bmatrix} \cdot \begin{bmatrix} \sigma_{11} & \sigma_{12} & \sigma_{13} \\ \sigma_{21} & \sigma_{22} & \sigma_{23} \\ \sigma_{31} & \sigma_{32} & \sigma_{33} \end{bmatrix}.$$

The Voigt notation representation of the Cauchy stress tensor takes advantage of the symmetry of the stress tensor to express the stress as a six-dimensional vector of the form:

$$\boldsymbol{\sigma} = \begin{bmatrix} \sigma_1 & \sigma_2 & \sigma_3 & \sigma_4 & \sigma_5 & \sigma_6 \end{bmatrix}^T \equiv \begin{bmatrix} \sigma_{11} & \sigma_{22} & \sigma_{33} & \sigma_{23} & \sigma_{31} & \sigma_{12} \end{bmatrix}^T.$$

The Voigt notation is used extensively in representing stress-strain relations in solid mechanics and for computational efficiency in numerical structural mechanics software.

Transformation rule of the stress tensor

It can be shown that the stress tensor is a contravariant second order tensor, which is a statement of how it transforms under a change of the coordinate system. From an x_i-system to an x_i'-system, the components σ_{ij} in the initial system are transformed into the components σ_{ij}' in the new system according to the tensor transformation rule (Figure 2.4):

$$\sigma'_{ij} = a_{im}a_{jn}\sigma_{mn} \quad \text{or} \quad \boldsymbol{\sigma}' = \mathbf{A}\boldsymbol{\sigma}\mathbf{A}^T,$$

where **A** is a rotation matrix with components a_{ij}. In matrix form this is

$$\begin{bmatrix} \sigma'_{11} & \sigma'_{12} & \sigma'_{13} \\ \sigma'_{21} & \sigma'_{22} & \sigma'_{23} \\ \sigma'_{31} & \sigma'_{32} & \sigma'_{33} \end{bmatrix} = \begin{bmatrix} a_{11} & a_{12} & a_{13} \\ a_{21} & a_{22} & a_{23} \\ a_{31} & a_{32} & a_{33} \end{bmatrix} \begin{bmatrix} \sigma_{11} & \sigma_{12} & \sigma_{13} \\ \sigma_{21} & \sigma_{22} & \sigma_{23} \\ \sigma_{31} & \sigma_{32} & \sigma_{33} \end{bmatrix} \begin{bmatrix} a_{11} & a_{21} & a_{31} \\ a_{12} & a_{22} & a_{32} \\ a_{13} & a_{23} & a_{33} \end{bmatrix}.$$

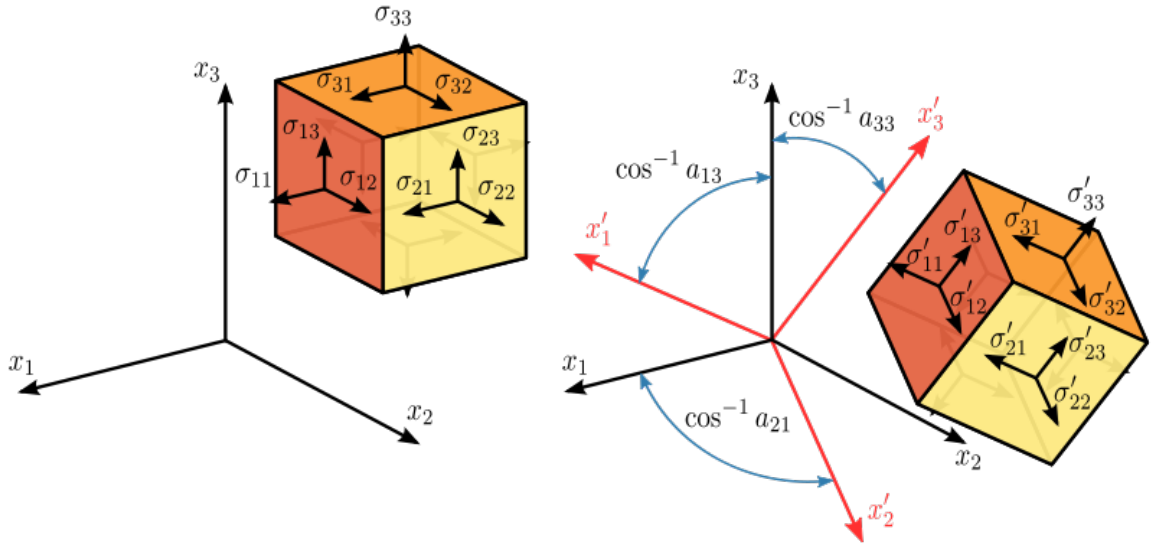

Figure 2.4 Transformation of the stress tensor

Expanding the matrix operation, and simplifying some terms by taking advantage of the symmetry of the stress tensor, gives

$$\begin{aligned}
\sigma'_{11} &= a_{11}^2\sigma_{11} + a_{12}^2\sigma_{22} + a_{13}^2\sigma_{33} + 2a_{11}a_{12}\sigma_{12} + 2a_{11}a_{13}\sigma_{13} + 2a_{12}a_{13}\sigma_{23}, \\
\sigma'_{22} &= a_{21}^2\sigma_{11} + a_{22}^2\sigma_{22} + a_{23}^2\sigma_{33} + 2a_{21}a_{22}\sigma_{12} + 2a_{21}a_{23}\sigma_{13} + 2a_{22}a_{23}\sigma_{23}, \\
\sigma'_{33} &= a_{31}^2\sigma_{11} + a_{32}^2\sigma_{22} + a_{33}^2\sigma_{33} + 2a_{31}a_{32}\sigma_{12} + 2a_{31}a_{33}\sigma_{13} + 2a_{32}a_{33}\sigma_{23}, \\
\sigma'_{12} &= a_{11}a_{21}\sigma_{11} + a_{12}a_{22}\sigma_{22} + a_{13}a_{23}\sigma_{33} \\
&\quad + (a_{11}a_{22} + a_{12}a_{21})\sigma_{12} + (a_{12}a_{23} + a_{13}a_{22})\sigma_{23} + (a_{11}a_{23} + a_{13}a_{21})\sigma_{13},
\end{aligned}$$

$$\begin{aligned}\sigma'_{23} =& a_{21}a_{31}\sigma_{11} + a_{22}a_{32}\sigma_{22} + a_{23}a_{33}\sigma_{33} \\ &+ (a_{21}a_{32} + a_{22}a_{31})\sigma_{12} + (a_{22}a_{33} + a_{23}a_{32})\sigma_{23} + (a_{21}a_{33} + a_{23}a_{31})\sigma_{13}, \\ \sigma'_{13} =& a_{11}a_{31}\sigma_{11} + a_{12}a_{32}\sigma_{22} + a_{13}a_{33}\sigma_{33} \\ &+ (a_{11}a_{32} + a_{12}a_{31})\sigma_{12} + (a_{12}a_{33} + a_{13}a_{32})\sigma_{23} + (a_{11}a_{33} + a_{13}a_{31})\sigma_{13}.\end{aligned}$$

The Mohr circle for stress is a graphical representation of this transformation of stresses.

Normal and shear stresses

The magnitude of the normal stress component σ_n of any stress vector $\mathbf{T}^{(\mathbf{n})}$ acting on an arbitrary plane with normal vector $\mathbf{n}$ at a given point, in terms of the components σ_{ij} of the stress tensor $\boldsymbol{\sigma}$, is the dot product of the stress vector and the normal vector:

$$\begin{aligned}\sigma_{\mathrm{n}} &= \mathbf{T}^{(\mathbf{n})} \cdot \mathbf{n} \\ &= T_i^{(\mathbf{n})} n_i \\ &= \sigma_{ij} n_i n_j.\end{aligned}$$

The magnitude of the shear stress component τ_n, acting in the plane spanned by the two vectors $\mathbf{T}^{(\mathbf{n})}$ and $\mathbf{n}$, can then be found using the Pythagorean theorem:

$$\begin{aligned}\tau_{\mathrm{n}} &= \sqrt{\left(T^{(\mathbf{n})}\right)^2 - \sigma_{\mathrm{n}}^2} \\ &= \sqrt{T_i^{(\mathbf{n})} T_i^{(\mathbf{n})} - \sigma_{\mathrm{n}}^2},\end{aligned}$$

where

$$\left(T^{(\mathbf{n})}\right)^2 = T_i^{(\mathbf{n})} T_i^{(\mathbf{n})} = \left(\sigma_{ij} n_j\right)\left(\sigma_{ik} n_k\right) = \sigma_{ij}\sigma_{ik} n_j n_k.$$

Equilibrium equations and symmetry of the stress tensor

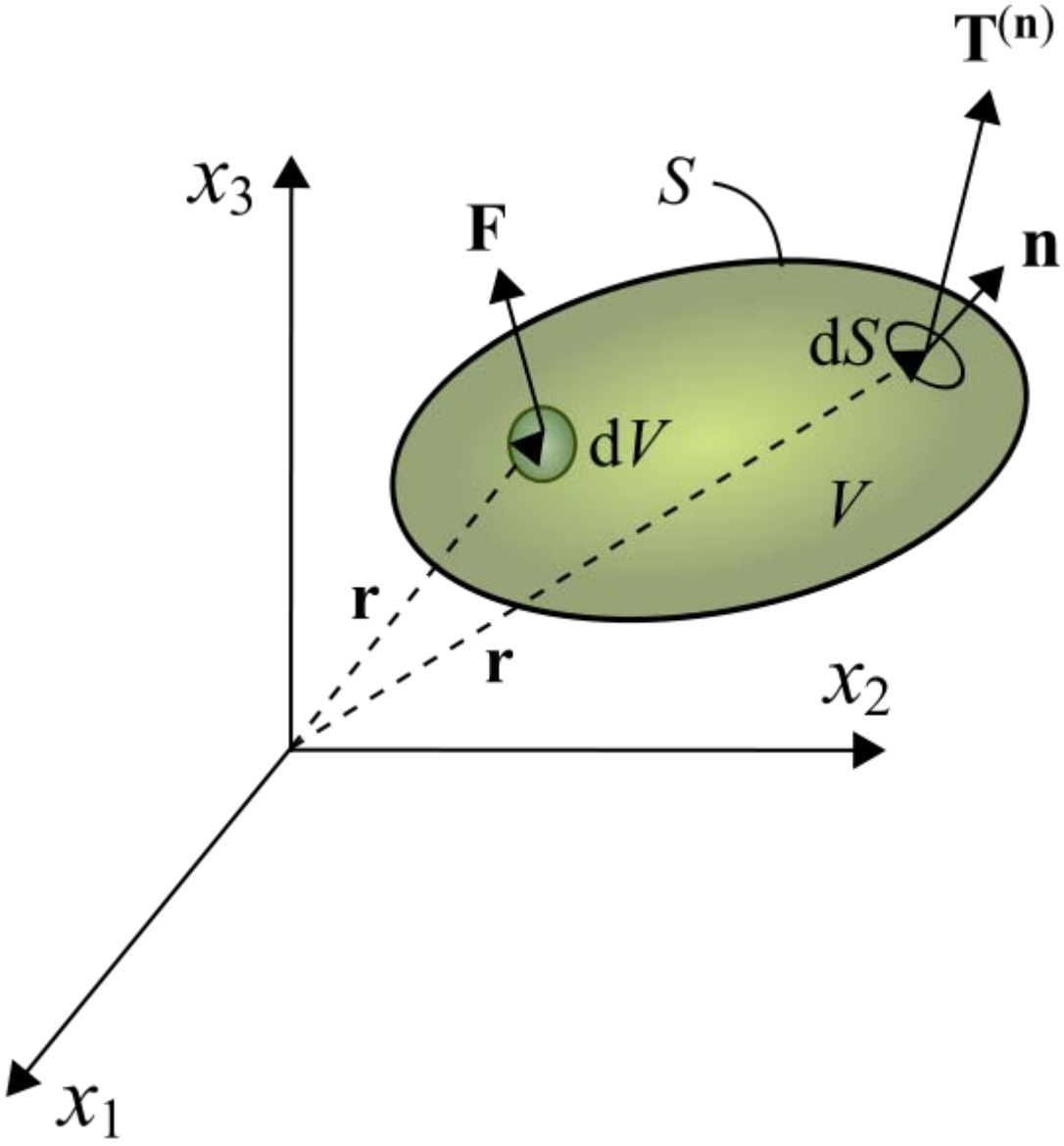

Figure 4. Continuum body in equilibrium

When a body is in equilibrium the components of the stress tensor in every point of the body satisfy the equilibrium equations,

$$\sigma_{ji,j} + F_i = 0$$

For example, for a hydrostatic fluid in equilibrium conditions, the stress tensor takes on the form:

$$\sigma_{ij} = -p\delta_{ij},$$

where *p* is the hydrostatic pressure, and $\delta_{ij}$is the kronecker delta.

At the same time, equilibrium requires that the summation of moments with respect to an arbitrary point is zero, which leads to the conclusion that the stress tensor is symmetric, i.e.

$$\sigma_{ij} = \sigma_{ji}$$

However, in the presence of couple-stresses, i.e. moments per unit volume, the stress tensor is non-symmetric. This also is the case when the Knudsen number is close to one, $K_n \rightarrow 1$, or the continuum is a non-Newtonian fluid, which can lead to rotationally non-invariant fluids, such as polymers.

Principal stresses and stress invariants

At every point in a stressed body there are at least three planes, called *principal planes*, with normal vectors $\mathbf{n}$, called *principal directions*, where the corresponding stress vector is perpendicular to the plane, i.e., parallel or in the same direction as the normal vector $\mathbf{n}$, and where there are no normal shear stresses $\tau_{\mathbf{n}}$. The three stresses normal to these principal planes are called *principal stresses*.

The components $\sigma_{ij}$of the stress tensor depend on the orientation of the coordinate system at the point under consideration. However, the stress tensor itself is a physical quantity and as such, it is independent of the coordinate system chosen to represent it. There are certain invariants associated with every tensor which are also independent of the coordinate system. For example, a vector is a simple tensor of rank one. In three dimensions, it has three components. The value of these components will depend on the coordinate system chosen to represent the vector, but the length of the vector is a physical quantity (a scalar) and is independent of the coordinate system chosen to represent the vector. Similarly, every second rank tensor (such as the stress and the strain tensors) has three independent invariant quantities associated with it. One set of such invariants are the principal stresses of the stress tensor, which are just the eigenvalues of the stress tensor. Their direction vectors are the principal directions or eigenvectors.

A stress vector parallel to the normal vector $\mathbf{n}$is given by:

$$\mathbf{T}^{(\mathbf{n})} = \lambda \mathbf{n} = \sigma_{\mathbf{n}} \mathbf{n}$$

where $\lambda$is a constant of proportionality, and in this particular case corresponds to the magnitudes $\sigma_{\mathrm{n}}$of the normal stress vectors or principal stresses.

Knowing that $T_i^{(n)} = \sigma_{ij} n_j$and $n_i = \delta_{ij} n_j$, we have

$$
\begin{aligned}
T_i^{(n)} &= \lambda n_i \\
\sigma_{ij} n_j &= \lambda n_i \\
\sigma_{ij} n_j - \lambda n_i &= 0 \\
\left(\sigma_{ij} - \lambda \delta_{ij}\right) n_j &= 0
\end{aligned}
$$

This is a homogeneous system, i.e. equal to zero, of three linear equations where n_j are the unknowns. To obtain a nontrivial (non-zero) solution for n_j, the determinant matrix of the coefficients must be equal to zero, i.e. the system is singular. Thus,

$$
\left|\sigma_{ij} - \lambda \delta_{ij}\right| = \begin{vmatrix} \sigma_{11} - \lambda & \sigma_{12} & \sigma_{13} \\ \sigma_{21} & \sigma_{22} - \lambda & \sigma_{23} \\ \sigma_{31} & \sigma_{32} & \sigma_{33} - \lambda \end{vmatrix} = 0
$$

Expanding the determinant leads to the *characteristic equation*

$$
\left|\sigma_{ij} - \lambda \delta_{ij}\right| = -\lambda^3 + I_1 \lambda^2 - I_2 \lambda + I_3 = 0
$$

where

$$
\begin{aligned}
I_1 &= \sigma_{11} + \sigma_{22} + \sigma_{33} \\
&= \sigma_{kk} \\
I_2 &= \begin{vmatrix} \sigma_{22} & \sigma_{23} \\ \sigma_{32} & \sigma_{33} \end{vmatrix} + \begin{vmatrix} \sigma_{11} & \sigma_{13} \\ \sigma_{31} & \sigma_{33} \end{vmatrix} + \begin{vmatrix} \sigma_{11} & \sigma_{12} \\ \sigma_{21} & \sigma_{22} \end{vmatrix} \\
&= \sigma_{11}\sigma_{22} + \sigma_{22}\sigma_{33} + \sigma_{11}\sigma_{33} - \sigma_{12}^2 - \sigma_{23}^2 - \sigma_{13}^2 \\
&= \frac{1}{2}\left(\sigma_{ii}\sigma_{jj} - \sigma_{ij}\sigma_{ji}\right) \\
I_3 &= \det(\sigma_{ij}) \\
&= \sigma_{11}\sigma_{22}\sigma_{33} + 2\sigma_{12}\sigma_{23}\sigma_{31} - \sigma_{12}^2\sigma_{33} - \sigma_{23}^2\sigma_{11} - \sigma_{13}^2\sigma_{22}
\end{aligned}
$$

The characteristic equation has three real roots λ, i.e. not imaginary due to the symmetry of the stress tensor. The three roots $\lambda_1 = \sigma_1$, $\lambda_2 = \sigma_2$, and $\lambda_3 = \sigma_3$ are the eigenvalues or principal stresses, and they are the roots of the Cayley–Hamilton theorem. The principal stresses are unique for a given stress tensor. Therefore, from the characteristic equation it is seen that the coefficients I_1, I_2 and I_3, called the first, second, and third *stress invariants*, respectively, have always the same value regardless of the orientation of the coordinate system chosen.

For each eigenvalue, there is a non-trivial solution for n_j in the equation $(\sigma_{ij} - \lambda\delta_{ij})\, n_j = 0$. These solutions are the principal directions or eigenvectors defining the plane where the principal stresses act. The principal stresses and principal directions characterize the stress at a point and are independent of the orientation of the coordinate system.

If we choose a coordinate system with axes oriented to the principal directions, then the normal stresses will be the principal stresses and the stress tensor is represented by a diagonal matrix:

$$\sigma_{ij} = \begin{bmatrix} \sigma_1 & 0 & 0 \\ 0 & \sigma_2 & 0 \\ 0 & 0 & \sigma_3 \end{bmatrix}$$

The principal stresses may be combined to form the stress invariants, I_1, I_2, and I_3.The first and third invariant are the trace and determinant respectively, of the stress tensor. Thus,

$$I_1 = \sigma_1 + \sigma_2 + \sigma_3$$
$$I_2 = \sigma_1\sigma_2 + \sigma_2\sigma_3 + \sigma_3\sigma_1$$
$$I_3 = \sigma_1\sigma_2\sigma_3$$

Because of its simplicity, working and thinking in the principal coordinate system is often very useful when considering the state of the elastic medium at a particular point.

Principal stresses are often expressed in the following equation for evaluating stresses in the x and y directions or axial and bending stresses on a part. The principal normal stresses can then be used to calculate the Von Mises stress and ultimately the safety factor and margin of safety.

$$\sigma_1, \sigma_2 = \frac{\sigma_x + \sigma_y}{2} \pm \sqrt{\left(\frac{\sigma_x - \sigma_y}{2}\right)^2 + \tau_{xy}^2}$$

Using just the part of the equation under the square root is equal to the maximum and minimum shear stress for plus and minus. This is shown as:

$$\tau_{max}, \tau_{min} = \pm\sqrt{\left(\frac{\sigma_x - \sigma_y}{2}\right)^2 + \tau_{xy}^2}$$

Maximum and minimum shear stresses

The maximum shear stress or maximum principal shear stress is equal to one-half the difference between the largest and smallest principal stresses, and acts on the plane that bisects the angle between the directions of the largest and smallest principal stresses, i.e. the plane of the maximum shear stress is oriented 45° from the principal stress planes. The maximum shear stress is expressed as

$$\tau_{\max} = \frac{1}{2}\left|\sigma_{\max} - \sigma_{\min}\right|$$

Assuming $\sigma_1 \geq \sigma_2 \geq \sigma_3$ then

$$\tau_{\max} = \frac{1}{2}\left|\sigma_1 - \sigma_3\right|$$

The normal stress component acting on the plane for the maximum shear stress is non-zero and it is equal to

$$\sigma_{\mathrm{n}} = \frac{1}{2}\left(\sigma_1 + \sigma_3\right)$$

Stress deviator tensor

The stress tensor σ_{ij} can be expressed as the sum of two other stress tensors:

1. a *mean hydrostatic stress tensor* or *volumetric stress tensor* or *mean normal stress tensor*, $p\delta_{ij}$, which tends to change the volume of the stressed body; and
2. a deviatoric component called the *stress deviator tensor*, s_{ij}, which tends to distort it.

So:

$$\sigma_{ij} = s_{ij} + p\delta_{ij},$$

where p is the mean stress given by

$$p = \frac{\sigma_{kk}}{3} = \frac{\sigma_{11} + \sigma_{22} + \sigma_{33}}{3} = \tfrac{1}{3}I_1.$$

Note that convention in solid mechanics differs slightly from what is listed above. In solid mechanics, pressure is generally defined as negative one-third the trace of the stress tensor.

The deviatoric stress tensor can be obtained by subtracting the hydrostatic stress tensor from the stress tensor:

$$s_{ij} = \sigma_{ij} - \frac{\sigma_{kk}}{3}\delta_{ij},$$

$$\begin{bmatrix} s_{11} & s_{12} & s_{13} \\ s_{21} & s_{22} & s_{23} \\ s_{31} & s_{32} & s_{33} \end{bmatrix} = \begin{bmatrix} \sigma_{11} & \sigma_{12} & \sigma_{13} \\ \sigma_{21} & \sigma_{22} & \sigma_{23} \\ \sigma_{31} & \sigma_{32} & \sigma_{33} \end{bmatrix} - \begin{bmatrix} p & 0 & 0 \\ 0 & p & 0 \\ 0 & 0 & p \end{bmatrix}$$

$$= \begin{bmatrix} \sigma_{11} - p & \sigma_{12} & \sigma_{13} \\ \sigma_{21} & \sigma_{22} - p & \sigma_{23} \\ \sigma_{31} & \sigma_{32} & \sigma_{33} - p \end{bmatrix}.$$

Invariants of the stress deviator tensor

As it is a second order tensor, the stress deviator tensor also has a set of invariants, which can be obtained using the same procedure used to calculate the invariants of the stress tensor. It can be shown that the principal directions of the stress deviator tensor s_{ij} are the same as the principal directions of the stress tensor σ_{ij}. Thus, the characteristic equation is

$$|s_{ij} - \lambda\delta_{ij}| = \lambda^3 - J_1\lambda^2 - J_2\lambda - J_3 = 0,$$

where J_1, J_2 and J_3 are the first, second, and third *deviatoric stress invariants*, respectively. Their values are the same (invariant) regardless of the orientation of the coordinate system chosen. These deviatoric stress invariants can be expressed as a function of the components of s_{ij} or its principal values s_1, s_2, and s_3, or alternatively, as a function of σ_{ij} or its principal values σ_1, σ_2, and σ_3. Thus,

$$\begin{aligned}
J_1 &= s_{kk} = 0, \\
J_2 &= \tfrac{1}{2}s_{ij}s_{ji} \\
&= -s_1s_2 - s_2s_3 - s_3s_1 \\
&= \tfrac{1}{6}\left[(\sigma_{11} - \sigma_{22})^2 + (\sigma_{22} - \sigma_{33})^2 + (\sigma_{33} - \sigma_{11})^2\right] + \sigma_{12}^2 + \sigma_{23}^2 + \sigma_{31}^2 \\
&= \tfrac{1}{6}\left[(\sigma_1 - \sigma_2)^2 + (\sigma_2 - \sigma_3)^2 + (\sigma_3 - \sigma_1)^2\right] \\
&= \tfrac{1}{3}I_1^2 - I_2, \\
J_3 &= \det(s_{ij}) \\
&= \tfrac{1}{3}s_{ij}s_{jk}s_{ki} \\
&= s_1s_2s_3 \\
&= \tfrac{2}{27}I_1^3 - \tfrac{1}{3}I_1I_2 + I_3.
\end{aligned}$$

Because $s_{kk} = 0$, the stress deviator tensor is in a state of pure shear.

A quantity called the equivalent stress or von Mises stress is commonly used in solid mechanics. The equivalent stress is defined as

$$\sigma_e = \sqrt{3\ J_2} = \sqrt{\tfrac{1}{2}\ [(\sigma_1 - \sigma_2)^2 + (\sigma_2 - \sigma_3)^2 + (\sigma_3 - \sigma_1)^2]}\ .$$

Octahedral stresses

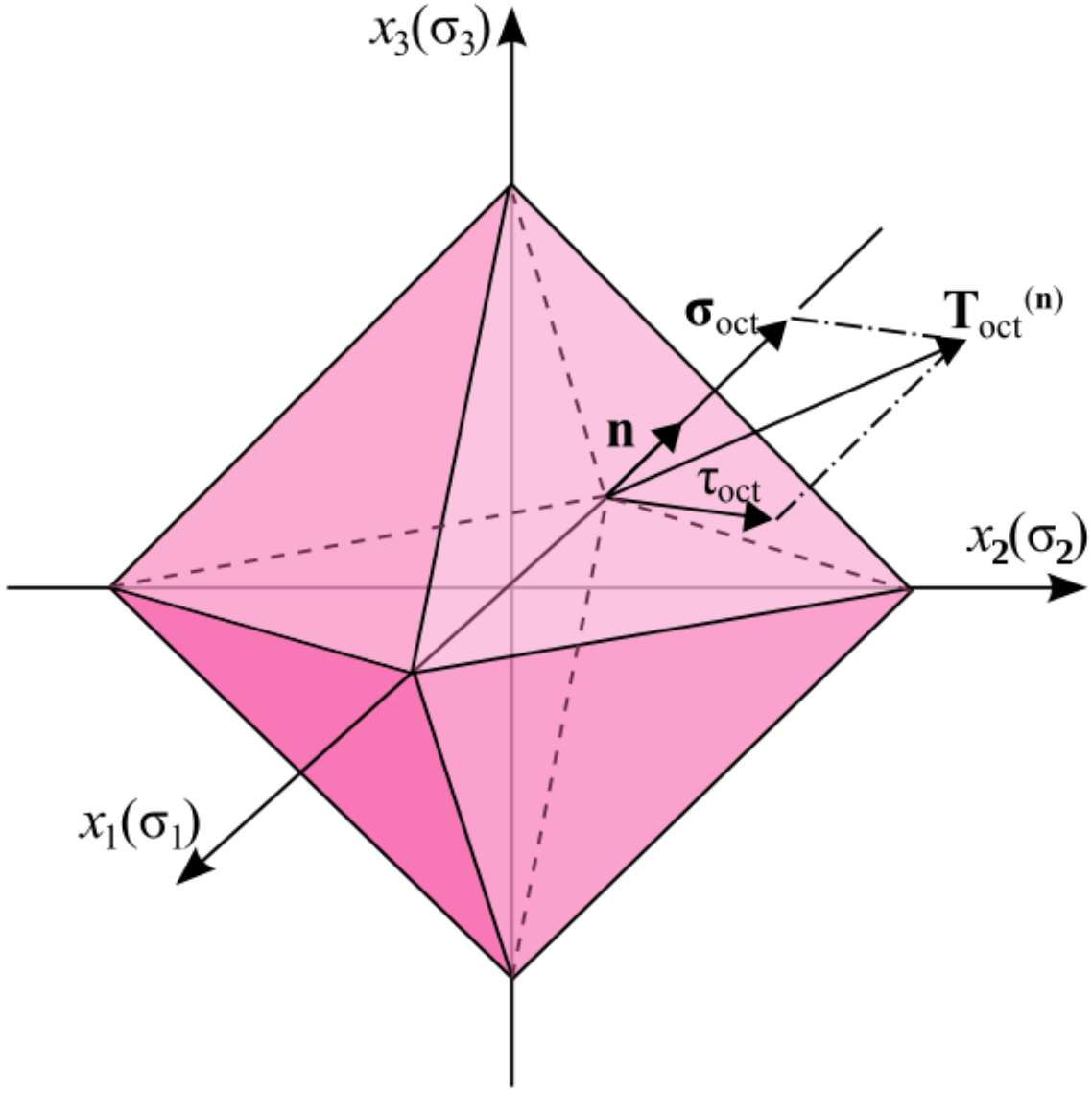

Figure 6. Octahedral stress planes

Considering the principal directions as the coordinate axes, a plane whose normal vector makes equal angles with each of the principal axes (i.e. having direction cosines equal to

$|1/\sqrt{3}|$) is called an *octahedral plane*. There are a total of eight octahedral planes (Figure 6). The normal and shear components of the stress tensor on these planes are called *octahedral normal stress* $\sigma_{\mathrm{oct}}$and *octahedral shear stress* τ_{oct}, respectively.

Knowing that the stress tensor of point O (Figure 6) in the principal axes is

$$\sigma_{ij} = \begin{bmatrix} \sigma_1 & 0 & 0 \\ 0 & \sigma_2 & 0 \\ 0 & 0 & \sigma_3 \end{bmatrix}$$

the stress vector on an octahedral plane is then given by:

$$\begin{aligned} \mathbf{T}_{\mathrm{oct}}^{(\mathbf{n})} &= \sigma_{ij} n_i \mathbf{e}_j \\ &= \sigma_1 n_1 \mathbf{e}_1 + \sigma_2 n_2 \mathbf{e}_2 + \sigma_3 n_3 \mathbf{e}_3 \\ &= \tfrac{1}{\sqrt{3}}(\sigma_1 \mathbf{e}_1 + \sigma_2 \mathbf{e}_2 + \sigma_3 \mathbf{e}_3) \end{aligned}$$

The normal component of the stress vector at point O associated with the octahedral plane is

$$\begin{aligned} \sigma_{\mathrm{oct}} &= T_i^{(n)} n_i \\ &= \sigma_{ij} n_i n_j \\ &= \sigma_1 n_1 n_1 + \sigma_2 n_2 n_2 + \sigma_3 n_3 n_3 \\ &= \tfrac{1}{3}(\sigma_1 + \sigma_2 + \sigma_3) = \tfrac{1}{3} I_1 \end{aligned}$$

which is the mean normal stress or hydrostatic stress. This value is the same in all eight octahedral planes. The shear stress on the octahedral plane is then

$$\begin{aligned} \tau_{\mathrm{oct}} &= \sqrt{T_i^{(n)} T_i^{(n)} - \sigma_{\mathrm{n}}^2} \\ &= \left[\tfrac{1}{3}(\sigma_1^2 + \sigma_2^2 + \sigma_3^2) - \tfrac{1}{9}(\sigma_1 + \sigma_2 + \sigma_3)^2\right]^{1/2} \\ &= \tfrac{1}{3}\left[(\sigma_1 - \sigma_2)^2 + (\sigma_2 - \sigma_3)^2 + (\sigma_3 - \sigma_1)^2\right]^{1/2} = \tfrac{1}{3}\sqrt{2I_1^2 - 6I_2} = \sqrt{\tfrac{2}{3} J_2} \end{aligned}$$

Alternative measures of stress

The Cauchy stress tensor is not the only measure of stress that is used in practice. Other measures of stress include the first and second Piola–Kirchhoff stress tensors, the Biot stress tensor, and the Kirchhoff stress tensor.

Piola–Kirchhoff stress tensor

In the case of finite deformations, the *Piola–Kirchhoff stress tensors* are used to express the stress relative to the reference configuration. This is in contrast to the Cauchy stress tensor which expresses the stress relative to the present configuration. For infinitesimal deformations or rotations, the Cauchy and Piola–Kirchhoff tensors are identical. These tensors take their names from Gabrio Piola and Gustav Kirchhoff.

Whereas the Cauchy stress tensor, $\boldsymbol{\sigma}$relates stresses in the current configuration, the deformation gradient and strain tensors are described by relating the motion to the reference configuration; thus not all tensors describing the state of the material are in either the reference or current configuration. Having the stress, strain and deformation all described either in the reference or current configuration would make it easier to define constitutive models (for example, the Cauchy Stress tensor is variant to a pure rotation, while the deformation strain tensor is invariant; thus creating problems in defining a constitutive model that relates a varying tensor, in terms of an invariant one during pure rotation; as by definition constitutive models have to be invariant to pure rotations). The 1st Piola–Kirchhoff stress tensor, $\boldsymbol{P}$is one possible solution to this problem. It defines a family of tensors, which describe the configuration of the body in either the current or the reference state.

The 1st Piola–Kirchhoff stress tensor, $\boldsymbol{P}$relates forces in the *present* configuration with areas in the *reference* ("material") configuration.

$$\boldsymbol{P} = J\ \boldsymbol{\sigma} \cdot \boldsymbol{F}^{-T}$$

where $\boldsymbol{F}$is the deformation gradient and $J = \det \boldsymbol{F}$is the Jacobian determinant.

In terms of components with respect to an orthonormal basis, the first Piola–Kirchhoff stress is given by

$$P_{iL} = J\ \sigma_{ik}\ F^{-1}_{Lk} = J\ \sigma_{ik}\ \frac{\partial X_L}{\partial x_k}$$

Because it relates different coordinate systems, the 1st Piola–Kirchhoff stress is a two-point tensor. In general, it is not symmetric. The 1st Piola–Kirchhoff stress is the 3D generalization of the 1D concept of engineering stress.

If the material rotates without a change in stress state (rigid rotation), the components of the 1st Piola–Kirchhoff stress tensor will vary with material orientation.

The 1st Piola–Kirchhoff stress is energy conjugate to the deformation gradient.

2nd Piola–Kirchhoff stress tensor

Whereas the 1st Piola–Kirchhoff stress relates forces in the current configuration to areas in the reference configuration, the 2nd Piola–Kirchhoff stress tensor $\boldsymbol{S}$ relates forces in the reference configuration to areas in the reference configuration. The force in the reference configuration is obtained via a mapping that preserves the relative relationship between the force direction and the area normal in the current configuration.

$$\boldsymbol{S} = J\ \boldsymbol{F}^{-1} \cdot \boldsymbol{\sigma} \cdot \boldsymbol{F}^{-T}\ .$$

In index notation with respect to an orthonormal basis,

$$S_{IL} = J\ F^{-1}_{Ik}\ F^{-1}_{Lm}\ \sigma_{km} = J\ \frac{\partial X_I}{\partial x_k}\ \frac{\partial X_L}{\partial x_m}\ \sigma_{km}$$

This tensor is symmetric.

If the material rotates without a change in stress state (rigid rotation), the components of the 2nd Piola–Kirchhoff stress tensor will remain constant, irrespective of material orientation.

The 2nd Piola–Kirchhoff stress tensor is energy conjugate to the Green–Lagrange finite strain tensor.

Chapter 4

Stress Concentration

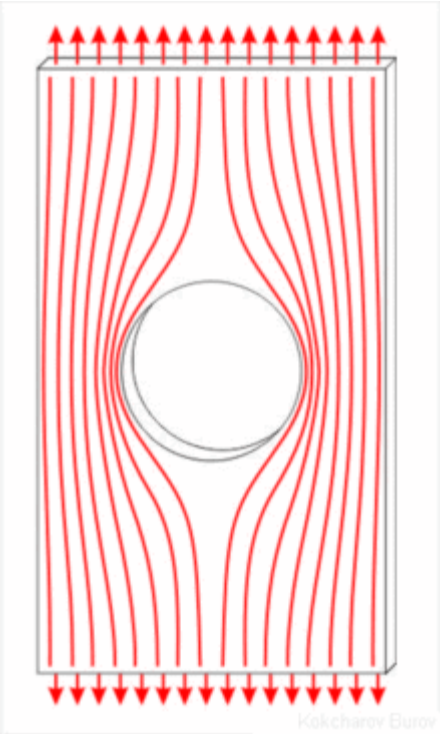

Internal force lines are denser near the hole

A **stress concentration** (often called **stress raisers** or **stress risers**) is a location in an object where stress is concentrated. An object is strongest when force is evenly distributed over its area, so a reduction in area, e.g. caused by a crack, results in a localized increase in stress. A material can fail, via a propagating crack, when a concentrated stress exceeds the material's theoretical cohesive strength. The real fracture strength of a material is always lower than the theoretical value because most materials contain small cracks that concentrate stress. Fatigue cracks always start at stress raisers, so removing such defects increases the fatigue strength.

Causes

The sharp corner at the brick has acted as a stress concentrator within the concrete causing it to crack

Geometric discontinuities cause an object to experience a local increase in the intensity of a stress field. The examples of shapes that cause these concentrations are: cracks, sharp corners, holes and, changes in the cross-sectional area of the object. High local stresses can cause the object to fail more quickly than if it wasn't there. Engineers must design the geometry to minimize stress concentrations.

Prevention

A counter-intuitive method of reducing one of the worst types of stress concentrations, a crack, is to drill a large hole at the end of the crack. The drilled hole, with its relatively large diameter, causes a smaller stress concentration than the sharp end of a crack. This is however, a temporary solution that must be corrected at the first opportune time.

It is important to systematically check for possible stress concentrations caused by cracks—there is a critical crack length of 2a for which, when this value is exceeded, the crack proceeds to definite catastrophic failure. This ultimate failure is definite since the crack will propagate on its own once the length is greater than 2a. (There is no additional

energy required to increase the crack length so the crack will continue to enlarge until the material fails.) The origins of the value 2a can be understood through Griffith's theory of brittle fracture.

Examples

This orthosis is implanted to support the femur after a fracture, but the concentration of stress at its bend increases the possibility that it may break under force.

The term "stress raiser" is used in orthopedics; a focus point of stress on an implanted orthosis is very likely to be its point of failure.

Classic cases of metal failures due to stress concentrations include metal fatigue at the corners of the windows of the De Havilland Comet aircraft and brittle fractures at the corners of hatches in Liberty ships in cold and stressful conditions in winter storms in the Atlantic Ocean.

Concentration factor for cracks

The maximum stress felt near a crack occurs in the area of lowest radius of curvature. In an elliptical crack of length 2*a* and width 2*b*, under an applied external stress σ, the stress at the ends of the major axes is given by:

$$\sigma_{max} = \sigma \left(1 + 2\frac{a}{b}\right) = \sigma \left(1 + 2\sqrt{\frac{a}{\rho}}\right)$$

where ρ is the radius of curvature of the crack tip. A **stress concentration factor** is the ratio of the highest stress (σ_{max}) to a reference stress (σ) of the gross cross-section. As the radius of curvature approaches zero, the maximum stress approaches infinity. Note that the stress concentration factor is a function of the geometry of a crack, and not of its size. These factors can be found in typical engineering reference materials to predict the stresses that could otherwise not be analyzed using strength of materials approaches. This is not to be confused with 'Stress Intensity Factor'.

Concentration factor calculation

There are experimental methods for measuring stress concentration factor including photoelastic stress analysis, brittle coatings or strain gauges. While all these approaches have been successful, all also have experimental, environmental, accuracy and/or measurement disadvantages.

During the design phase, there are multiple approaches to estimating stress concentration factors. Several catalogs of stress concentration factors have been published. Perhaps most famous is *Stress Concentration Design Factors* by Peterson, first published in 1953. Finite element methods are commonly used in design today. Theoretical approaches, using elasticity or strength of material considerations, can lead to equations similar to the one shown above.

There may be small differences between the catalog, FEM and theoretical values calculated. Each method has advantages and disadvantages. Many catalog curves were derived from experimental data. FEM calculates the peak stresses directly and nominal stresses may be easily found by integrating stresses in the surrounding material. The result is that engineering judgment may have to be used when selecting which data applies to making a design decision. Many theoretical stress concentration factors have been derived for infinite or semi-infinite geometries which may not be analyzable and are

not testable in a stress lab, but tackling a problem using two or more of these approaches will allow an engineer to achieve an accurate conclusion.

Chapter 5

Yield Surface

A **yield surface** is a five-dimensional surface in the six-dimensional space of stresses. The yield surface is usually convex and the state of stress of *inside* the yield surface is elastic. When the stress state lies on the surface the material is said to have reached its yield point and the material is said to have become plastic. Further deformation of the material causes the stress state to remain on the yield surface, even though the surface itself may change shape and size as the plastic deformation evolves. This is because stress states that lie outside the yield surface are non-permissible in rate-independent plasticity, though not in some models of viscoplasticity.

The yield surface is usually expressed in terms of (and visualized in) a three-dimensional principal stress space (σ_1,σ_2,σ_3), a two- or three-dimensional space spanned by stress invariants (I_1,J_2,J_3) or a version of the three-dimensional Haigh–Westergaard stress space. Thus we may write the equation of the yield surface (that is, the yield function) in the forms:

- $f(\sigma_1, \sigma_2, \sigma_3) = 0$ where σ_i are the principal stresses.
- $f(I_1, J_2, J_3) = 0$ where I_1 is the first principal invariant of the Cauchy stress and J_2,J_3 are the second and third principal invariants of the deviatoric part of the Cauchy stress.
- $f(p, q, r) = 0$ where p,q are scaled versions of I_1 and J_2 and r is a function of J_2,J_3.
- $f(\xi, \rho, \theta) = 0$ where ξ,ρ are scaled versions of I_1 and J_2, and θ is the **Lode angle**.

Invariants used to describe yield surfaces

The first principal invariant of the Cauchy stress (I_1), and the second and third principal invariants of the deviatoric part of the Cauchy stress (J_2,J_3) are defined as

$$I_1 = \operatorname{Tr}(\boldsymbol{\sigma}) = \sigma_1 + \sigma_2 + \sigma_3$$
$$J_2 = \frac{1}{2}\boldsymbol{s} : \boldsymbol{s} = \frac{1}{6}\left[(\sigma_1 - \sigma_2)^2 + (\sigma_2 - \sigma_3)^2 + (\sigma_3 - \sigma_1)^2\right]$$
$$J_3 = \det(\boldsymbol{s}) = \frac{1}{3}(\boldsymbol{s} \cdot \boldsymbol{s}) : \boldsymbol{s} = s_1 s_2 s_3$$

where $\boldsymbol{\sigma}$ is the Cauchy stress and $\sigma_1,\sigma_2,\sigma_3$ are its principal values, $\boldsymbol{s}$ is the deviatoric part of the Cauchy stress and s_1,s_2,s_3 are its principal values.

The quantities p, q, r are usually used to describe yield surfaces for cohesive frictional materials such as rocks, soils, and ceramics. These quantities are defined as

$$p = \frac{1}{3}\, I_1 \;\; : \;\; q = \sqrt{3\; J_2} = \sigma_{\text{eq}} \; ; \;\; r = 3 \left(\frac{J_3}{2}\right)^{1/3}$$

where σ_{eq} is the **equivalent stress**.

The quantities ξ, ρ, θ describe a cylindrical coordinate system (the **Haigh–Westergaard** coordinates) and are defined as

$$\xi = \frac{1}{\sqrt{3}}\, I_1 = \sqrt{3}\, p \; ; \;\; \rho = \sqrt{2J_2} = \sqrt{\frac{2}{3}}\, q \; ; \;\; \cos(3\theta) = \left(\frac{r}{q}\right)^3 = \frac{3\sqrt{3}}{2}\, \frac{J_3}{J_2^{3/2}}$$

The $\xi - \rho$ plane is also called the **Rendulic plane**. The angle θ is called the **Lode angle** and the relation between θ and J_2,J_3 was first given by Nayak and Zienkiewicz in 1972

The principal stresses and the Haigh–Westergaard coordinates are related by

$$\begin{bmatrix} \sigma_1 \\ \sigma_2 \\ \sigma_3 \end{bmatrix} = \frac{1}{\sqrt{3}} \begin{bmatrix} \xi \\ \xi \\ \xi \end{bmatrix} + \sqrt{\frac{2}{3}}\, \rho \begin{bmatrix} \cos\theta \\ \cos\left(\theta - \dfrac{2\pi}{3}\right) \\ \cos\left(\theta + \dfrac{2\pi}{3}\right) \end{bmatrix}$$

Examples of yield surfaces

There are several different yield surfaces known in engineering, and those most popular are listed below.

Tresca yield surface

The Tresca or *maximum shear stress* yield criterion is taken to be the work of Henri Tresca. It is also referred as the Tresca–Guest (TG) criterion. The functional form of this yield criterion is

$$f(\sigma_1, \sigma_2, \sigma_3) = 0 \ .$$

In terms of the principal stresses the Tresca criterion is expressed as

$$\max(|\sigma_1 - \sigma_2|, |\sigma_2 - \sigma_3|, |\sigma_3 - \sigma_1|) = \sigma_0$$

Figure 1 shows the Tresca–Guest yield surface in the three-dimensional space of principal stresses. It is a prism of six sides and having infinite length. This means that the material remains elastic when all three principal stresses are roughly equivalent (a hydrostatic pressure), no matter how much it is compressed or stretched. However, when one of principal stresses becomes smaller (or larger) than the others the material is subject to shearing. In such situations, if the shear stress reaches the yield limit then the material enters the plastic domain. Figure 2 shows the Tresca–Guest yield surface in two-dimensional stress space, it is a cross section of the prism along the σ_1,σ_2 plane.

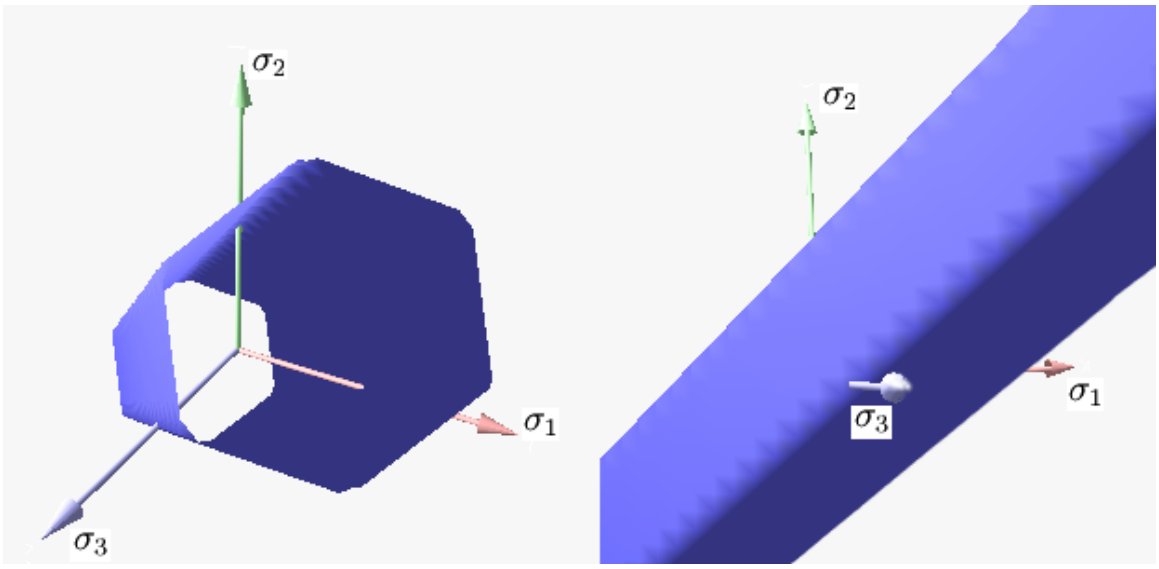

Figure 1: View of Tresca–Guest yield surface in 3D space of principal stresses

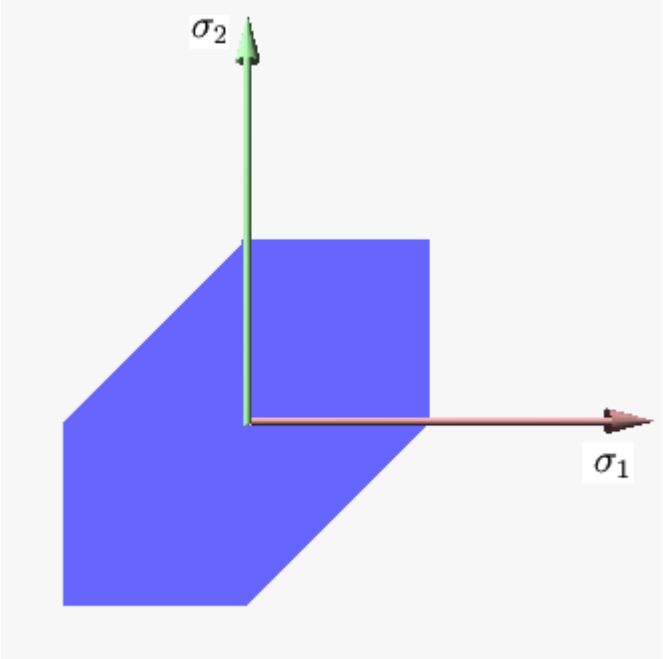

Figure 2: Tresca–Guest yield surface in 2D space (σ_1,σ_2)

Huber–von Mises yield surface

The von Mises yield criterion (also known as Prandtl–Reuss yield criterion) has the functional form

$$f(J_2) = 0 \ .$$

This yield criterion is often credited to Maximilian Huber and Richard von Mises. It is also referred to as the Huber–Mises–Hencky (HMH) criterion.

The von Mises yield criterion is expressed in the principal stresses as

$$\sqrt{3J_2} = \sigma_y \quad \text{or,} \quad (\sigma_1 - \sigma_2)^2 + (\sigma_2 - \sigma_3)^2 + (\sigma_3 - \sigma_1)^2 = 2{\sigma_y}^2$$

where σ_y is the yield stress in uniaxial tension.

Figure 3 shows the von Mises yield surface in the three-dimensional space of principal stresses. It is a circular cylinder of infinite length with its axis inclined at equal angles to the three principal stresses. Figure 4 shows the von Mises yield surface in two-dimensional space compared with Tresca–Guest criterion. A cross section of the von Mises cylinder on the plane of σ_1,σ_2 produces the elliptical shape of the yield surface.

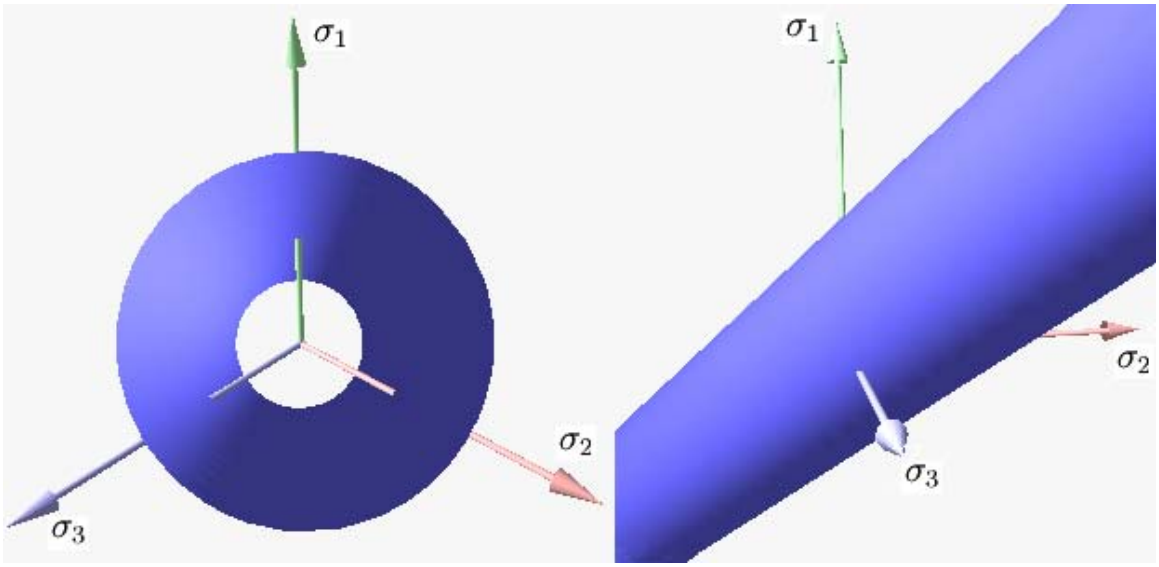

Figure 3: View of Huber–Mises–Hencky yield surface in 3D space of principal stresses

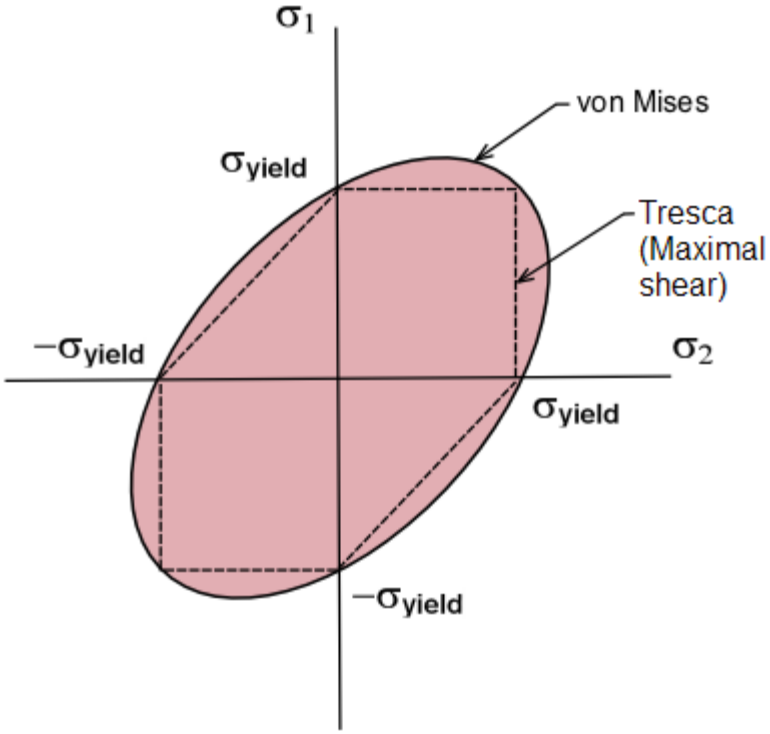

Figure 4: Comparison of Tresca–Guest and Huber–Mises–Hencky criteria in 2D space (σ_1,σ_2)

Mohr–Coulomb yield surface

The Mohr–Coulomb yield (failure) criterion is a two-parameter yield criterion which has the functional form

$f(\sigma_1,\sigma_2,\sigma_3) = 0$

This model is often used to model concrete, soil or granular materials.

The Mohr–Coulomb yield criterion may be expressed as:

$$\pm\frac{\sigma_1-\sigma_2}{2} = c-K\left(\frac{\sigma_1+\sigma_2}{2}\right)\ ;\ \pm\frac{\sigma_2-\sigma_3}{2} = c-K\left(\frac{\sigma_2+\sigma_3}{2}\right)\ ;\ \pm\frac{\sigma_3-\sigma_1}{2} = c-K\left(\frac{\sigma_3+\sigma_1}{2}\right)$$

where

$$m = \frac{\sigma_c}{\sigma_t}\ ,\quad K = \frac{m-1}{m+1}\ ;\quad c = \left(\frac{1}{m+1}\right)\sigma_c = \left(\frac{m}{m+1}\right)\sigma_t$$

and the parameters σ_c and σ_t are the yield (failure) stresses of the material in uniaxial compression and tension, respectively. If $K = 0$ then the Mohr–Coulomb criterion reduces to the Tresca–Guest criterion.

Figure 5 shows Mohr–Coulomb yield surface in the three-dimensional space of principal stresses. It is a conical prism and K determines the inclination angle of conical surface. Figure 6 shows Mohr–Coulomb yield surface in two-dimensional stress space. It is a cross section of this conical prism on the plane of σ_1,σ_2.

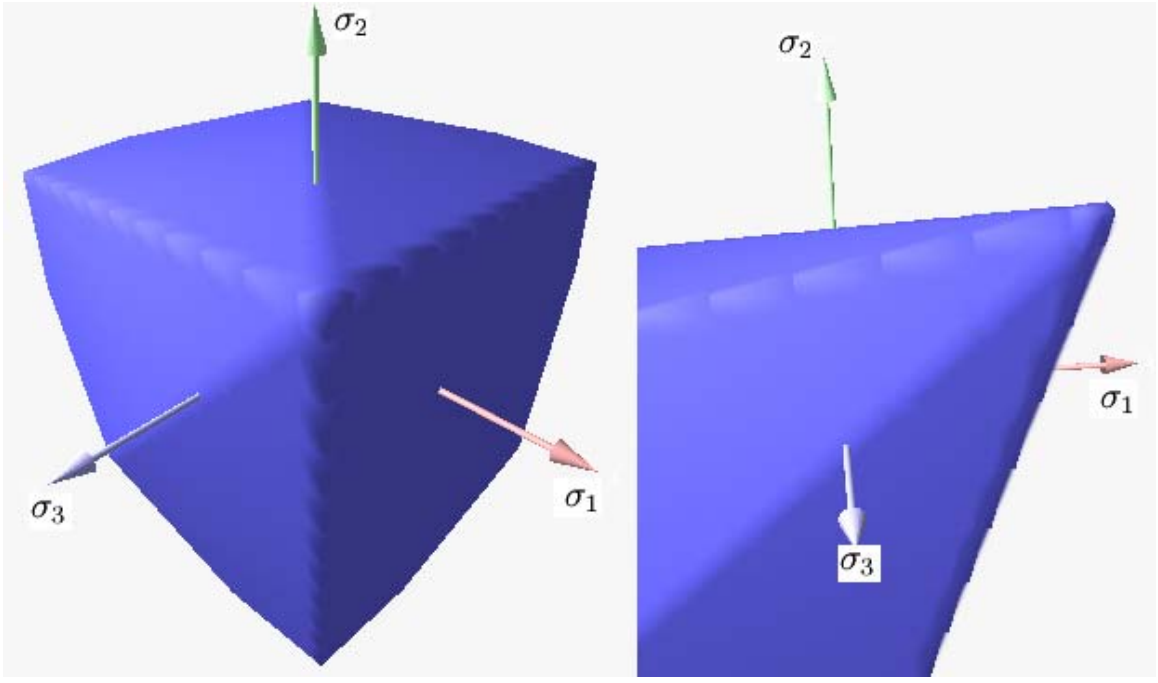

Figure 5: View of Mohr–Coulomb yield surface in 3D space of principal stresses

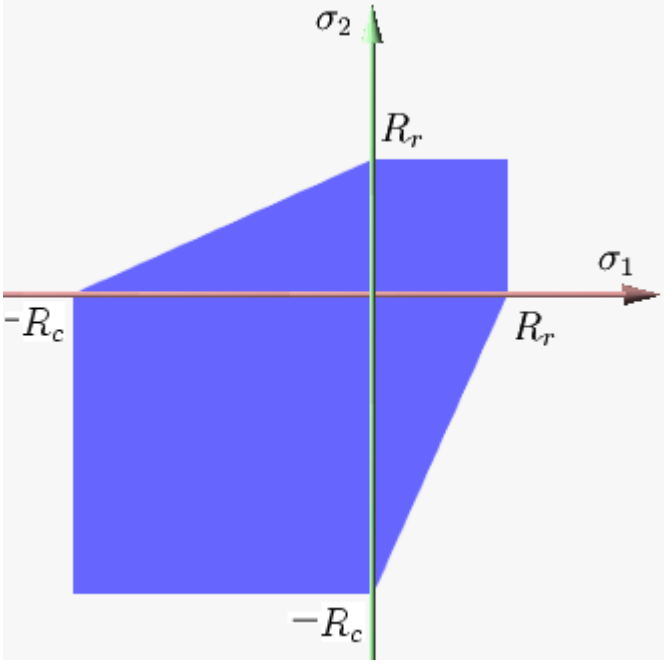

Figure 6: Mohr–Coulomb yield surface in 2D space (σ_1,σ_2)

The following formula was used to plot the surface in Fig. 5 :

$$\max\left(\frac{|\sigma_1-\sigma_2|}{2}-c+K\frac{\sigma_1+\sigma_2}{2},\ \frac{|\sigma_2-\sigma_3|}{2}-c+K\frac{\sigma_2+\sigma_3}{2},\ \frac{|\sigma_3-\sigma_1|}{2}-c+K\frac{\sigma_3+\sigma_1}{2}\right)=0$$

Drucker–Prager yield surface

The Drucker–Prager yield criterion has the function form

$$f(I_1, J_2) = 0\ .$$

This criterion is most often used for concrete where both normal and shear stresses can determine failure. The Drucker–Prager yield criterion may be expressed as

$$\alpha\left(\sigma_1+\sigma_2+\sigma_3\right)+\sqrt{\frac{(\sigma_1-\sigma_2)^2+(\sigma_2-\sigma_3)^2+(\sigma_3-\sigma_1)^2}{6}}=K$$

where

$$m=\frac{\sigma_c}{\sigma_t}\ ;\quad K=\frac{2\sigma_c}{\sqrt{3}(m+1)}\ ;\quad \alpha=\frac{m-1}{\sqrt{3}(m+1)}$$

and σ_c,σ_t are the uniaxial yield stresses in compression and tension respectively.

Figure 7 shows Drucker–Prager yield surface in the three-dimensional space of principal stresses. It is a regular cone. Figure 8 shows Drucker–Prager yield surface in two-dimensional space. The ellipsoidal-shaped elastic domain is a cross section of the cone on the plane of σ_1,σ_2; here it is shown enclosing the elastic domain for the Mohr–Coulomb yield criterion, although the converse scenario is also possible.

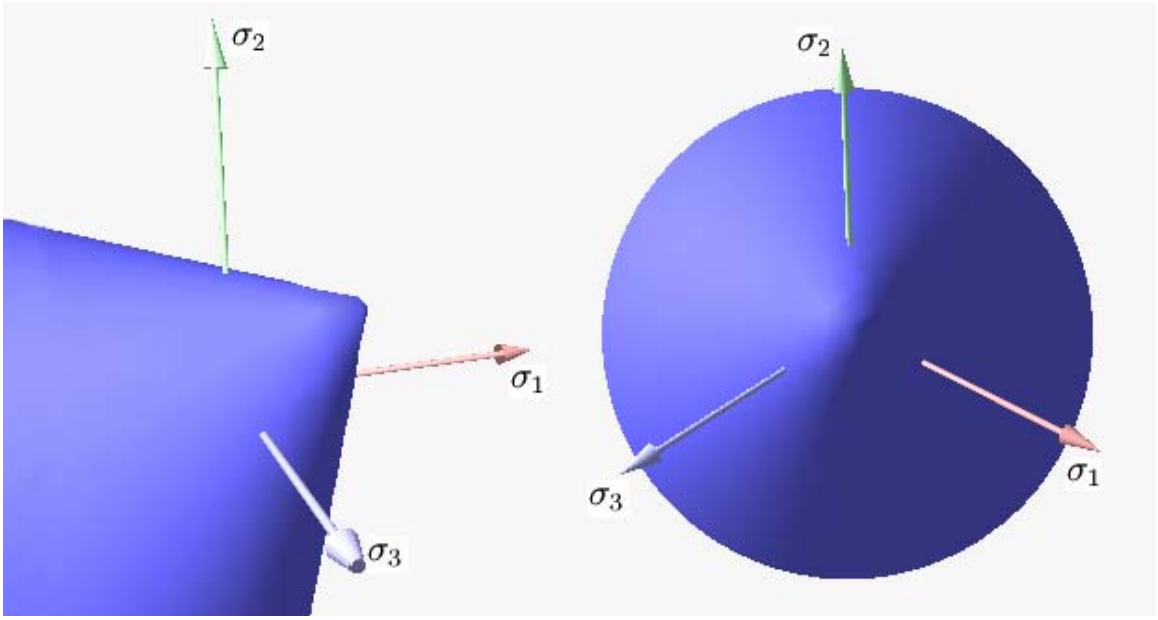

Figure 7: View of Drucker–Prager yield surface in 3D space of principal stresses

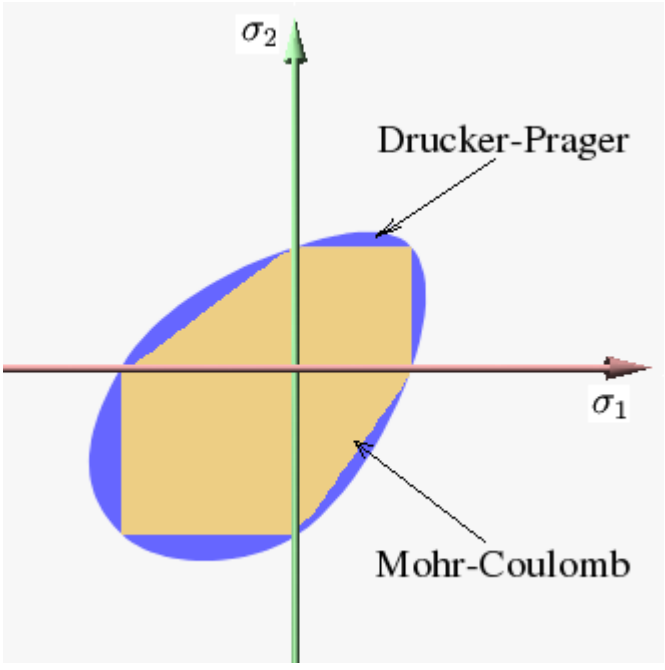

Figure 8: Drucker–Prager and Mohr–Coulomb yield surface in 2D space (σ_1,σ_2)

Bresler–Pister yield surface

The Bresler–Pister yield criterion is an extension of the Drucker–Prager yield criterion that uses three parameters.

The Bresler–Pister yield surface has the functional form

$$f(I_1, J_2) = 0 \ .$$

In terms of the principal stresses, this yield criterion may be expressed as

$$f := \frac{1}{\sqrt{6}}\left[(\sigma_1 - \sigma_2)^2 + (\sigma_2 - \sigma_3)^2 + (\sigma_3 - \sigma_1)^2\right]^{1/2} - c_0 - c_1\,(\sigma_1+\sigma_2+\sigma_3) - c_2\,(\sigma_1+\sigma_2+\sigma_3)^2$$

where c_0,c_1,c_2 are material constants. The additional parameter c_2 gives the yield surface a ellipsoidal cross section when viewed from a direction perpendicular to its axis. If σ_c is the yield stress in uniaxial compression, σ_t is the yield stress in uniaxial tension, and σ_b is the yield stress in biaxial compression, the parameters can be expressed as

$$c_1 = \left(\frac{\sigma_t - \sigma_c}{\sqrt{3}(\sigma_t + \sigma_c)}\right)\left(\frac{4\sigma_b^2 - \sigma_b(\sigma_c + \sigma_t) + \sigma_c\sigma_t}{4\sigma_b^2 + 2\sigma_b(\sigma_t - \sigma_c) - \sigma_c\sigma_t}\right)$$

$$c_2 = \left(\frac{1}{\sqrt{3}(\sigma_t + \sigma_c)}\right)\left(\frac{\sigma_b(3\sigma_t - \sigma_c) - 2\sigma_c\sigma_t}{4\sigma_b^2 + 2\sigma_b(\sigma_t - \sigma_c) - \sigma_c\sigma_t}\right)$$

$$c_0 = \frac{\sigma_c}{\sqrt{3}} + c_1\sigma_c - c_2\sigma_c^2$$

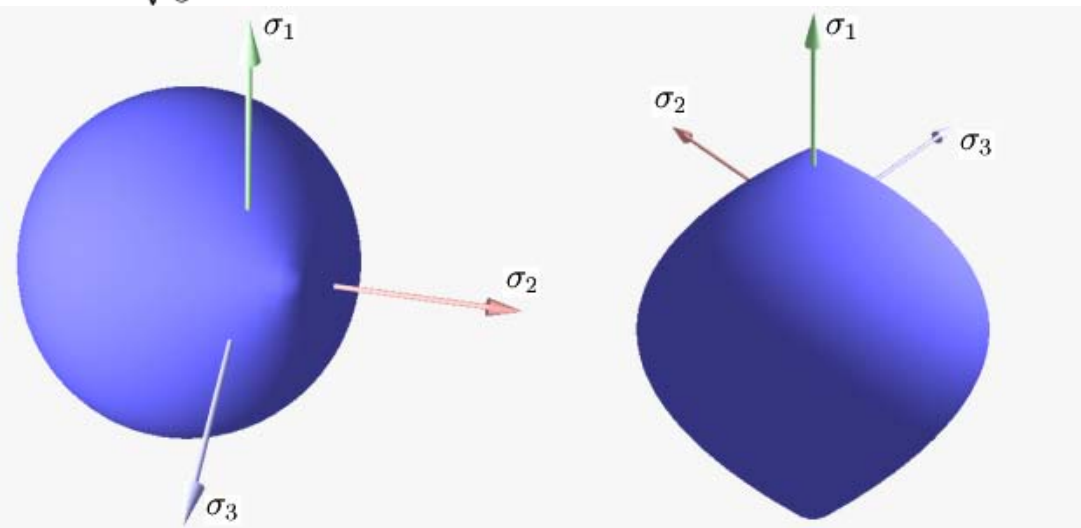

Figure 9: View of Bresler–Pister yield surface in 3D space of principal stresses

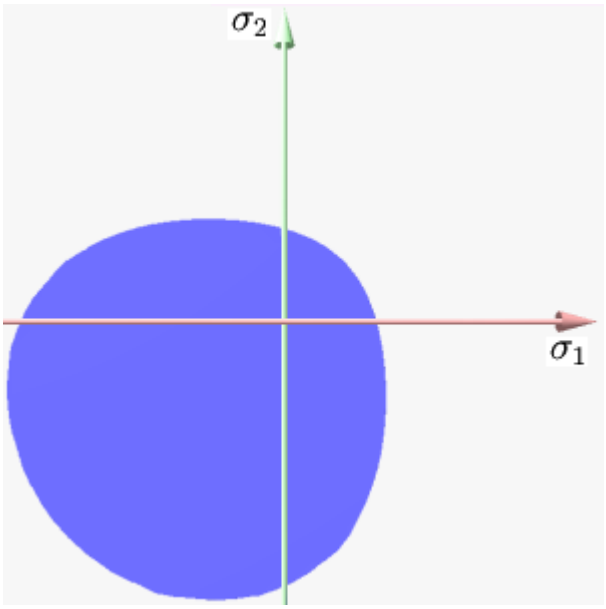

Figure 10: Bresler–Pister yield surface in 2D space (σ_1,σ_2)

Willam–Warnke yield surface

The Willam–Warnke yield criterion is a three-parameter smoothed version of the Mohr–Coulomb yield criterion that has similarities in form to the Drucker–Prager and Bresler–Pister yield criteria.

The yield criterion has the functional form

$$f(I_1, J_2, J_3) = 0 \ .$$

However, it is more commonly expressed in Haigh–Westergaard coordinates as

$$f(\xi, \rho, \theta) = 0 \ .$$

The cross-section of the surface when viewed along its axis is a smoothed triangle (unlike Mohr–Coulumb). The Willam–Warnke yield surface is convex and has unique and well defined first and second derivatives on every point of its surface. Therefore the Willam–Warnke model is computationally robust and has been used for a variety of cohesive-frictional materials.

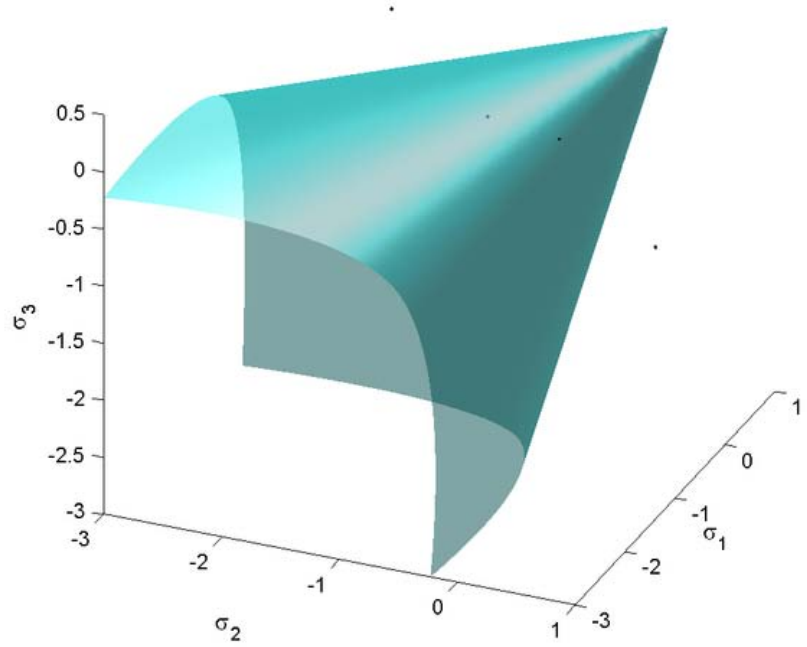

Figure 11: View of Willam–Warnke yield surface in 3D space of principal stresses

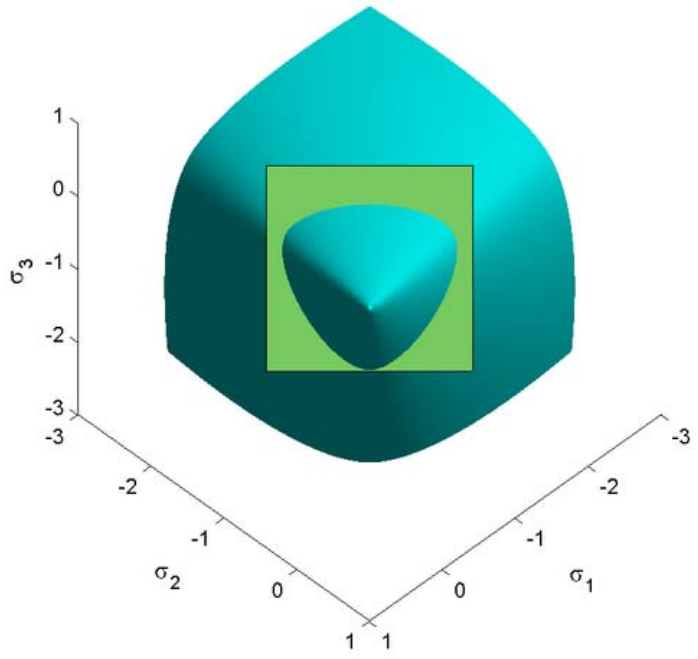

Figure 12: Willam–Warnke yield surface in the π-plane

Chapter 6

Hill Yield Criteria

Rodney Hill has developed several yield criteria for anisotropic plastic deformations. The earliest version was a straightforward extension of the von Mises yield criterion and had a quadratic form. This model was later generalized by allowing for an exponent *m*. Variations of these criteria are in wide use for metals, polymers, and certain composites.

Quadratic Hill yield criterion

The quadratic Hill yield criterion. has the form

$$F(\sigma_{22}-\sigma_{33})^2+G(\sigma_{33}-\sigma_{11})^2+H(\sigma_{11}-\sigma_{22})^2+2L\sigma_{23}^2+2M\sigma_{31}^2+2N\sigma_{12}^2=1\ .$$

Here *F, G, H, L, M, N* are constants that have to be determined experimentally and σ_{ij} are the stresses. The quadratic Hill yield criterion depends only on the deviatoric stresses and is pressure independent. It predicts the same yield stress in tension and in compression.

Expressions for F, G, H, L, M, N

If the axes of material anisotropy are assumed to be orthogonal, we can write

$$(G+H)\ (\sigma_1^y)^2=1\ ;\quad (F+H)\ (\sigma_2^y)^2=1\ ;\quad (F+G)\ (\sigma_3^y)^2=1$$

where $\sigma_1^y,\sigma_2^y,\sigma_3^y$ are the normal yield stresses with respect to the axes of anisotropy. Therefore we have

$$F=\frac{1}{2}\left[\frac{1}{(\sigma_2^y)^2}+\frac{1}{(\sigma_3^y)^2}-\frac{1}{(\sigma_1^y)^2}\right]$$
$$G=\frac{1}{2}\left[\frac{1}{(\sigma_3^y)^2}+\frac{1}{(\sigma_1^y)^2}-\frac{1}{(\sigma_2^y)^2}\right]$$

$$H = \frac{1}{2}\left[\frac{1}{(\sigma_1^y)^2} + \frac{1}{(\sigma_2^y)^2} - \frac{1}{(\sigma_3^y)^2}\right]$$

Similarly, if $\tau_{12}^y, \tau_{23}^y, \tau_{31}^y$ are the yield stresses in shear (with respect to the axes of anisotropy), we have

$$L = \frac{1}{2\ (\tau_{23}^y)^2}\ ; \quad M = \frac{1}{2\ (\tau_{31}^y)^2}\ ; \quad N = \frac{1}{2\ (\tau_{12}^y)^2}$$

Quadratic Hill yield criterion for plane stress

The quadratic Hill yield criterion for thin rolled plates (plane stress conditions) can be expressed as

$$\sigma_1^2 + \frac{R_0\ (1 + R_{90})}{R_{90}\ (1 + R_0)}\ \sigma_2^2 - \frac{2\ R_0}{1 + R_0}\ \sigma_1\sigma_2 = (\sigma_1^y)^2$$

where the principal stresses σ_1,σ_2 are assumed to be aligned with the axes of anisotropy with σ_1 in the rolling direction and σ_2 perpendicular to the rolling direction, $\sigma_3 = 0$, R_0 is the R-value in the rolling direction, and R_{90} is the R-value perpendicular to the rolling direction.

For the special case of transverse isotropy we have $R = R_0 = R_{90}$ and we get

$$\sigma_1^2 + \sigma_2^2 - \frac{2\ R}{1 + R}\ \sigma_1\sigma_2 = (\sigma_1^y)^2$$

Generalized Hill yield criterion

The generalized Hill yield criterion has the form

$$\begin{aligned} F|\sigma_2 - \sigma_3|^m + G|\sigma_3 - \sigma_1|^m + H|\sigma_1 - \sigma_2|^m + L|2\sigma_1 - \sigma_2 - \sigma_3|^m \\ + M|2\sigma_2 - \sigma_3 - \sigma_1|^m + N|2\sigma_3 - \sigma_1 - \sigma_2|^m = \sigma_y^m\ . \end{aligned}$$

where σ_i are the principal stresses (which are aligned with the directions of anisotropy), σ_y is the yield stress, and *F, G, H, L, M, N* are constants. The value of *m* is determined by the degree of anisotropy of the material and must be greater than 1 to ensure convexity of the yield surface.

Generalized Hill yield criterion for plane stress

For transversely isotropic materials with 1 − 2 being the plane of symmetry, the generalized Hill yield criterion reduces to (with $F = G$ and $L = M$)

$$f := F|\sigma_2 - \sigma_3|^m + F|\sigma_3 - \sigma_1|^m + H|\sigma_1 - \sigma_2|^m + L|2\sigma_1 - \sigma_2 - \sigma_3|^m + L|2\sigma_2 - \sigma_3 - \sigma_1|^m + N|2\sigma_3 - \sigma_1 - \sigma_2|^m - \sigma_y^m \leq 0$$

The R-value or Lankford coefficient can be determined by considering the situation where $\sigma_1 > (\sigma_2 = \sigma_3 = 0)$. The R-value is then given by

$$R = \frac{(2^{m-1} + 2)L - N + H}{(2^{m-1} - 1)L + 2N + F}.$$

Under plane stress conditions and with some assumptions, the generalized Hill criterion can take several forms.

- **Case 1:** $L = 0, H = 0$.

$$f := \frac{1 + 2R}{1 + R}(|\sigma_1|^m + |\sigma_2|^m) - \frac{R}{1 + R}|\sigma_1 + \sigma_2|^m - \sigma_y^m \leq 0$$

- **Case 2:** $N = 0, F = 0$.

$$f := \frac{2^{m-1}(1 - R) + (R + 2)}{(1 - 2^{m-1})(1 + R)}|\sigma_1 - \sigma_2|^m - \frac{1}{(1 - 2^{m-1})(1 + R)}(|2\sigma_1 - \sigma_2|^m + |2\sigma_2 - \sigma_1|^m) - \sigma_y^m \leq 0$$

- **Case 3:** $N = 0, H = 0$.

$$f := \frac{2^{m-1}(1 - R) + (R + 2)}{(2 + 2^{m-1})(1 + R)}(|\sigma_1|^m - |\sigma_2|^m) + \frac{R}{(2 + 2^{m-1})(1 + R)}(|2\sigma_1 - \sigma_2|^m + |2\sigma_2 - \sigma_1|^m) - \sigma_y^m \leq 0$$

- **Case 4:** $L = 0, F = 0$.

$$f := \frac{1 + 2R}{2(1 + R)}|\sigma_1 - \sigma_2|^m + \frac{1}{2(1 + R)}|\sigma_1 + \sigma_2|^m - \sigma_y^m \leq 0$$

- **Case 5:** $L = 0, N = 0$.. This is the Hosford yield criterion.

$$f := \frac{1}{1 + R}(|\sigma_1|^m + |\sigma_2|^m) + \frac{R}{1 + R}|\sigma_1 - \sigma_2|^m - \sigma_y^m \leq 0$$

Care must be exercised in using these forms of the generalized Hill yield criterion because the yield surfaces become concave (sometimes even unbounded) for certain combinations of R and *m*.

Hill 1993 yield criterion

In 1993, Hill proposed another yield criterion for plane stress problems with planar anisotropy. The Hill93 criterion has the form

$$\left(\frac{\sigma_1}{\sigma_0}\right)^2 + \left(\frac{\sigma_2}{\sigma_{90}}\right)^2 + \left[(p+q-c) - \frac{p\sigma_1 + q\sigma_2}{\sigma_b}\right]\left(\frac{\sigma_1\sigma_2}{\sigma_0\sigma_{90}}\right) = 1$$

where σ_0 is the uniaxial tensile yield stress in the rolling direction, σ_{90} is the uniaxial tensile yield stress in the direction normal to the rolling direction, σ_b is the yield stress under uniform biaxial tension, and c,p,q are parameters defined as

$$c = \frac{\sigma_0}{\sigma_{90}} + \frac{\sigma_{90}}{\sigma_0} - \frac{\sigma_0\sigma_{90}}{\sigma_b^2}$$

$$\left(\frac{1}{\sigma_0} + \frac{1}{\sigma_{90}} - \frac{1}{\sigma_b}\right) \quad p = \frac{2R_0(\sigma_b - \sigma_{90})}{(1+R_0)\sigma_0^2} - \frac{2R_{90}\sigma_b}{(1+R_{90})\sigma_{90}^2} + \frac{c}{\sigma_0}$$

$$\left(\frac{1}{\sigma_0} + \frac{1}{\sigma_{90}} - \frac{1}{\sigma_b}\right) \quad q = \frac{2R_{90}(\sigma_b - \sigma_0)}{(1+R_{90})\sigma_{90}^2} - \frac{2R_0\sigma_b}{(1+R_0)\sigma_0^2} + \frac{c}{\sigma_{90}}$$

and R_0 is the R-value for uniaxial tension in the rolling direction, and R_{90} is the R-value for uniaxial tension in the in-plane direction perpendicular to the rolling direction.

Extensions of Hill's yield criteria

The original versions of Hill's yield criteria were designed for material that did not have pressure-dependent yield surfaces which are needed to model polymers and foams.

The Caddell-Raghava-Atkins yield criterion

An extension that allows for pressure dependence is Caddell-Raghava-Atkins (CRA) model which has the form

$$F(\sigma_{22}-\sigma_{33})^2+G(\sigma_{33}-\sigma_{11})^2+H(\sigma_{11}-\sigma_{22})^2+2L\sigma_{23}^2+2M\sigma_{31}^2+2N\sigma_{12}^2+I\sigma_{11}+J\sigma_{22}+K\sigma_{33}=1\,.$$

The Deshpande-Fleck-Ashby yield criterion

Another pressure-dependent extension of Hill's quadratic yield criterion which has a form similar to the Bresler Pister yield criterion is the Deshpande, Fleck and Ashby (DFA) yield criterion for honeycomb structures (used in sandwich composite construction). This yield criterion has the form

$$F(\sigma_{22}-\sigma_{33})^2+G(\sigma_{33}-\sigma_{11})^2+H(\sigma_{11}-\sigma_{22})^2+2L\sigma_{23}^2+2M\sigma_{31}^2+2N\sigma_{12}^2+K(\sigma_{11}+\sigma_{22}+\sigma_{33})^2=1\,.$$

Chapter 7

Hosford Yield Criterion

The Hosford yield criterion is a function that is used to determine whether a material has undergone plastic yielding under the action of stress.

Hosford yield criterion for isotropic plasticity

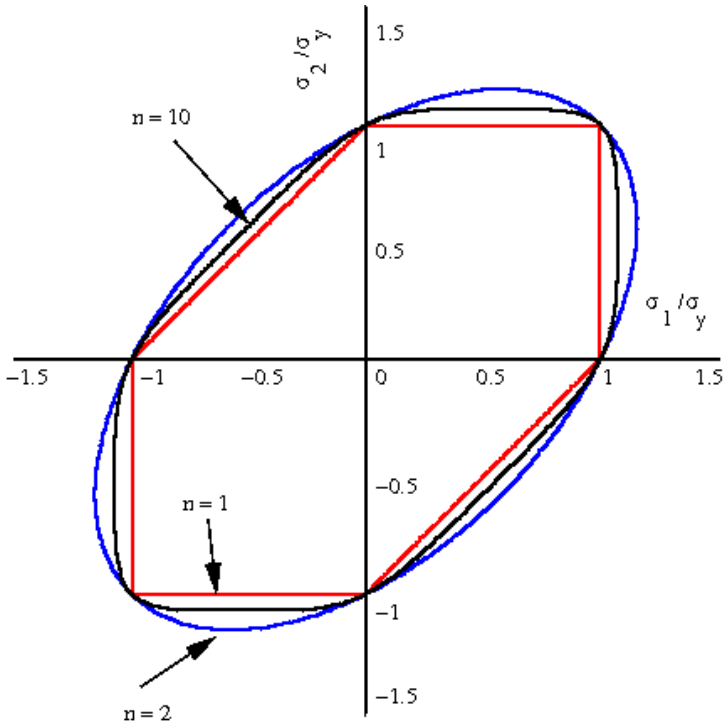

The plane stress, isotropic, Hosford yield surface for three values of *n*

The Hosford yield criterion for isotropic materials is a generalization of the von Mises yield criterion. It has the form

$$\tfrac{1}{2}|\sigma_2 - \sigma_3|^n + \tfrac{1}{2}|\sigma_3 - \sigma_1|^n + \tfrac{1}{2}|\sigma_1 - \sigma_2|^n = \sigma_y^n$$

where σ_i, i=1,2,3 are the principal stresses, *n* is a material-dependent exponent and σ_y is the yield stress in uniaxial tension/compression.

Alternatively, the yield criterion may be written as

$$\sigma_y = \left(\tfrac{1}{2}|\sigma_2 - \sigma_3|^n + \tfrac{1}{2}|\sigma_3 - \sigma_1|^n + \tfrac{1}{2}|\sigma_1 - \sigma_2|^n\right)^{1/n} .$$

This expression has the form of an L^p norm which is defined as

$$\|x\|_p = \left(|x_1|^p + |x_2|^p + \cdots + |x_n|^p\right)^{1/p} .$$

When $p = \infty$, the we get the L^∞ norm,

$\|x\|_\infty = \max\{|x_1|, |x_2|, \ldots, |x_n|\}$. Comparing this with the Hosford criterion

indicates that if $n = \infty$, we have

$$(\sigma_y)_{n\to\infty} = \max\left(|\sigma_2 - \sigma_3|, |\sigma_3 - \sigma_1|, |\sigma_1 - \sigma_2|\right) .$$

This is identical to the Tresca yield criterion.

Therefore, when *n = 1* or *n* goes to infinity the Hosford criterion reduces to the Tresca yield criterion. When *n = 2* the Hosford criterion reduces to the von Mises yield criterion.

Note that the exponent *n* does not need to be an integer.

Hosford yield criterion for plane stress

For the practically important situation of plane stress, the Hosford yield criterion takes the form

$$\frac{1}{2}\left(|\sigma_1|^n + |\sigma_2|^n\right) + \frac{1}{2}|\sigma_1 - \sigma_2|^n = \sigma_y^n$$

A plot of the yield locus in plane stress for various values of the exponent $n \geq 1$is shown in the adjacent figure.

Logan-Hosford yield criterion for anisotropic plasticity

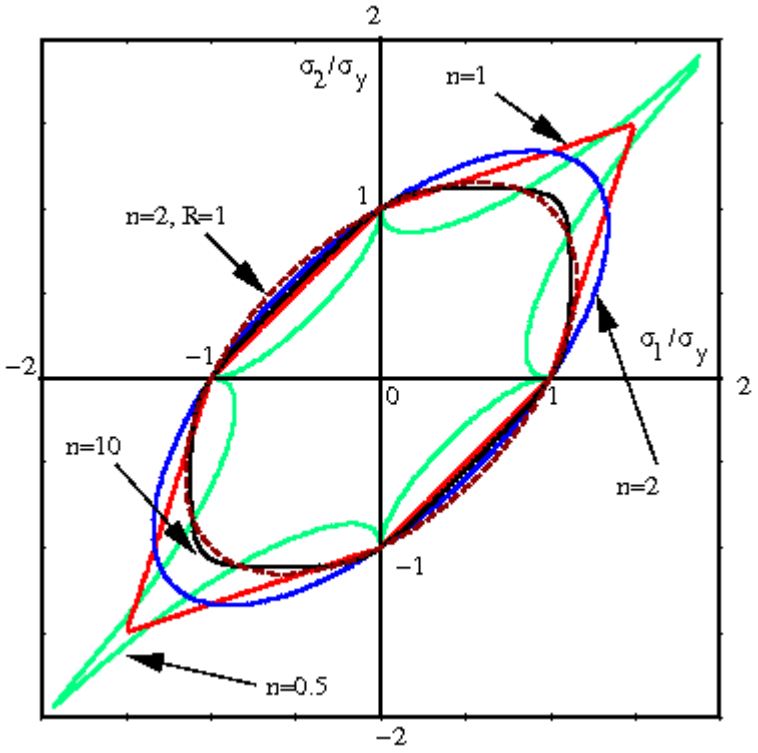

The plane stress, anisotropic, Hosford yield surface for four values of *n* and R=2.0

The Logan-Hosford yield criterion for anisotropic plasticity is similar to Hill's generalized yield criterion and has the form

$$F|\sigma_2 - \sigma_3|^n + G|\sigma_3 - \sigma_1|^n + H|\sigma_1 - \sigma_2|^n = 1$$

where *F,G,H* are constants, σ_i are the principal stresses, and the exponent *n* depends on the type of crystal (bcc, fcc, hcp, etc.) and has a value much greater than 2. Accepted values of *n* are 6 for bcc materials and 8 for fcc materials.

Though the form is similar to Hill's generalized yield criterion, the exponent *n* is independent of the R-value unlike the Hill's criterion.

Logan-Hosford criterion in plane stress

Under plane stress conditions, the Logan-Hosford criterion can be expressed as

$$\frac{1}{1+R}(|\sigma_1|^n + |\sigma_2|^n) + \frac{R}{1+R}|\sigma_1 - \sigma_2|^n = \sigma_y^n$$

where *R* is the R-value and σ_y is the yield stress in uniaxial tension/compression. For a derivation of this relation see Hill's yield criteria for plane stress. A plot of the yield locus

for the anisotropic Hosford criterion is shown in the adjacent figure. For values of n that are less than 2, the yield locus exhibits corners and such values are not recommended.

Chapter 8

Mohr–Coulomb Theory

Mohr–Coulomb theory is a mathematical model describing the response of brittle materials such as concrete, or rubble piles, to shear stress as well as normal stress. Most of the classical engineering materials somehow follow this rule in at least a portion of their shear failure envelope. Generally the theory applies to materials for which the compressive strength far exceeds the tensile strength.

In Geotechnical Engineering it is used to define shear strength of soils and rocks at different effective stresses.

In structural engineering it is used to determine failure load as well as the angle of fracture of a displacement fracture in concrete and similar materials. Coulomb's friction hypothesis is used to determine the combination of shear and normal stress that will cause a fracture of the material. Mohr's circle is used to determine which principal stresses that will produce this combination of shear and normal stress, and the angle of the plane in which this will occur. According to the principle of normality the stress introduced at failure will be perpendicular to the line describing the fracture condition.

It can be shown that a material failing according to Coulomb's friction hypothesis will show the displacement introduced at failure forming an angle to the line of fracture equal to the angle of friction. This makes the strength of the material determinable by comparing the external mechanical work introduced by the displacement and the external load with the internal mechanical work introduced by the strain and stress at the line of failure. By conservation of energy the sum of these must be zero and this will make it possible to calculate the failure load of the construction.

A common improvement of this model is to combine Coulomb's friction hypothesis with Rankine's principal stress hypothesis to describe a separation fracture.

History of the development

The Mohr–Coulomb theory is named in honour of Charles-Augustin de Coulomb and Christian Otto Mohr. Coulomb's contribution was a 1776 essay entitled "*Essai sur une application des règles des maximis et minimis à quelques problèmes de statique relatifs à l'architecture*" . Mohr developed a generalised form of the theory around the end of the 19th century. As the generalised form affected the interpretation of the criterion, but not the substance of it, some texts continue to refer to the criterion as simply the **'Coulomb criterion'** .

Mohr–Coulomb failure criterion

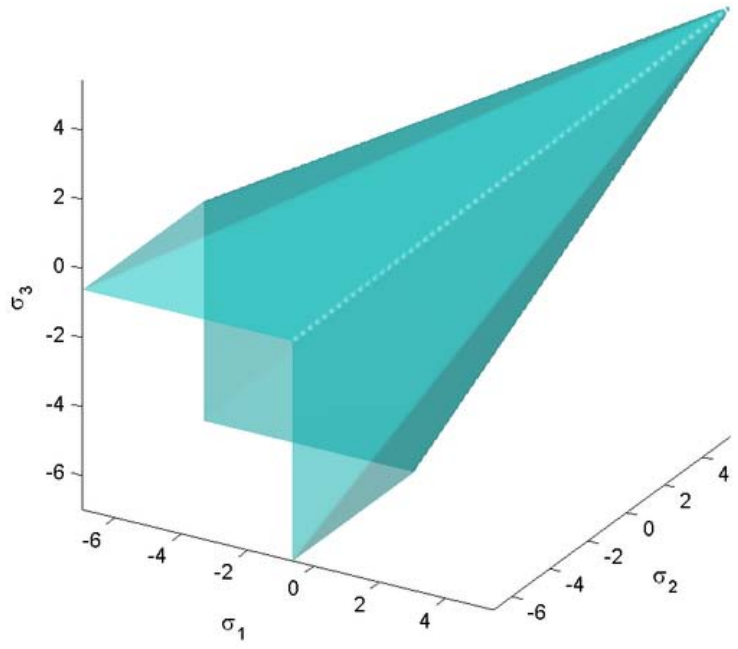

Figure 1: View of Mohr–Coulomb failure surface in 3D space of principal stresses for $c = 2, \phi = -20^\circ$

The Mohr–Coulomb failure criterion represents the linear envelope that is obtained from a plot of the shear strength of a material versus the applied normal stress. This relation is expressed as

$$\tau = \sigma \ \tan(\phi) + c$$

where τ is the shear strength, σ is the normal stress, *c* is the intercept of the failure envelope with the τ axis, and φ is the slope of the failure envelope. The quantity *c* is often called the **cohesion** and the angle φ is called the **angle of internal friction** . Compression is assumed to be positive in the following discussion. If compression is assumed to be negative then σ should be replaced with − σ.

If φ = 0, the Mohr–Coulomb criterion reduces to the Tresca criterion. On the other hand, if $\phi = 90^\circ$ the Mohr–Coulomb model is equivalent to the Rankine model. Higher values of φ are not allowed.

From Mohr's circle we have

$$\sigma = \sigma_m - \tau_m \sin\phi \ ; \quad \tau = \tau_m \cos\phi$$

where

$$\tau_m = \frac{\sigma_1 - \sigma_3}{2} \ ; \quad \sigma_m = \frac{\sigma_1 + \sigma_3}{2}$$

and σ_1 is the maximum principal stress and σ_3 is the minimum principal stress.

Therefore the Mohr–Coulomb criterion may also be expressed as

$$\tau_m = \sigma_m \sin\phi + c\cos\phi \ .$$

This form of the Mohr–Coulomb criterion is applicable to failure on a plane that is parallel to the σ_2 direction.

Mohr–Coulomb failure criterion in three dimensions

The Mohr–Coulomb criterion in three dimensions is often expressed as

$$\begin{cases} \pm\dfrac{\sigma_1 - \sigma_2}{2} = \left[\dfrac{\sigma_1 + \sigma_2}{2}\right]\sin(\phi) + c\cos(\phi) \\ \pm\dfrac{\sigma_2 - \sigma_3}{2} = \left[\dfrac{\sigma_2 + \sigma_3}{2}\right]\sin(\phi) + c\cos(\phi) \\ \pm\dfrac{\sigma_3 - \sigma_1}{2} = \left[\dfrac{\sigma_3 + \sigma_1}{2}\right]\sin(\phi) + c\cos(\phi) \end{cases}$$

The Mohr–Coulomb failure surface is a cone with a hexagonal cross section in deviatoric stress space.

The expressions for τ and σ can be generalized to three dimensions by developing expressions for the normal stress and the resolved shear stress on a plane of arbitrary orientation with respect to the coordinate axes (basis vectors). If the unit normal to the plane of interest is

$$\mathbf{n} = n_1\ \mathbf{e}_1 + n_2\ \mathbf{e}_2 + n_3\ \mathbf{e}_3$$

where $\mathbf{e}_i, \quad i = 1, 2, 3$ are three orthonormal unit basis vectors, and if the principal stresses $\sigma_1,\sigma_2,\sigma_3$ are aligned with the basis vectors $\mathbf{e}_1, \mathbf{e}_2, \mathbf{e}_3$, then the expressions for σ,τ are

$$\begin{aligned}\sigma &= n_1^2\sigma_1 + n_2^2\sigma_2 + n_3^2\sigma_3 \\ \tau &= \sqrt{(n_1\sigma_1)^2 + (n_2\sigma_2)^2 + (n_3\sigma_3)^2 - \sigma^2} \\ &= \sqrt{n_1^2n_2^2(\sigma_1 - \sigma_2)^2 + n_2^2n_3^2(\sigma_2 - \sigma_3)^2 + n_3^2n_1^2(\sigma_3 - \sigma_1)^2}\end{aligned}$$

The Mohr–Coulomb failure criterion can then be evaluated using the usual expression

$$\tau = \sigma\ \tan(\phi) + c$$

for the six planes of maximum shear stress.

Derivation of normal and shear stress on a plane

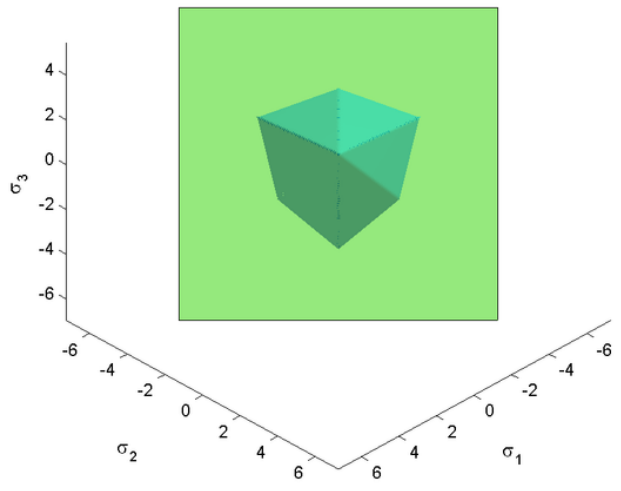

Figure 2: Mohr–Coulomb yield surface in the π-plane for $c = 2, \phi = -20°$

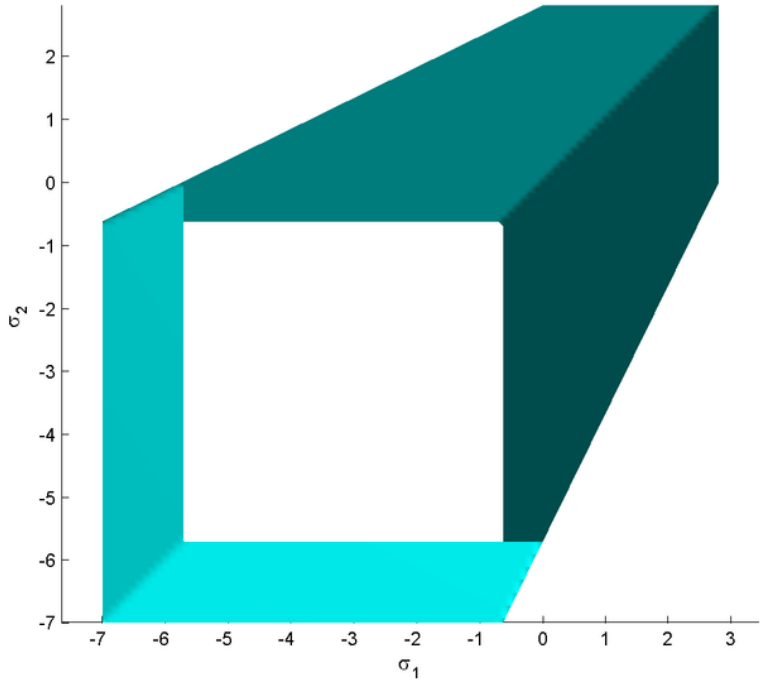

Figure 3: Trace of the Mohr–Coulomb yield surface in the $\sigma_1 - \sigma_2$-plane for $c = 2, \phi = -20^\circ$

Mohr–Coulomb failure surface in Haigh–Westergaard space

The Mohr–Coulomb failure (yield) surface is often expressed in Haigh–Westergaad coordinates. For example, the function

$$\frac{\sigma_1 - \sigma_3}{2} = \frac{\sigma_1 + \sigma_3}{2} \sin\phi + c\cos\phi$$

can be expressed as

$$\left[\sqrt{3}\ \sin\left(\theta + \frac{\pi}{3}\right) - \sin\phi\cos\left(\theta + \frac{\pi}{3}\right)\right]\rho - \sqrt{2}\sin(\phi)\xi = \sqrt{6}c\cos\phi$$

Alternatively, in terms of the invariants *p*,*q*,*r* we can write

$$\left[\frac{1}{\sqrt{3}\ \cos\phi}\ \sin\left(\theta + \frac{\pi}{3}\right) - \frac{1}{3}\tan\phi\ \cos\left(\theta + \frac{\pi}{3}\right)\right]q - p\ \tan\phi = c$$

where

$$\theta = \frac{1}{3}\arccos\left[\left(\frac{r}{q}\right)^3\right] \quad .$$

Mohr–Coulomb yield and plasticity

The Mohr–Coulomb yield surface is often used to model the plastic flow of geomaterials (and other cohesive-frictional materials). Many such materials show dilatational behavior under triaxial states of stress which the Mohr–Coulomb model does not include. Also, since the yield surface has corners, it may be inconvenient to use the original Mohr–Coulomb model to determine the direction of plastic flow (in the flow theory of plasticity).

A common approach that is used is to use a **non-associated** plastic flow potential that is smooth. An example of such a potential is the function

$$g := \sqrt{(\alpha c_{\mathrm{y}} \tan\psi)^2 + G^2(\phi,\theta)\ q^2} - p\tan\phi$$

where α is a parameter, c_{y} is the value of c when the plastic strain is zero (also called the **initial cohesion yield stress**), ψ is the angle made by the yield surface in the **Rendulic plane** at high values of p (this angle is also called the **dilation angle**), and $G(\varphi,\theta)$ is an appropriate function that is also smooth in the deviatoric stress plane.

Chapter 9

Drucker Prager Yield Criterion

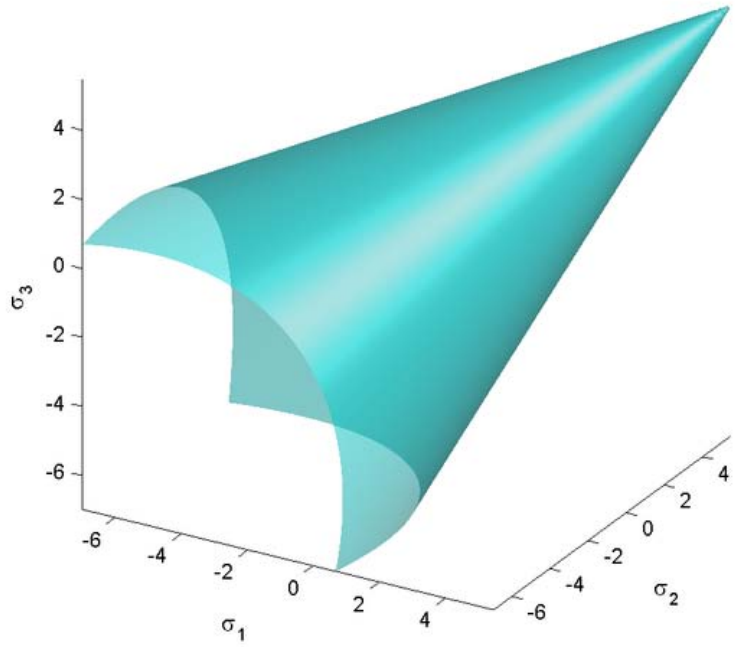

Figure 1: View of Drucker–Prager yield surface in 3D space of principal stresses for $c = 2, \phi = -20^\circ$

The Drucker–Prager yield criterion is a pressure-dependent model for determining whether a material has failed or undergone plastic yielding. The criterion was introduced to deal with the plastic deformation of soils. It and its many variants have been applied to rock, concrete, polymers, foams, and other pressure-dependent materials.

The Drucker–Prager yield criterion has the form

$$\sqrt{J_2} = A + B\ I_1$$

where I_1 is the first invariant of the Cauchy stress and J_2 is the second invariant of the deviatoric part of the Cauchy stress. The constants A,B are determined from experiments.

In terms of the equivalent stress (or von Mises stress) and the hydrostatic (or mean) stress, the Drucker–Prager criterion can be expressed as

$$\sigma_e = a + b\ \sigma_m$$

where σ_e is the equivalent stress, σ_m is the hydrostatic stress, and a,b are material constants. The Drucker–Prager yield criterion expressed in Haigh–Westergaard coordinates is

$$\tfrac{1}{\sqrt{2}}\rho - \sqrt{3}\ B\xi = A$$

The Drucker–Prager yield surface is a smooth version of the Mohr–Coulomb yield surface.

Expressions for A and B

The Drucker–Prager model can be written in terms of the principal stresses as

$$\sqrt{\frac{1}{6}[(\sigma_1 - \sigma_2)^2 + (\sigma_2 - \sigma_3)^2 + (\sigma_3 - \sigma_1)^2]} = A + B\ (\sigma_1 + \sigma_2 + \sigma_3)\ .$$

If σ_t is the yield stress in uniaxial tension, the Drucker–Prager criterion implies

$$\frac{1}{\sqrt{3}}\,\sigma_t = A + B\ \sigma_t\ .$$

If σ_c is the yield stress in uniaxial compression, the Drucker–Prager criterion implies

$$\frac{1}{\sqrt{3}}\,\sigma_c = A - B\ \sigma_c\ .$$

Solving these two equations gives

$$A = \frac{2}{\sqrt{3}}\ \left(\frac{\sigma_c\ \sigma_t}{\sigma_c + \sigma_t}\right)\ ;\quad B = \frac{1}{\sqrt{3}}\ \left(\frac{\sigma_t - \sigma_c}{\sigma_c + \sigma_t}\right)\ .$$

Uniaxial asymmetry ratio

Different uniaxial yield stresses in tension and in compression are predicted by the Drucker–Prager model. The uniaxial asymmetry ratio for the Drucker–Prager model is

$$\beta = \frac{\sigma_{\mathrm{c}}}{\sigma_{\mathrm{t}}} = \frac{1 - \sqrt{3}\ B}{1 + \sqrt{3}\ B}\ .$$

Expressions in terms of cohesion and friction angle

Since the Drucker–Prager yield surface is a smooth version of the Mohr–Coulomb yield surface, it is often expressed in terms of the cohesion (*c*) and the angle of internal friction (φ) that are used to describe the Mohr–Coulomb yield surface. If we assume that the Drucker–Prager yield surface **circumscribes** the Mohr–Coulomb yield surface then the expressions for *A* and *B* are

$$A = \frac{6\ c\ \cos\phi}{\sqrt{3}(3 + \sin\phi)}\ ; \quad B = \frac{2\ \sin\phi}{\sqrt{3}(3 + \sin\phi)}$$

If the Drucker–Prager yield surface **inscribes** the Mohr–Coulomb yield surface then

$$A = \frac{6\ c\ \cos\phi}{\sqrt{3}(3 - \sin\phi)}\ ; \quad B = \frac{2\ \sin\phi}{\sqrt{3}(3 - \sin\phi)}$$

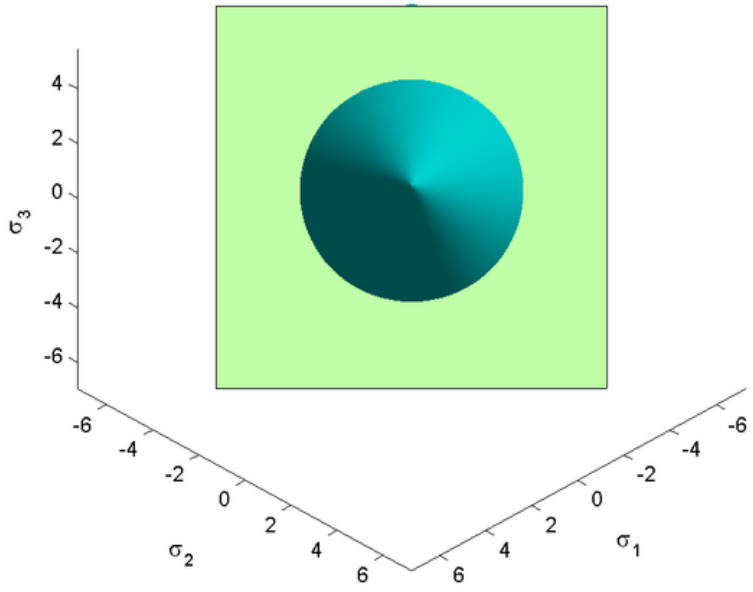

Figure 2: Drucker–Prager yield surface in the π-plane for $c = 2, \phi = -20^\circ$

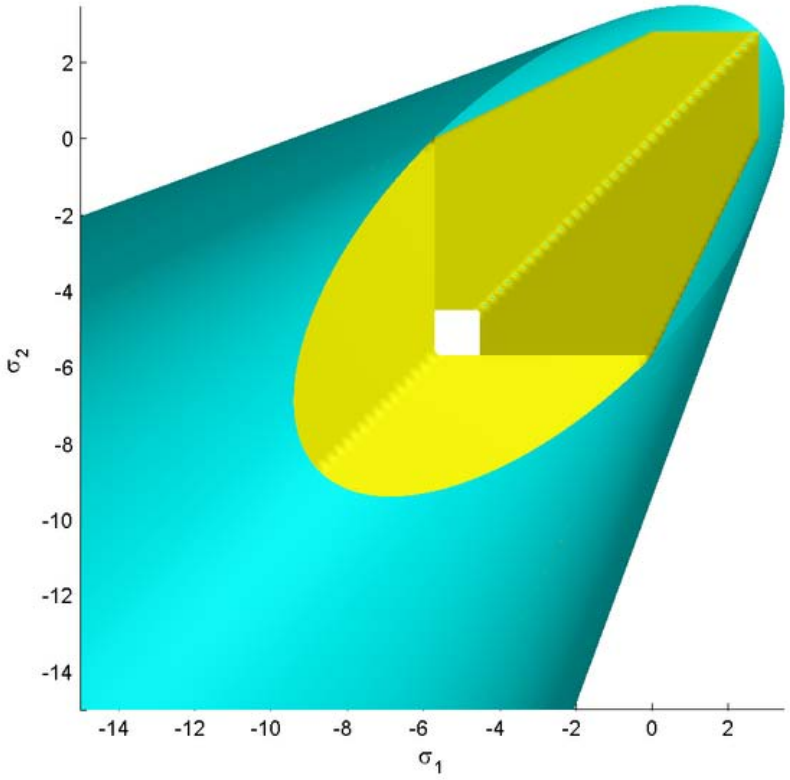

Figure 3: Trace of the Drucker–Prager and Mohr–Coulomb yield surfaces in the $\sigma_1 - \sigma_2$-plane for $c = 2, \phi = -20^\circ$. Yellow = Mohr–Coulomb, Cyan = Drucker–Prager.

Drucker–Prager model for polymers

The Drucker–Prager model has been used to model polymers such as polyoxymethylene and polypropylene. For polyoxymethylene the yield stress is a linear function of the pressure. However, polypropylene shows a quadratic pressure-dependence of the yield stress.

Drucker–Prager model for foams

For foams, the GAZT model uses

$$A = \pm \frac{\sigma_y}{\sqrt{3}}; \quad B = \mp \frac{1}{\sqrt{3}} \left(\frac{\rho}{5\ \rho_s} \right)$$

where σ_y is a critical stress for failure in tension or compression, ρ is the density of the foam, and ρ_s is the density of the base material.

Extensions of the isotropic Drucker–Prager model

The Drucker–Prager criterion can also be expressed in the alternative form

$$J_2 = (A + B\ I_1)^2 = a + b\ I_1 + c\ I_1^2\ .$$

Deshpande–Fleck yield criterion

The Deshpande–Fleck yield criterion for foams has the form given in above equation. The parameters *a*,*b*,*c* for the Deshpande–Fleck criterion are

$$a = (1 + \beta^2)\ \sigma_y^2\ , \quad b = 0\ , \quad c = -\frac{\beta^2}{3}$$

where β is a parameter that determines the shape of the yield surface, and σ_y is the yield stress in tension or compression.

Anisotropic Drucker–Prager yield criterion

An anisotropic form of the Drucker–Prager yield criterion is the Liu–Huang–Stout yield criterion . This yield criterion is an extension of the generalized Hill yield criterion and has the form

$$\begin{aligned} f :=& \sqrt{F(\sigma_{11}-\sigma_{22})^2 + G(\sigma_{22}-\sigma_{33})^2 + H(\sigma_{33}-\sigma_{11})^2 + 2L\sigma_{23}^2 + 2M\sigma_{31}^2 + 2N\sigma_{12}^2} \\ &+ I\sigma_{11} + J\sigma_{22} + K\sigma_{33} - 1 \le 0 \end{aligned}$$

The coefficients *F*,*G*,*H*,*L*,*M*,*N*,*I*,*J*,*K* are

$$\begin{aligned} F =& \frac{1}{2}\left[\Sigma_2^2 + \Sigma_3^2 - \Sigma_1^2\right]\ ;\quad G = \frac{1}{2}\left[\Sigma_3^2 + \Sigma_1^2 - \Sigma_2^2\right]\ ;\quad H = \frac{1}{2}\left[\Sigma_1^2 + \Sigma_2^2 - \Sigma_3^2\right] \\ L =& \frac{1}{2(\sigma_{23}^y)^2}\ ;\quad M = \frac{1}{2(\sigma_{31}^y)^2}\ ;\quad N = \frac{1}{2(\sigma_{12}^y)^2} \\ I =& \frac{\sigma_{1c} - \sigma_{1t}}{2\sigma_{1c}\sigma_{1t}}\ ;\quad J = \frac{\sigma_{2c} - \sigma_{2t}}{2\sigma_{2c}\sigma_{2t}}\ ;\quad K = \frac{\sigma_{3c} - \sigma_{3t}}{2\sigma_{3c}\sigma_{3t}} \end{aligned}$$

where

$$\Sigma_1 := \frac{\sigma_{1c} + \sigma_{1t}}{2\sigma_{1c}\sigma_{1t}}\ ;\quad \Sigma_2 := \frac{\sigma_{2c} + \sigma_{2t}}{2\sigma_{2c}\sigma_{2t}}\ ;\quad \Sigma_3 := \frac{\sigma_{3c} + \sigma_{3t}}{2\sigma_{3c}\sigma_{3t}}$$

and $\sigma_{ic}, i = 1,2,3$ are the uniaxial yield stresses in **compression** in the three principal directions of anisotropy, $\sigma_{it}, i = 1,2,3$ are the uniaxial yield stresses in **tension**, and $\sigma_{23}^{y}, \sigma_{31}^{y}, \sigma_{12}^{y}$ are the yield stresses in pure shear.

The Drucker yield criterion

The Drucker–Prager criterion should not be confused with the earlier Drucker criterion which is independent of the pressure (I_1). The Drucker yield criterion has the form

$$f := J_2^3 - \alpha\ J_3^2 - k^2 \leq 0$$

where J_2 is the second invariant of the deviatoric stress, J_3 is the third invariant of the deviatoric stress, α is a constant that lies between -27/8 and 9/4 (for the yield surface to be convex), k is a constant that varies with the value of α. For α = 0, $k^2 = \frac{\sigma_y^6}{27}$ where σ_y is the yield stress in uniaxial tension.

Anisotropic Drucker Criterion

An anisotropic version of the Drucker yield criterion is the Cazacu–Barlat (CZ) yield criterion which has the form

$$f := (J_2^0)^3 - \alpha\ (J_3^0)^2 - k^2 \leq 0$$

where J_2^0, J_3^0 are generalized forms of the deviatoric stress and are defined as

$$J_2^0 := \frac{1}{6}\left[a_1(\sigma_{22}-\sigma_{33})^2 + a_2(\sigma_{33}-\sigma_{11})^2 + a_3(\sigma_{11}-\sigma_{22})^2\right] + a_4\sigma_{23}^2 + a_5\sigma_{31}^2 + a_6\sigma_{12}^2$$

$$\begin{aligned} J_3^0 := {} & \frac{1}{27}\left[(b_1+b_2)\sigma_{11}^3 + (b_3+b_4)\sigma_{22}^3 + \{2(b_1+b_4)-(b_2+b_3)\}\sigma_{33}^3\right] \\ & - \frac{1}{9}\left[(b_1\sigma_{22}+b_2\sigma_{33})\sigma_{11}^2 + (b_3\sigma_{33}+b_4\sigma_{11})\sigma_{22}^2 + \{(b_1-b_2+b_4)\sigma_{11}+(b_1-b_3+b_4)\sigma_{22}\}\sigma_{33}^2\right] \\ & + \frac{2}{9}(b_1+b_4)\sigma_{11}\sigma_{22}\sigma_{33} + 2b_{11}\sigma_{12}\sigma_{23}\sigma_{31} \\ & - \frac{1}{3}\left[\{2b_9\sigma_{22} - b_8\sigma_{33} - (2b_9-b_8)\sigma_{11}\}\sigma_{31}^2 + \{2b_{10}\sigma_{33} - b_5\sigma_{22} - (2b_{10}-b_5)\sigma_{11}\}\sigma_{12}^2\right. \\ & \left. \{(b_6+b_7)\sigma_{11} - b_6\sigma_{22} - b_7\sigma_{33}\}\sigma_{23}^2\right] \end{aligned}$$

Cazacu–Barlat yield criterion for plane stress

For thin sheet metals, the state of stress can be approximated as plane stress. In that case the Cazacu–Barlat yield criterion reduces to its two-dimensional version with

$$J_2^0 = \frac{1}{6}\left[(a_2+a_3)\sigma_{11}^2 + (a_1+a_3)\sigma_{22}^2 - 2a_3\sigma_1\sigma_2\right] + a_6\sigma_{12}^2$$

$$J_3^0 = \frac{1}{27}\left[(b_1+b_2)\sigma_{11}^3 + (b_3+b_4)\sigma_{22}^3\right] - \frac{1}{9}\left[b_1\sigma_{11} + b_4\sigma_{22}\right]\sigma_{11}\sigma_{22} + \frac{1}{3}\left[b_5\sigma_{22} + (2b_{10}-b_5)\sigma_{11}\right]\sigma_{12}^2$$

For thin sheets of metals and alloys, the parameters of the Cazacu–Barlat yield criterion are

Table 1. **Cazacu–Barlat yield criterion parameters for sheet metals and alloys**

Material	a_1	a_2	a_3	a_6	b_1	b_2	b_3	b_4	b_5	b_{10}	α
6016-T4 Aluminum Alloy	0.815	0.815	0.334	0.42	0.04	-1.205	-0.958	0.306	0.153	-0.02	1.4
2090-T3 Aluminum Alloy	1.05	0.823	0.586	0.96	1.44	0.061	-1.302	-0.281	-0.375	0.445	1.285

Chapter 10

Bresler Pister Yield Criterion

The **Bresler-Pister yield criterion** is a function that was originally devised to predict the strength of concrete under multiaxial stress states. This yield criterion is an extension of the Drucker-Prager yield criterion and can be expressed on terms of the stress invariants as

$$\sqrt{J_2} = A + B\ I_1 + C\ I_1^2$$

where I_1 is the first invariant of the Cauchy stress, J_2 is the second invariant of the deviatoric part of the Cauchy stress, and A,B,C are material constants.

Yield criteria of this form have also been used for polypropylene and polymeric foams .

The parameters A,B,C have to be chosen with care for reasonably shaped yield surfaces. If σ_c is the yield stress in uniaxial compression, σ_t is the yield stress in uniaxial tension, and σ_b is the yield stress in biaxial compression, the parameters can be expressed as

$$B = \left(\frac{\sigma_t - \sigma_c}{\sqrt{3}(\sigma_t + \sigma_c)}\right)\left(\frac{4\sigma_b^2 - \sigma_b(\sigma_c + \sigma_t) + \sigma_c\sigma_t}{4\sigma_b^2 + 2\sigma_b(\sigma_t - \sigma_c) - \sigma_c\sigma_t}\right)$$

$$C = \left(\frac{1}{\sqrt{3}(\sigma_t + \sigma_c)}\right)\left(\frac{\sigma_b(3\sigma_t - \sigma_c) - 2\sigma_c\sigma_t}{4\sigma_b^2 + 2\sigma_b(\sigma_t - \sigma_c) - \sigma_c\sigma_t}\right)$$

$$A = \frac{\sigma_c}{\sqrt{3}} + c_1\sigma_c - c_2\sigma_c^2$$

Derivation of expressions for parameters A, B, C

The Bresler-Pister yield criterion in terms of the principal stresses σ_1,σ_2,σ_3 is

$$\frac{1}{\sqrt{6}}\left[(\sigma_1-\sigma_2)^2+(\sigma_2-\sigma_3)^2+(\sigma_3-\sigma_1)^2\right]^{1/2}-A-B\,(\sigma_1+\sigma_2+\sigma_3)-C\,(\sigma_1+\sigma_2+\sigma_3)^2=0\,.$$

If $\sigma_t = \sigma_1$ is the yield stress in uniaxial tension, then

$$\frac{1}{\sqrt{3}}\,\sigma_t - A - B\sigma_t - C\sigma_t^2 = 0\ .$$

If $-\sigma_c = \sigma_1$ is the yield stress in uniaxial compression, then

$$\frac{1}{\sqrt{3}}\,\sigma_c - A + B\sigma_c - C\sigma_c^2 = 0\ .$$

If $-\sigma_b = \sigma_1 = \sigma_2$ is the yield stress in equibiaxial compression, then

$$\frac{1}{\sqrt{3}}\,\sigma_b - A + 2B\sigma_b - 4C\sigma_b^2 = 0\ .$$

Solving these three equations for A,B,C (using Maple) gives us

$$A := \frac{1}{\sqrt{3}}\,\frac{\sigma_c\sigma_t\sigma_b(\sigma_t+8\sigma_b-3\sigma_c)}{(\sigma_c+\sigma_t)(2\sigma_b-\sigma_c)(2\sigma_b+\sigma_t)}$$

$$B := \frac{1}{\sqrt{3}}\,\frac{(\sigma_c-\sigma_t)(\sigma_b\sigma_c+\sigma_b\sigma_t-\sigma_c\sigma_t-4\sigma_b^2)}{(\sigma_c+\sigma_t)(2\sigma_b-\sigma_c)(2\sigma_b+\sigma_t)}$$

$$C := \frac{1}{\sqrt{3}}\,\frac{3\sigma_b\sigma_t-\sigma_b\sigma_c-2\sigma_c\sigma_t}{(\sigma_c+\sigma_t)(2\sigma_b-\sigma_c)(2\sigma_b+\sigma_t)}$$

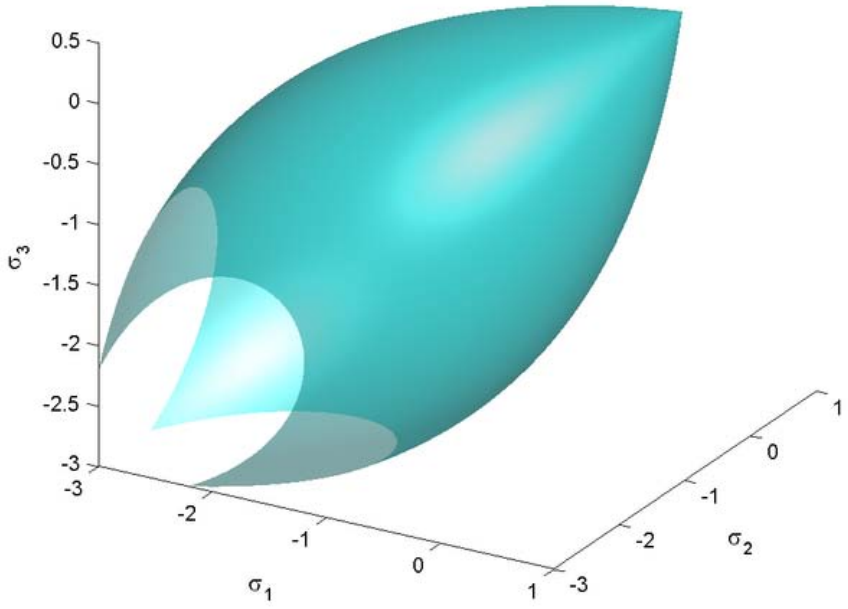

Figure 1: View of the three-parameter Bresler-Pister yield surface in 3D space of principal stresses for $\sigma_c = 1, \sigma_t = 0.3, \sigma_b = 1.7$

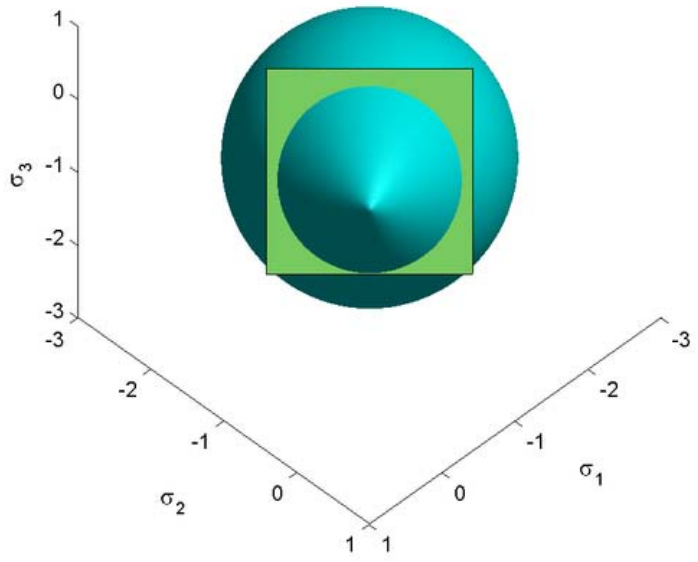

Figure 2: The three-parameter Bresler-Pister yield surface in the π-plane for $\sigma_c = 1, \sigma_t = 0.3, \sigma_b = 1.7$

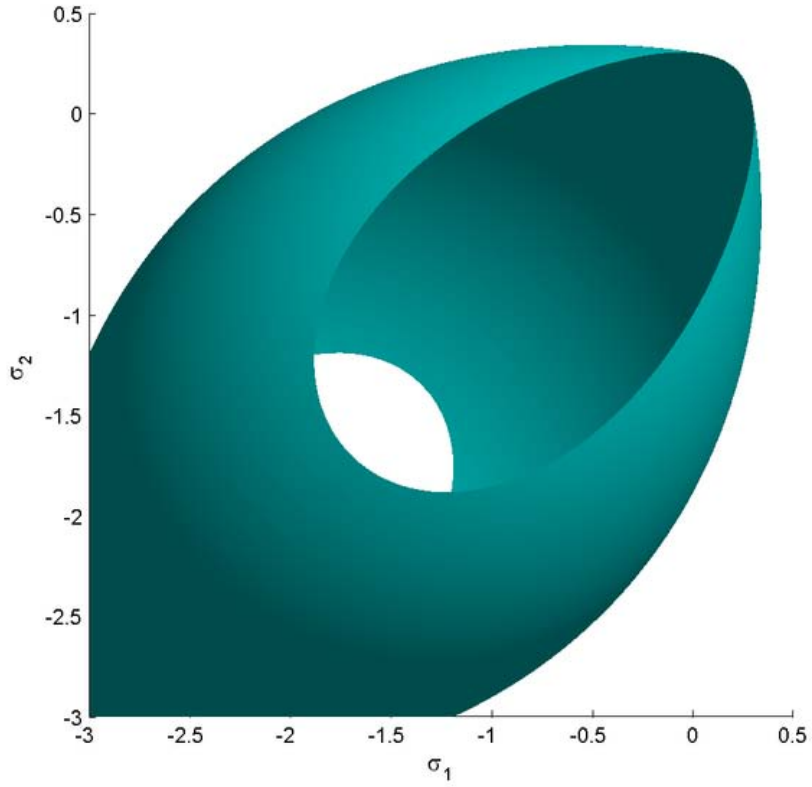

Figure 3: Trace of the three-parameter Bresler-Pister yield surface in the $\sigma_1 - \sigma_2$-plane for $\sigma_c = 1, \sigma_t = 0.3, \sigma_b = 1.7$

Alternative forms of the Bresler-Pister yield criterion

In terms of the equivalent stress (σ_e) and the mean stress (σ_m), the Bresler-Pister yield criterion can be written as

$$\sigma_e = a + b\,\sigma_m + c\,\sigma_m^2\;; \quad \sigma_e = \sqrt{3J_2}\;, \quad \sigma_m = I_1/3\;.$$

The Etse-Willam form of the Bresler-Pister yield criterion for concrete can be expressed as

$$\sqrt{J_2} = \frac{1}{\sqrt{3}}\,I_1 - \frac{1}{2\sqrt{3}}\left(\frac{\sigma_t}{\sigma_c^2 - \sigma_t^2}\right)\,I_1^2$$

where σ_c is the yield stress in uniaxial compression and σ_t is the yield stress in uniaxial tension.

The GAZT yield criterion for plastic collapse of foams also has a form similar to the Bresler-Pister yield criterion and can be expressed as

$$\sqrt{J_2} = \begin{cases} \frac{1}{\sqrt{3}}\,\sigma_t - 0.03\sqrt{3}\frac{\rho}{\rho_m\ \sigma_t}\ I_1^2 \\ -\frac{1}{\sqrt{3}}\,\sigma_c + 0.03\sqrt{3}\frac{\rho}{\rho_m\ \sigma_c}\ I_1^2 \end{cases}$$

where ρ is the density of the foam and ρ_m is the density of the matrix material.

Chapter 11

Willam-Warnke Yield Criterion

The **Willam-Warnke yield criterion** is a function that is used to predict when failure will occur in concrete and other cohesive-frictional materials such as rock, soil, and ceramics. This yield criterion has the functional form

$$f(I_1, J_2, J_3) = 0$$

where I_1 is the first invariant of the Cauchy stress tensor, and J_2,J_3 are the second and third invariants of the deviatoric part of the Cauchy stress tensor. There are three material parameters (σ_c - the uniaxial compressive strength, σ_t - the uniaxial tensile strength, σ_b - the equibiaxial compressive strength) that have to be determined before the Willam-Warnke yield criterion may be applied to predict failure.

In terms of I_1,J_2,J_3, the Willam-Warnke yield criterion can be expressed as

$$f := \sqrt{J_2} + \lambda(J_2, J_3)\ (\tfrac{I_1}{3} - B) = 0$$

where λ is a function that depends on J_2,J_3 and the three material parameters and B depends only on the material parameters. The function λ can be interpreted as the friction angle which depends on the Lode angle (θ). The quantity B is interpreted as a cohesion pressure. The Willam-Warnke yield criterion may therefore be viewed as a combination of the Mohr-Coulomb and the Drucker-Prager yield criteria.

Willam-Warnke yield function

In the original paper, the three-parameter Willam-Warnke yield function was expressed as

$$f := \frac{1}{3z}\frac{I_1}{\sigma_c} + \sqrt{\frac{2}{5}}\frac{1}{r(\theta)}\frac{\sqrt{J_2}}{\sigma_c} - 1 \leq 0$$

where I_1 is the first invariant of the stress tensor, J_2 is the second invariant of the deviatoric part of the stress tensor, σ_c is the yield stress in uniaxial compression, and θ is the Lode angle given by

$$\theta = \tfrac{1}{3}\cos^{-1}\left(\frac{3\sqrt{3}}{2}\frac{J_3}{J_2^{3/2}}\right) .$$

The locus of the boundary of the stress surface in the deviatoric stress plane is expressed in polar coordinates by the quantity $r(\theta)$ which is given by

$$r(\theta) := \frac{u(\theta) + v(\theta)}{w(\theta)}$$

where

$$\begin{aligned} u(\theta) :=& 2\ r_c\ (r_c^2 - r_t^2)\ \cos\theta \\ v(\theta) :=& r_c\ (2\ r_t - r_c)\sqrt{4\ (r_c^2 - r_t^2)\ \cos^2\theta + 5\ r_t^2 - 4\ r_t\ r_c} \\ w(\theta) :=& 4(r_c^2 - r_t^2)\cos^2\theta + (r_c - 2\ r_t)^2 \end{aligned}$$

The quantities r_t and r_c describe the position vectors at the locations $\theta = 0^\circ, 60^\circ$ and can be expressed in terms of σ_c,σ_b,σ_t as

$$r_c := \sqrt{\frac{6}{5}}\left[\frac{\sigma_b\sigma_t}{3\sigma_b\sigma_t + \sigma_c(\sigma_b - \sigma_t)}\right] \quad ; \quad r_t := \sqrt{\frac{6}{5}}\left[\frac{\sigma_b\sigma_t}{\sigma_c(2\sigma_b + \sigma_t)}\right]$$

The parameter z in the model is given by

$$z := \frac{\sigma_b\sigma_t}{\sigma_c(\sigma_b - \sigma_t)} .$$

The Haigh-Westergaard representation of the Willam-Warnke yield condition can be written as

$$f(\xi, \rho, \theta) = 0 \quad \equiv \quad f := \bar{\lambda}(\theta)\ \rho + \bar{B}\ \xi - \sigma_c \leq 0$$

where

$$\bar{B} := \frac{1}{\sqrt{3}\ z} ; \quad \bar{\lambda} := \frac{1}{\sqrt{5}\ r(\theta)} .$$

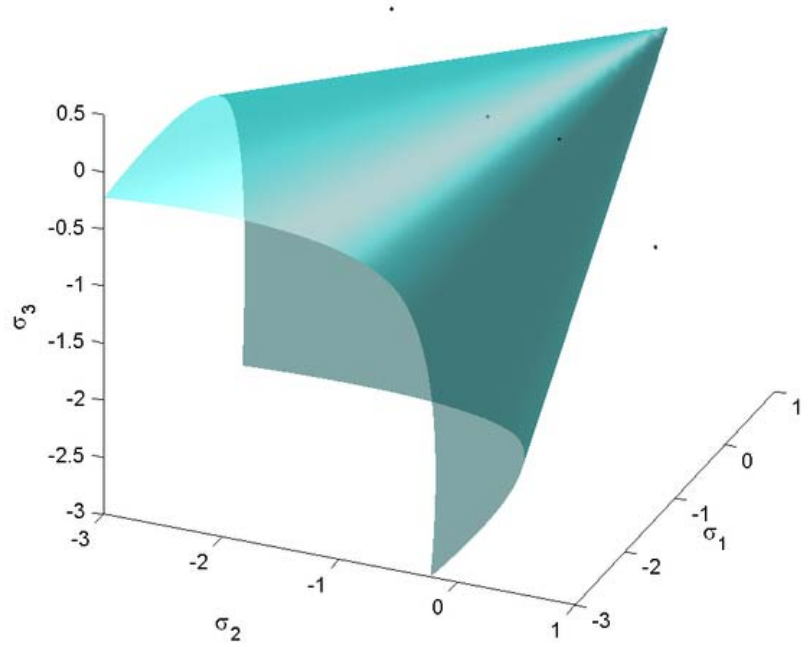

Figure 1: View of three-parameter Willam-Warnke yield surface in 3D space of principal stresses for $\sigma_c = 1, \sigma_t = 0.3, \sigma_b = 1.7$

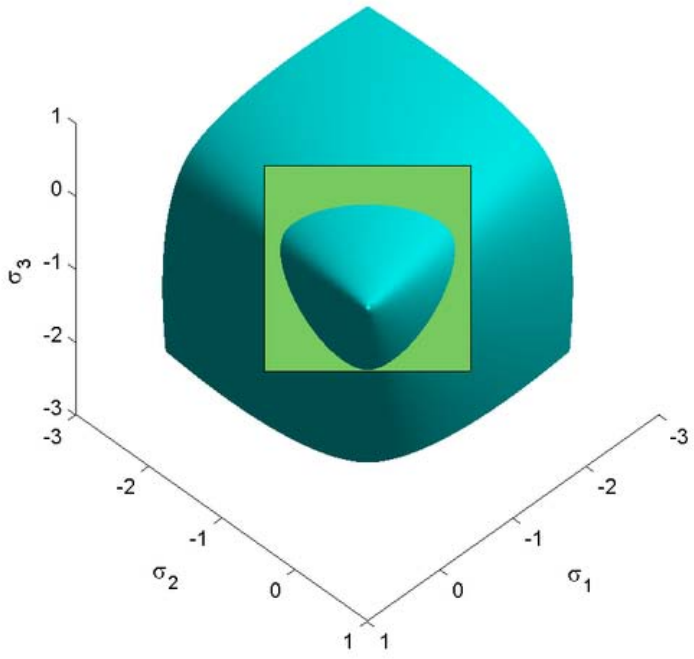

Figure 2: Three-parameter Willam-Warnke yield surface in the π-plane for $\sigma_c = 1, \sigma_t = 0.3, \sigma_b = 1.7$

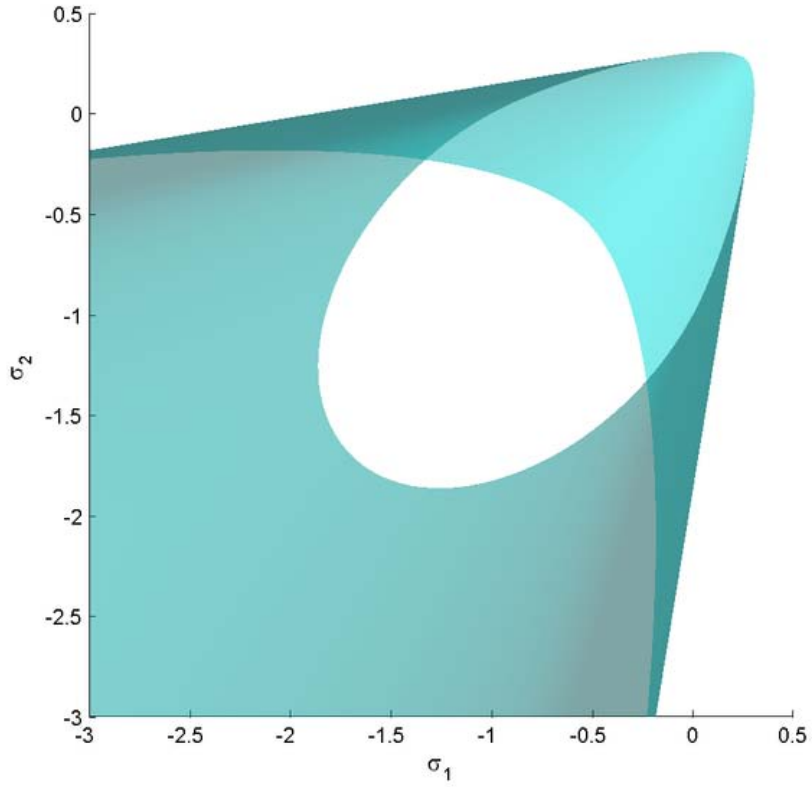

Figure 3: Trace of the three-parameter Willam-Warnke yield surface in the $\sigma_1 - \sigma_2$-plane for $\sigma_c = 1, \sigma_t = 0.3, \sigma_b = 1.7$

Modified forms of the Willam-Warnke yield criterion

An alternative form of the Willam-Warnke yield criterion in Haigh-Westergaard coordinates is the Ulm-Coussy-Bazant form :

$$f(\xi, \rho, \theta) = 0 \quad \text{or} \quad f := \rho + \bar{\lambda}(\theta) \ \left(\xi - \bar{B}\right) = 0$$

where

$$\bar{\lambda} := \sqrt{\tfrac{2}{3}} \ \frac{u(\theta) + v(\theta)}{w(\theta)} \ ; \quad \bar{B} := \tfrac{1}{\sqrt{3}} \ \left[\frac{\sigma_b \sigma_t}{\sigma_b - \sigma_t}\right]$$

and

$$r_t := \frac{\sqrt{3}\,(\sigma_b - \sigma_t)}{2\sigma_b - \sigma_t}$$

$$r_c := \frac{\sqrt{3}\,\sigma_c\,(\sigma_b - \sigma_t)}{(\sigma_c + \sigma_t)\sigma_b - \sigma_c\sigma_t}$$

The quantities r_c,r_t are interpreted as friction coefficients. For the yield surface to be convex, the Willam-Warnke yield criterion requires that $2\,r_t \geq r_c \geq r_t/2$and $0 \leq \theta \leq \frac{\pi}{3}$.

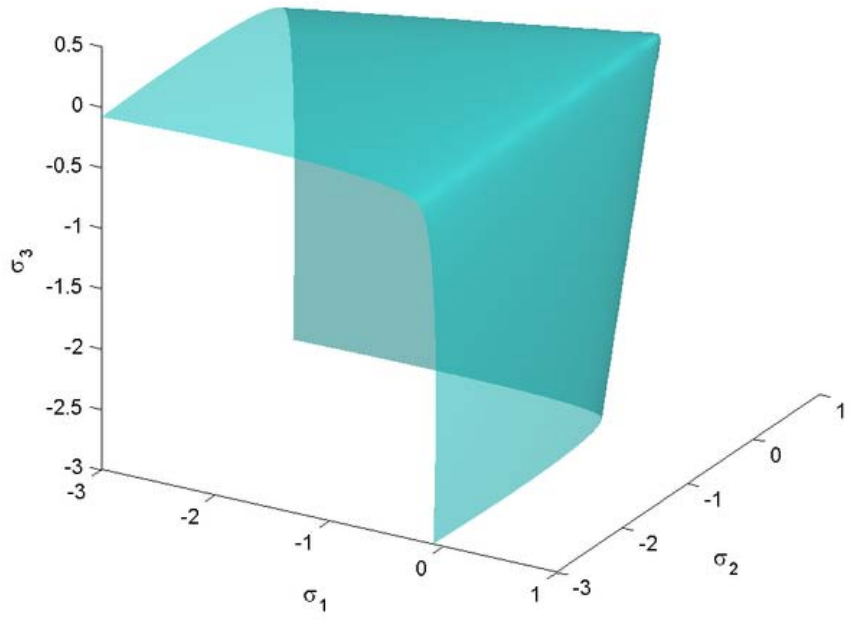

Figure 4: View of Ulm-Coussy-Bazant version of the three-parameter Willam-Warnke yield surface in 3D space of principal stresses for $\sigma_c = 1$,$\sigma_t = 0.3$,$\sigma_b = 1.7$

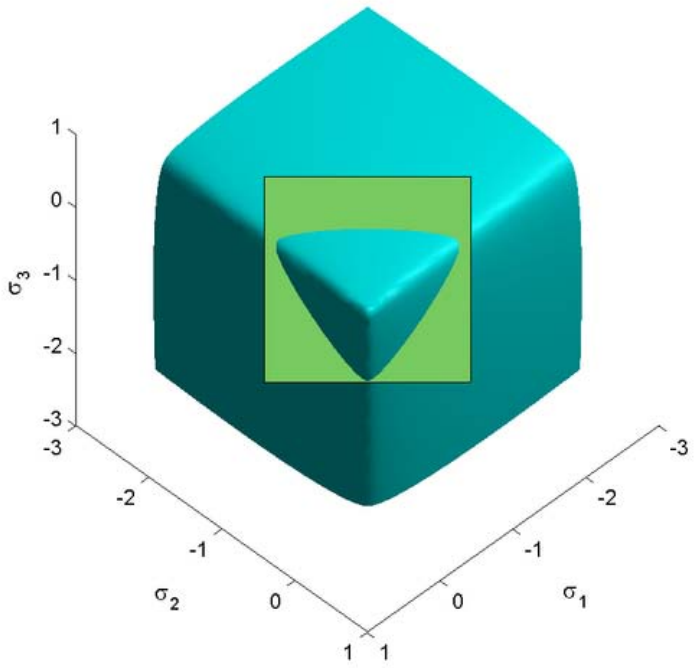

Figure 5: Ulm-Coussy-Bazant version of the three-parameter Willam-Warnke yield surface in the π-plane for $\sigma_c = 1, \sigma_t = 0.3, \sigma_b = 1.7$

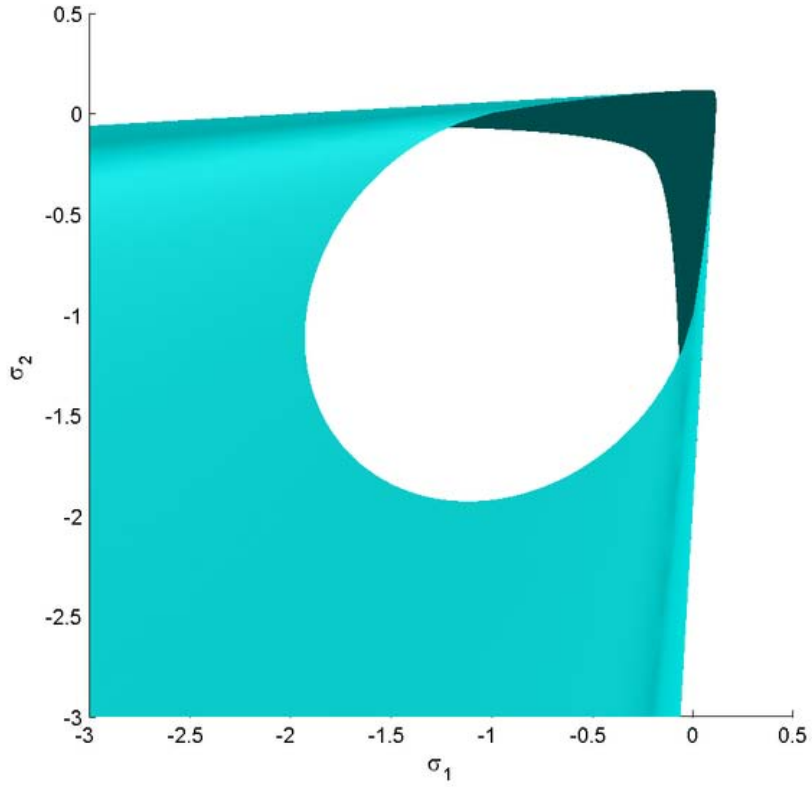

Figure 6: Trace of the Ulm-Coussy-Bazant version of the three-parameter Willam-Warnke yield surface in the $\sigma_1 - \sigma_2$-plane for $\sigma_c = 1, \sigma_t = 0.3, \sigma_b = 1.7$

Chapter 12

Grain Boundary Strengthening

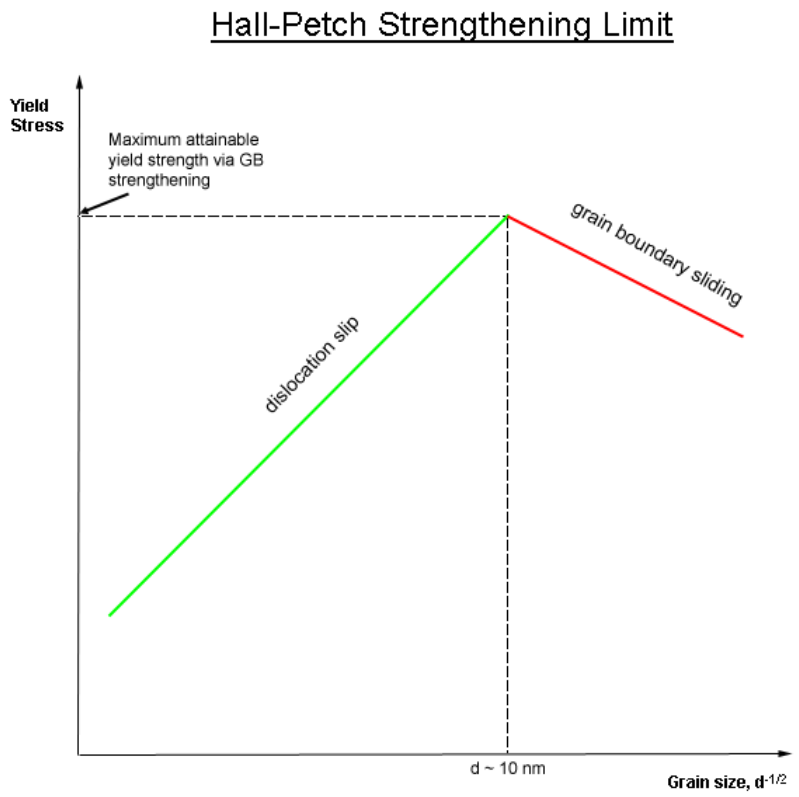

Figure 1: Hall-Petch Strengthening is limited by the size of dislocations. Once the grain size reaches about 10 nanometres (3.9×10^{-7} in), grain boundaries start to slide.

Grain-boundary strengthening (or **Hall-Petch strengthening**) is a method of strengthening materials by changing their average crystallite (grain) size. It is based on the observation that grain boundaries impede dislocation movement and that the number of dislocations within a grain have an effect on how easily dislocations can traverse grain boundaries and travel from grain to grain. So, by changing grain size one can influence

dislocation movement and yield strength. For example, heat treatment after plastic deformation and changing the rate of solidification are ways to alter grain size.

Theory

In grain-boundary strengthening the grain boundaries act as pinning points impeding further dislocation propagation. Since the lattice structure of adjacent grains differs in orientation, it requires more energy for a dislocation to change directions and move into the adjacent grain. The grain boundary is also much more disordered than inside the grain, which also prevents the dislocations from moving in a continuous slip plane. Impeding this dislocation movement will hinder the onset of plasticity and hence increase the yield strength of the material.

Under an applied stress, existing dislocations and dislocations generated by Frank-Read Sources will move through a crystalline lattice until encountering a grain boundary, where the large atomic mismatch between different grains creates a repulsive stress field to oppose continued dislocation motion. As more dislocations propagate to this boundary, dislocation 'pile up' occurs as a cluster of dislocations are unable to move past the boundary. As dislocations generate repulsive stress fields, each successive dislocation will apply a repulsive force to the dislocation incident with the grain boundary. These repulsive forces act as a driving force to reduce the energetic barrier for diffusion across the boundary, such that additional pile up causes dislocation diffusion across the grain boundary, allowing further deformation in the material. Decreasing grain size decreases the amount of possible pile up at the boundary, increasing the amount of applied stress necessary to move a dislocation across a grain boundary. The higher the applied stress to move the dislocation, the higher the yield strength. Thus, there is then an inverse relationship between grain size and yield strength, as demonstrated by the Hall-Petch equation. However, when there is a large direction change in the orientation of the two adjacent grains, the dislocation may not necessarily move from one grain to the other but instead create a new source of dislocation in the adjacent grain. The theory remains the same that more grain boundaries create more opposition to dislocation movement and in turn strengthens the material.

Obviously, there is a limit to this mode of strengthening, as infinitely strong materials do not exist. Grain sizes can range from about 100 μm (0.0039 in) (large grains) to 1 μm (3.9×10^{-5} in) (small grains). Lower than this, the size of dislocations begins to approach the size of the grains. At a grain size of about 10 nm (3.9×10^{-7} in), only one or two dislocations can fit inside of a grain. This scheme prohibits dislocation pile-up and never results in grain boundary diffusion. The lattice resolves the applied stress by grain boundary sliding, resulting in a *decrease* in the material's yield strength.

To understand the mechanism of grain boundary strengthening one must understand the nature of dislocation-dislocation interactions. Dislocations create a stress field around them given by:

$$\sigma \propto Gbln(\frac{r}{r_0}),$$

where G is the material's shear modulus, and b is the Burgers vector. If the dislocations are in the right alignment with respect to each other, the local stress fields they create will repel each other. This helps dislocation movement along grains and across grain boundaries. Hence, the more dislocations are present in a grain, the greater the stress field felt by a dislocation near a grain boundary:

$$\tau_{felt} = \tau_{applied} + n_{dislocation}\tau_{dislocation}$$

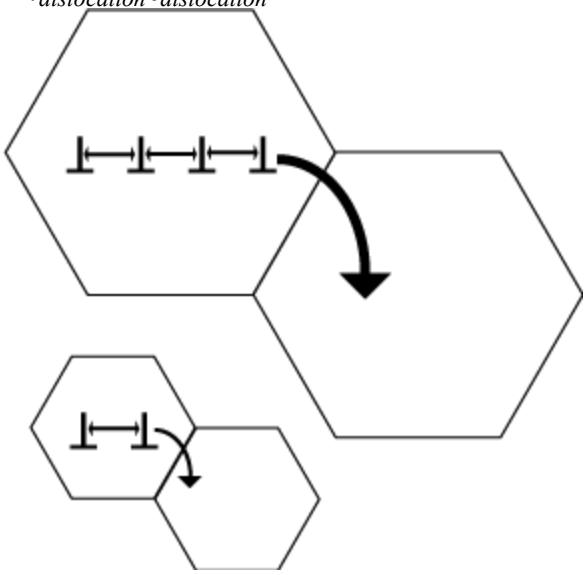

This is a schematic roughly illustrating the concept of dislocation pile up and how it affects the strength of the material. A material with larger grain size is able to have more dislocation to pile up leading to a bigger driving force for dislocations to move from one grain to another. Thus you will have to apply less force to move a dislocation from a larger than from a smaller grain, leading materials with smaller grains to exhibit higher yield stress.

Subgrain strengthening

A subgrain is a part of the grain that is only slightly disoriented from other parts of the grain. Current research is being done to see the effect of subgrain strengthening in materials. Depending on the processing of the material, subgrains can form within the grains of the material. For example, when Fe-based material is ball-milled for long periods of time (e.g. 100+ hours), subgrains of 60-90 nm are formed. It has been shown that the higher the density of the subgrains, the higher the yield stress of the material due to the increased subgrain boundary. The strength of the metal was found to vary reciprocally with the size of the subgrain, which is analogous to the Hall-Petch equation. The subgrain boundary strengthening also has a breakdown point of around a subgrain size of 0.1 nm, which is the size where any subgrains smaller than that size would decrease yield strength. .

Hall-Petch relationship

Hall-Petch constants

Material	σ_o [MPa]	k [MPa $m^{1/2}$]
Copper	25	0.11
Titanium	80	0.40
Mild steel	70	0.74
Ni_3Al	300	1.70

There is an inverse relationship between delta yield strength and grain size to some power, *x*.

$$\Delta\tau \propto \frac{k}{d^x}$$

where *k* is the strengthening coefficient and both *k* and *x* are material specific. The smaller the grain size, the smaller the repulsion stress felt by a grain boundary dislocation and the higher the applied stress needed to propagate dislocations through the material.

The relation between yield stress and grain size is described mathematically by the Hall-Petch equation:

$$\sigma_y = \sigma_0 + \frac{k_y}{\sqrt{d}}$$

where σ_y is the yield stress, σ_o is a materials constant for the starting stress for dislocation movement (or the resistance of the lattice to dislocation motion), k_y is the strengthening coefficient (a constant unique to each material), and *d* is the average grain diameter.

Theoretically, a material could be made infinitely strong if the grains are made infinitely small. This is impossible though, because the lower limit of grain size is a single unit cell of the material. Even then, if the grains of a material are the size of a single unit cell, then the material is in fact amorphous, not crystalline, since there is no long range order, and dislocations can not be defined in an amorphous material. It has been observed experimentally that the microstructure with the highest yield strength is a grain size of about 10 nm (3.9×10^{-7} in), because grains smaller than this undergo another yielding mechanism, grain boundary sliding. Producing engineering materials with this ideal grain size is difficult because only thin films can be reliably produced with grains of this size.

History

In the early 1950s two groundbreaking series of papers were written independently on the relationship between grain boundaries and strength.

In 1951, while at the University of Sheffield, E.O. Hall wrote three papers which appeared in volume 64 of the Proceedings of the Physical Society. In his third paper, Hall showed that the length of slip bands or crack lengths correspond to grain sizes and thus a relationship could be established between the two. Hall concentrated on the yielding properties of mild steels.

Based on his experimental work carried out in 1946–1949, N.J. Petch of the University of Leeds, England published a paper in 1953 independent from Hall's. Petch's paper concentrated more on brittle fracture. By measuring the variation in cleavage strength with respect to ferritic grain size at very low temperatures, Petch found a relationship exact to that of Hall's. Thus this important relationship is named after both Hall and Petch.

Reverse or inverse Hall-Petch relation

The Hall-Petch relation predicts that as the grain size decreases the yield strength increases. The Hall-Petch relation was experimentally found to be an effective model for materials with grain sizes ranging from 1 millimeter to 1 micrometre. Consequently it was believed that if average grain size could be decreased even further to the nanometer length scale the yield strength would increase as well. However, experiments on many nanocrystalline materials demonstrated that if the grains reached a small enough size, the critical grain size which is typically less than 100 nm (3.9×10^{-6} in), the yield strength would either remain constant or decrease with decreasing grains size. This phenomenon has been termed the reverse or inverse Hall-Petch Relation. A number of different mechanisms have been proposed for this relation. As suggested by Carlton et al. they fall into four categories: (1) Dislocation based (2) Diffusion based (3) Grain boundary shearing based (4) Two phase based.

Other explanations that have been proposed to rationalize the apparent softening of metals with nanosized grains include poor sample quality and the suppression of dislocation pileups.

Many of the early measurements of a reverse Hall-Petch effect were likely the result of unrecognized pores in samples. The presence of voids in nanocrystalline metals would undoubtedly lead to their having weaker mechanical properties.

The pileup of dislocations at grain boundaries is a hallmark mechanism of the Hall-Petch relationship. Once grain sizes drop below the equilibrium distance between dislocations, though, this relationship should no longer be valid. Nevertheless, it is not entirely clear what exactly the dependency of yield stress should be on grain sizes below this point.

Grain refinement

Grain refinement, also known as *inoculation*, is the set of techniques used to implement grain boundary strengthening in metallurgy. The specific techniques and corresponding mechanisms will vary based on what materials are being considered.

One method for controlling grain size in aluminum alloys is by introducing particles to serve as nucleants, such as Al-5%Ti. Grains will grow via heterogeneous nucleation; that is, for a given degree of undercooling beneath the melting temperature, aluminum particles in the melt will nucleate on the surface of the added particles. Grains will grow in the form of dendrites growing radially away from the surface of the nucleant. Solute particles can then be added (called grain refiners) which limit the growth of dendrites, leading to grain refinement. TiB2 is a common grain refiner for Al alloys; however, novel refiners such as Al3Sc have been suggested.

One common technique is to induce a very small fraction of the melt to solidify at a much higher temperature than the rest; this will generate seed crystals that act as a template when the rest of the material falls to its (lower) melting temperature and begins to solidify. Since a huge number of minuscule seed crystals are present, a nearly equal number of crystallites result, and the size of any one grain is limited.

Typical inoculants for various casting alloys

Metal	Inoculant
Cast iron	FeSi, SiCa, graphite
Mg alloys	Zr, C
Cu alloys	Fe, Co, Zr
Al-Si alloys	P, Ti, B
Pb alloys	As, Te
Zn alloys	Ti
Ti alloys	Al-Ti intermetallics

Chapter 13

Work Hardening

Work hardening, also known as **strain hardening** or **cold working**, is the strengthening of a metal by plastic deformation. This strengthening occurs because of dislocation movements within the crystal structure of the material. Any material with a reasonably high melting point such as metals and alloys can be strengthened in this fashion. Alloys not amenable to heat treatment, including low-carbon steel, are often work-hardened. Some materials cannot be work-hardened at normal ambient temperatures, such as indium, however others can only be strengthened via work hardening, such as pure copper and aluminum.

Work hardening may be desirable or undesirable depending on the context. An example of undesirable work hardening is during machining when early passes of a cutter inadvertently work-harden the workpiece surface, causing damage to the cutter during the later passes. An example of desirable work hardening is that which occurs in metalworking processes that intentionally induce plastic deformation to exact a shape change. These processes are known as **cold working** or **cold forming** processes. They are characterized by shaping the workpiece at a temperature below its recrystallization temperature, usually at the ambient temperature. Cold forming techniques are usually classified into four major groups: squeezing, bending, drawing, and shearing.

History

Copper was the first metal in common use for tools and containers since it is one of the few metals available in non-oxidized form, not requiring the smelting of an ore. Copper is easily softened by heating and cooling (it does not harden by quenching, as in cool water). In this annealed state it may then be hammered, stretched and otherwise formed, progressing toward the desired final shape, but becoming harder and less ductile as work progresses. If work continues beyond a certain hardness the metal will tend to fracture when worked and so it may be re-annealed periodically as the shape progresses. Annealing is stopped when the workpiece is near its final desired shape, and so the final product will have a desired stiffness and hardness. The technique of repoussé exploits these properties of copper, enabling the construction of durable jewelry articles and sculptures (including the Statue of Liberty).

For metal objects designed to flex, such as springs, specialized alloys are usually employed in order to avoid work hardening (a result of plastic deformation) and metal fatigue, with specific heat treatments required to obtain the necessary characteristics.

Devices made from aluminum and its alloys, such as aircraft, must be carefully designed to minimize or evenly distribute flexure, which can lead to work hardening and in turn stress cracking, possibly causing catastrophic failure. For this reason modern aluminum aircraft will have an imposed working lifetime (dependent upon the type of loads encountered), after which the aircraft must be retired.

Theory

Before work hardening, the lattice of the material exhibits a regular, defect-free (no dislocations) pattern. The defect-free lattice can be created or restored at any time by annealing. As the material is work hardened it becomes increasingly saturated with new dislocations, and more dislocations are prevented from nucleating (a resistance to dislocation-formation develops). This resistance to dislocation-formation manifests itself as a resistance to plastic deformation; hence, the observed strengthening.

In metallic crystals, irreversible deformation is usually carried out on a microscopic scale by defects called dislocations, which are created by fluctuations in local stress fields within the material culminating in a lattice rearrangement as the dislocations propagate through the lattice. At normal temperatures the dislocations are not annihilated by annealing. Instead, the dislocations accumulate, interact with one another, and serve as pinning points or obstacles that significantly impede their motion. This leads to an increase in the yield strength of the material and a subsequent decrease in ductility.

Such deformation increases the concentration of dislocations which may subsequently form low-angle grain boundaries surrounding sub-grains. Cold working generally results in a higher yield strength as a result of the increased number of dislocations and the Hall-Petch effect of the sub-grains, and a decrease in ductility. The effects of cold working may be reversed by annealing the material at high temperatures where recovery and recrystallization reduce the dislocation density.

A material's work hardenability can be predicted by analyzing a stress-strain curve, or studied in context by performing hardness tests before and after a process.

Elastic and plastic deformation

Work hardening is a consequence of plastic deformation, a permanent change in shape. This is distinct from elastic deformation, which is reversible. Most materials do not exhibit only one or the other, but rather a combination of the two. The following discussion mostly applies to metals, especially steels, which are well studied. Work hardening occurs most notably for ductile materials such as metals. Ductility is the ability of a material to undergo large plastic deformations before fracture (for example, bending a steel rod until it finally breaks).

The tensile test is widely used to study deformation mechanisms. This is because under compression, most materials will experience trivial (lattice mismatch) and non-trivial (buckling) events before plastic deformation or fracture occur. Hence the intermediate processes that occur to the material under uniaxial compression before the incidence of plastic deformation make the compressive test fraught with difficulties.

A material generally deforms elastically if it is under the influence of small forces, allowing the material to readily return to its original shape when the deforming force is removed. This phenomenon is called *elastic deformation*. This behavior in materials is described by Hooke's Law. Materials behave elastically until the deforming force increases beyond the elastic limit, also known as the yield stress. At this point, the material is rendered permanently deformed and fails to return to its original shape when the force is removed. This phenomenon is called *plastic deformation*. For example, if one stretches a coil spring up to a certain point, it will return to its original shape, but once it is stretched beyond the elastic limit, it will remain deformed and won't return to its original state.

Elastic deformation stretches atomic bonds in the material away from their equilibrium radius of separation of a bond, without applying enough energy to break the inter-atomic bonds. Plastic deformation, on the other hand, breaks inter-atomic bonds, and involves the rearrangement of atoms in a solid material.

Dislocations and lattice strain fields

In materials science parlance, dislocations are defined as line defects in a material's crystal structure. They are surrounded by relatively strained (and weaker) bonds than the bonds between the constituents of the regular crystal lattice. This explains why these bonds break first during plastic deformation. Like any thermodynamic system, the crystals tend to lower their energy through bond formation between constituents of the crystal. Thus the dislocations interact with one another and the atoms of the crystal. This results in a lower but energetically favorable energy conformation of the crystal. Dislocations are a "negative-entity" in that they do not exist: they are merely vacancies in the host medium which does exist. As such, the material itself does not move much. To a much greater extent visible "motion" is movement in a bonding pattern of largely stationary atoms.

The strained bonds around a dislocation are characterized by lattice strain fields. For example, there are compressively strained bonds directly next to an edge dislocation and tensilely strained bonds beyond the end of an edge dislocation. These form compressive strain fields and tensile strain fields, respectively. Strain fields are analogous to electric fields in certain ways. Additionally, the strain fields of dislocations, obey the laws of attraction and repulsion.

The visible (macroscopic) results of plastic deformation are the result of microscopic dislocation motion. For example, the stretching of a steel rod in a tensile tester is accommodated through dislocation motion on the atomic scale.

Increase of dislocations and work hardening

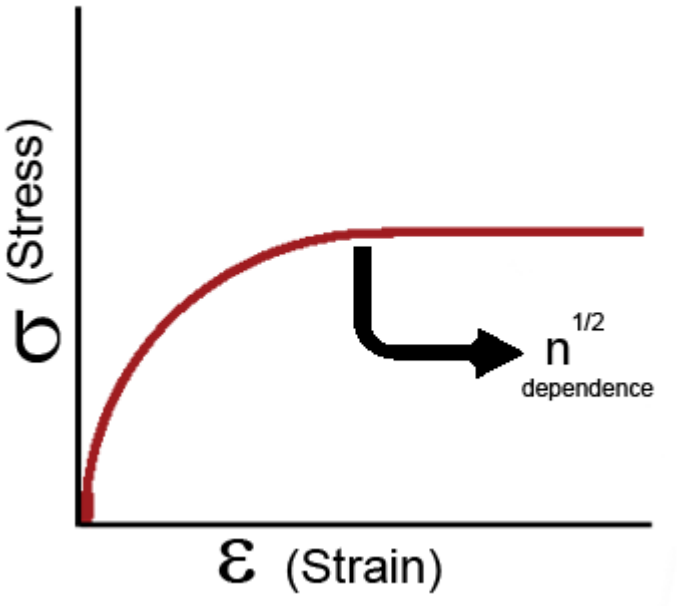

Figure 1: The yield stress of an ordered material has a half-root dependency on the number of dislocations present.

Increase in the number of dislocations is a quantification of work hardening. Plastic deformation occurs as a consequence of work being done on a material; energy is added to the material. In addition, the energy is almost always applied fast enough and in large enough magnitude to not only move existing dislocations, but also to *produce* a great number of new dislocations by jarring or working the material sufficiently enough. New dislocations are generated by Frank-Read source.

Yield strength is increased in a cold-worked material. Using lattice strain fields, it can be shown that an environment filled with dislocations will hinder the movement of any one dislocation. Because dislocation motion is hindered, plastic deformation cannot occur at normal stresses. Upon application of stresses just beyond the yield strength of the non-cold-worked material, a cold-worked material will continue to deform using the only mechanism available: elastic deformation. The regular scheme of stretching or compressing of electrical bonds (without dislocation motion) continues to occur, and the modulus of elasticity is unchanged. Eventually the stress is great enough to overcome the strain-field interactions and plastic deformation resumes.

However, ductility of a work-hardened material is decreased. Ductility is the extent to which a material can undergo plastic deformation, that is, it is how far a material can be plastically deformed before fracture. A cold-worked material is, in effect, a normal material that has already been extended through part of its allowed plastic deformation. If dislocation motion and plastic deformation have been hindered enough by dislocation

accumulation, and stretching of electronic bonds and elastic deformation have reached their limit, a third mode of deformation occurs: fracture.

Quantification of work hardening

The stress, τ, of dislocation is dependent on the shear modulus, G, the lattice constant, b, and the dislocation density, $\rho_{\perp}$:

$$\tau = \tau_0 + G\alpha b\rho_{\perp}^{1/2}$$

where τ_0 is the intrinsic strength of the material with low dislocation density and α is a correction factor specific to the material.

As shown in Figure 1 and the equation above, work hardening has a half root dependency on the number of dislocations. The material exhibits high strength if there are either high levels of dislocations (greater than 10^{14} dislocations per m^2) or no dislocations. A moderate number of dislocations (between 10^7 and 10^9 dislocations per m^2) typically results in low strength.

Example

For an extreme example, in a tensile test a bar of steel is strained to just before the distance at which it usually fractures. The load is released smoothly and the material relieves some of its strain by decreasing in length. The decrease in length is called the elastic recovery, and the end result is a work-hardened steel bar. The fraction of length recovered (length recovered/original length) is equal to the yield-stress divided by the modulus of elasticity. (Here we discuss true stress in order to account for the drastic decrease in diameter in this tensile test.) The length recovered after removing a load from a material just before it breaks is equal to the length recovered after removing a load just before it enters plastic deformation.

The work-hardened steel bar has a large enough number of dislocations that the strain field interaction prevents all plastic deformation. Subsequent deformation requires a stress that varies linearly with the strain observed, the slope of the graph of stress vs. strain is the modulus of elasticity, as usual.

The work-hardened steel bar fractures when the applied stress exceeds the usual fracture stress and the strain exceeds usual fracture strain. This may be considered to be the elastic limit and the yield stress is now equal to the fracture toughness, which is of course, much higher than a non-work-hardened-steel yield stress.

The amount of plastic deformation possible is zero, which is obviously less than the amount of plastic deformation possible for a non-work-hardened material. Thus, the ductility of the cold-worked bar is reduced.

Substantial and prolonged cavitation can also produce strain hardening.

Additionally, jewelers will construct structurally sound rings and other wearable objects (especially those worn on the hands) that require much more durability (than earrings for example) by utilizing a material's ability to be work hardened. While casting rings is done for a number of economical reasons (saving a great deal of time and cost of labor), a master jeweler may utilize the ability of a material to be work hardened and apply some combination of cold forming techniques during the production of a piece.

Empirical relations

There are two common mathematical descriptions of the work hardening phenomenon. Hollomon's equation is a power law relationship between the stress and the amount of plastic strain:

$$\sigma = K\epsilon_p^n$$

where σ is the stress, K is the strength index, ε_p is the plastic strain and n is the strain hardening index. Ludwik's equation is similar but includes the yield stress:

$$\sigma = \sigma_y + K\epsilon_p^n$$

If a material has been subjected to prior deformation (at low temperature) then the yield stress will be increased by a factor depending on the amount of prior plastic strain ε_0:

$$\sigma = \sigma_y + K(\epsilon_0 + \epsilon_p)^n$$

The constant K is structure dependent and is influenced by processing while n is a material property normally lying in the range 0.2–0.5. The strain hardening index can be described by:

$$n = \frac{d\log(\sigma)}{d\log(\epsilon)} = \frac{\epsilon}{\sigma}\frac{d\sigma}{d\epsilon}$$

This equation can be evaluated from the slope of a log(σ) - log(ε) plot. Rearranging allows a determination of the rate of strain hardening at a given stress and strain:

$$\frac{d\sigma}{d\epsilon} = n\frac{\sigma}{\epsilon}$$

Processes

The following is a list of cold forming processes:

- Squeezing
  - Rolling
  - Swaging
  - Extrusion
  - Forging
  - Sizing
  - Riveting
  - Staking
  - Coining
  - Peening
  - Burnishing
  - Hubbing
  - Thread rolling
- Bending
  - Angle bending
  - Roll bending
  - Draw and compression
  - Roll forming
  - Seaming
  - Flanging
  - Straightening
- Shearing
  - Slitting
  - Blanking
  - Piercing
  - Lancing
  - Perforating
  - Notching
  - Nibbling
  - Shaving
  - Trimming
  - Cutoff
  - Dinking
- Drawing
  - Tube drawing
  - Wire drawing
  - Spinning
  - Embossing
  - Stretch forming
  - Sheet metal drawing
  - Ironing
  - Superplastic forming

Techniques have been designed to maintain the general shape of the workpiece during work hardening, including shot peening and equal channel angular extrusion.

Advantages and disadvantages

Advantages:

- No heating required
- Better surface finish
- Superior dimensional control
- Better reproducibility and interchangeability
- Directional properties can be imparted into the metal
- Contamination problems are minimized

The increase in strength due to strain hardening is comparable to that of heat treating. Therefore, it is sometimes more economical to cold work a less costly and weaker metal than to hot work a more expensive metal that can be heat treated, especially if precision or a fine surface finish is required as well. The cold working process also reduces waste as compared to machining, or even eliminates with near net shape methods. The material savings becomes even more significant at larger volumes, and even more so when using expensive materials, such as copper. The saving on raw material as a result of cold forming can be very significant, as is saving machining time. Production cycle times when cold working are very short. On multi-station machinery, production cycle times are even less. This can be very advantageous for large production runs.

During cold working the part undergoes work hardening and the microstructure deforms to follow the contours of the part surface. Unlike hot working, the inclusions and grains distort to follow the contour of the surface, resulting in anisotropic engineering properties.

Disadvantages:

- Greater forces are required
- Heavier and more powerful equipment and stronger tooling are required
- Metal is less ductile
- Metal surfaces must be clean and scale-free
- Intermediate anneals may be required to compensate for loss of ductility that accompanies strain hardening
- The imparted directional properties may be detrimental
- Undesirable residual stress may be produced

Due to the large capital costs required to set up a cold working process the process is usually only suitable for large volume productions.

Intermediate annealings may be required to reach the required ductility to continue cold working a workpiece, otherwise it may fracture if the ultimate tensile strength is exceeded. An anneal may also be used to obtain the proper engineering properties required in the final workpiece. Also, the distorted grain structure that gives the workpiece its superior strength can lead to residual stresses.

Cold worked items suffer from a phenomenon known as *springback*, or *elastic springback*. After the deforming force is removed from the workpiece, the workpiece springs back slightly. The amount a material springs back is equal to Young's modulus for the material from the final stress.

Chapter 14

Solid Solution Strengthening

Solid solution strengthening is a type of alloying that can be used to improve the strength of a pure metal. The technique works by adding atoms of one element (the alloying element) to the crystalline lattice of another element (the base metal). The alloying element diffuses into the matrix, forming a solid solution. In most binary systems, when alloyed above a certain concentration, a second phase will form. When this increases the strength of the material, the process is known as precipitation strengthening, but this is not always the case.

Types

Depending on the size of the alloying element, a substitutional solid solution or an interstitial solid solution can form. In both cases, the overall crystal structure is essentially unchanged.

Substitutional solid solution strengthening occurs when the solute atom is large enough that it can replace solvent atoms in their lattice positions. According to the Hume-Rothery rules, solvent and solute atoms must differ in atomic size by less than 15% in order to form this type of solution. Because both elements exist in the same crystalline lattice, both elements in their pure form must be of the same crystal structure. Examples of substitutional solid solutions include the Cu-Ni and the Ag-Au FCC binary systems, and the Mo-W BCC binary system.

When the solute atom is much smaller than the solvent atoms, an interstitial solid solution forms. This typically occurs when the solute atoms are less than half as small as the solvent atoms. The smaller solute atom essentially "crowds" into the spacings within the lattice structure, causing defects in the material. Elements commonly used to form interstitial solid solutions include H, N, C, and O. Carbon in iron (steel) is one example of interstitial diffusion.

Mechanism

The strength of a material is dependent on how easily dislocations in its crystal lattice can be propagated. These dislocations create stress fields within the material depending on their character. When solute atoms are introduced, local stress fields are formed that interact with those of the dislocations, impeding their motion and causing an increase in the yield stress of the material, which means an increase in strength of the material. This gain is a result of both lattice distortion and the modulus effect.

When solute and solvent atoms differ in size, local stress fields are created (if solute atom size is larger than solvent atom size, this field is compressive, and similarly, when solute atoms are smaller than solvent atoms, this field is tensile). Depending on their relative locations, solute atoms will either attract or repel dislocations in their vicinity. This is known as the size effect. This allows the solute atoms to relieve either tensile or compressive strain in the lattice, which in turn puts the dislocation in a lower energy state. In substitutional solid solutions, these stress fields are spherically symmetric, meaning they have no shear stress component. As such, substitutional solute atoms do not interact with the shear stress fields characteristic of screw dislocations. Conversely, in interstitial solid solutions, solute atoms cause a tetragonal distortion, generating a shear field that can interact with both edge, screw, and mixed dislocations. The attraction or repulsion of the dislocation centers to the solute particles increase the stress it takes to propagate the dislocation in any other direction. Increasing the applied stress to move the dislocation increases the yield strength of the material.

The energy density of a dislocation is dependent on its Burgers vector as well as the modulus of the local atoms. When the modulus of solute atoms differs from that of the host element, the local energy around the dislocation is changed, increasing the amount of force necessary to move past this energy well. This is known as the modulus effect. Meanwhile, in the specific case of a lattice distortion, the difference in lattice parameter leads to a high stress field around that solute atom that impedes dislocation movement.

Surface carburizing, or case hardening, is one example of solid solution strengthening in which the density of solute carbon atoms is increased close to the surface of the steel, resulting in a gradient of carbon atoms throughout the material. This provides superior mechanical properties to the surface of the steel.

Governing equations

Solid solution strengthening increases yield strength of the material by increasing the stress τ to move dislocations:

$$\Delta\tau = Gb\epsilon^{\frac{3}{2}}\sqrt{c}$$

where c is the concentration of the solute atoms, G is the shear modulus, b is the magnitude of the Burger's vector, and ε is the lattice strain due to the solute. This is

composed of two terms, one describing lattice distortion and the other local modulus change.

$\varepsilon = | \varepsilon_a - \beta\varepsilon_G |$ Here, ε_a is the lattice distortion term, β a constant dependent on the solute atoms and ε_G the term that captures the local modulus change.

The lattice distortion term can be described as:

$\epsilon_a = \frac{\Delta a}{a \Delta c}$, where *a* is the lattice parameter of the material.

Meanwhile, the local modulus change is captured in the following expression:

$\epsilon_G = \frac{\Delta G}{G \Delta c}$, where *G* is shear modulus of the solute material,

Implications

In order to achieve noticeable material strengthening via solute solution strengthening one should alloy with solutes of higher shear modulus, hence increasing the local shear modulus in the material. In addition, one should alloy with elements of different equilibrium lattice constants. The greater the different in lattice parameter, the higher the local stress fields introduced by alloying. Alloying with elements of higher shear modulus or of very different lattice parameters will increase the stiffness and introduce local stress fields respectively. In either case, the dislocation propagation will be hindered at these sites, impeding plasticity and increasing yield strength proportionally with solute concentration.

Solid solution strengthening depends on:
- Concentration of solute atoms
- Shear modulus of solute atoms
- Size of solute atoms
- Valency of solute atoms (for ionic materials)

Nevertheless, one should not add so much solute as to precipitate a new phase. This occurs if the concentration of the solute reaches a high critical point given by the binary system phase diagram. This critical concentration therefore puts a limit to the amount of solid solution strengthening a material can have, as the material cannot be infinitely strengthened.